CHALMERS
UNIVERSITY OF TECHNOLOGY

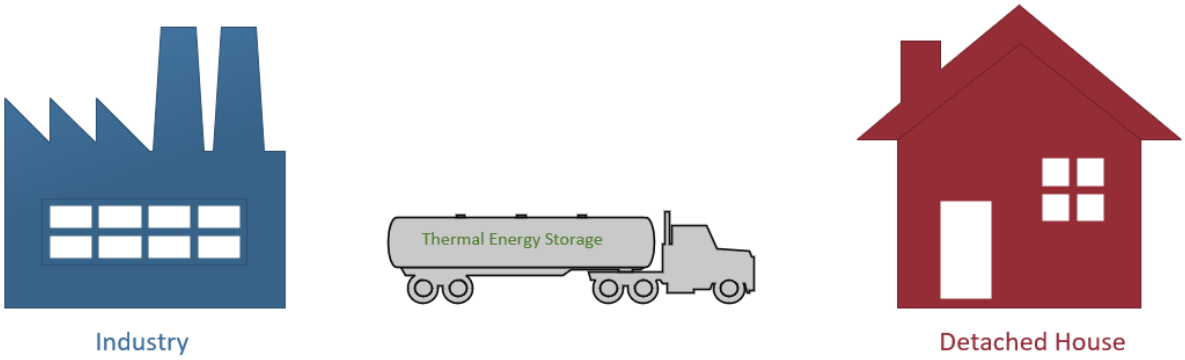

Technoeconomic Analysis of Storing Industrial Waste Heat in a Novel Heat Storage

Master's Thesis in Innovative Sustainable Energy Engineering (Nordic Five Tech) Programme

DORIN JAVAHERNESHAN

DEPARTMENT OF ENERGY AND ENVIRONMENT

DIVISION OF ENERGY TECHNOLOGY

CHALMERS UNIVERSITY OF TECHNOLOGY

Gothenburg, Sweden 2023
www.chalmers.se

Master's Thesis in ISEE (N5T)

Technoeconomic Analysis of Storing Industrial Waste Heat in a Novel Heat Storage

DORIN JAVAHERNESHAN

CHALMERS
UNIVERSITY OF TECHNOLOGY

Department of Space, Earth and Environment

Division of Energy Technology

Chalmers University of Technology

Gothenburg, Sweden 2023

Technoeconomic Analysis of Storing Industrial Waste Heat in a Novel Heat Storage

DORIN JAVAHERNESHAN

Supervisor: Timo Laukkanen, Aalto University
Examiner: Simon Harvey, Department of Energy and Environment

Master's Thesis in ISEE (N5T)
Department of Space, Earth and Environment
Division of Energy Technology
Chalmers University of Technology
SE-412 96 Gothenburg

Technoeconomic Analysis of Storing Industrial Waste Heat in a Novel Heat Storage

DORIN JAVAHERNESHAN
Department of Space, Earth and Environment
Chalmers University of Technology

Abstract

In remote areas where direct electric heating is the dominant heating system, it is essential to provide alternative heat supply options. Electricity prices fluctuate considerably, and considerable amounts of electricity are still produced from fossil fuels with a negative impact on the environment. Detached houses in Nordic countries, including Finland, require a lot of heating, but at the same time, a considerable amount of excess heat is available from industrial processes. A significant amount of this excess heat cannot be utilized for energy efficiency enhancement at the process site and is therefore wasted. In rural areas, there is normally no heating network connecting houses to one another, and there is thus no existing infrastructure to enable usage of waste heat from industries for space-heating purposes. Thermal Energy Storage (TES) is an option that can store the unused heat of industry and transfer it to houses. A novel Latent TES has been developed utilizing cold-crystallization material (CCM) that enables long storage periods which can be suitable for satisfying the annual space heating demand of a small house. The storage medium can be charged once or several times at the industry during a year and store the heat for months.

This thesis aims to identify and select industries that can efficiently recover and distribute their excess heat using the CCM TES system. Thereafter, various storage models and case studies are proposed, taking into account factors such as the number of charging and transportation cycles, and storage unit quantities. For each model, the design entails storage size (s), heat exchanger (s), potential pipe network, valves, and the pump. Technoeconomic analysis is conducted for each model and case study in order to assess the economic efficiency of the CCM TES for domestic space heating purposes. Net Present Value (NPV) and Levelized Cost of Energy (LCOE) are used to conduct an economic evaluation and make comparisons with alternative heating systems for single-family houses, such as direct electric heating, air source heat pumps, and ground source heat pumps. In this regard, the study aimed to determine the most cost-effective solution. The study's findings demonstrate that increasing the TES's number of charging cycles per year decreases its size and improves the system's economic efficiency beyond the other options explored. The LCOE decreased from 0.59 to 0.15 €/kWh, which is comparable with the average household electricity price of 0.09 €/kWh.

Keywords: Thermal Energy Storage, Cold Crystallization Material, Industrial Waste Heat, Detached Houses Heating System, Technoeconomic Analysis

Acknowledgements

My sincere appreciation goes out to my advisors, D.Sc. Timo Laukkanen and D.Sc. Behnam Talebjedi from Aalto University for their unwavering leadership, priceless guidance, and constructive feedback. Their insights and mentorship have played a pivotal role in the successful completion of this thesis.

I would also like to express my special gratitude to my examiners, Professor Simon Harvey from Chalmers University of Technology and Professor Risto Lahdelma from Aalto University for their insightful comments and dedicated supervision.

I want to express my deepest appreciation to my parents for their unending support, unwavering encouragement, and consistent presence during hard and successful times throughout my academic journey. Their faith in my abilities and the chance they gave me to study in two top universities in Europe have been absolutely life changing.

I am externally thankful to my partner, Mohammad Ali Zonoobi, for his continuous support and assistance especially throughout the writing process. His presence during challenging times has been a source of strength and encouragement, contributing significantly to the completion of this thesis.

Espoo, December 2023

Dorin Javaherneshan

Contents

Symbols and Abbreviations

Symbols

ΔT_{min}	Minimum temperature difference
C_p	Specific heat capacity (kJ/kg°C)
E	Thermal Energy (J)
Q	Heat (W)
V	Volume (m^3)
U	Overall heat transfer coefficient ($W/m^{2\circ}K$)
h_h	Hot fluid convective heat transfer coefficient ($W/m^{2\circ}K$)
h_c	Cold fluid convective heat transfer coefficient ($W/m^{2\circ}K$)
T	Temperature (°C)
ΔT_{LM}	logarithmic mean temperature difference ($^{\circ}K$)
A	Area (m^2)
D	Diameter (m)
L	Length (m)
C	Cost (€)
i	Interest rate (%)
F	Annual Cash flow (€/a)
I_0	Capital Cost (€)
r	Annuity Factor

Abbreviations

TES	Thermal Energy Storage
M-TES	Mobilized Thermal Energy Storage
IWH	Industrial Waste Heat
HX	Heat Exchanger
PCM	Phase Change Material
CCM	Cold Crystallization Material
ErNa	Erythritol in cross-linked sodium polyacrylate matrix
Er	Erythritol
GCC	Grand Composite Curve
TMP	Thermomechanical Pulp Mill
CAPEX	Capital Expenditures
OPEX	Operational Expenditures
NPV	Net Present Value
LCOE	Levelized Cost of Energy
k€	Thousand Euros
HP	Heat Pump
COP	Coefficient of Performance
ASHP	Air Source Heat Pump
GSHP	Ground Source Heat Pump

1
Introduction

1.1 Background

One of the greatest issues humans are facing is climate change arising from anthropogenic greenhouse gas emissions. The International Panel on Climate Change (IPCC) stated that human activities are the major driver behind climate change [1]. The European Union has planned to achieve carbon neutrality by 2050 and has set a target to reduce greenhouse gas emissions by 40% compared to the year 1990 by 2030 [2]**.** Almost 40% of emissions are associated with the supply of heat [3]. Approximately, 52% of this heat is supplied to industrial processes and 46% is used for space and water heating of buildings [4]. Therefore, reducing heat supply from fossil fuel sources will have a significant impact on carbon emissions. Decarbonization of buildings' heating system can be done by utilizing heat pumps, renewable sources and improving energy efficiency.

By 2030, it is expected that energy efficiency will increase by 27% compared to the year 1990, which will reduce the primary energy usage as well as greenhouse gas emissions [2]. One of the major measures that can improve energy efficiency is to utilize the excess heat from industry as an energy source for other sectors. Approximately between 20% and 50% of consumed energy in the industrial processes is wasted in EU, which corresponds to 300 TWh per year [5], [6].

In Nordic countries, specifically Finland, due to severe cold weather conditions, buildings are among the most energy-intensive sectors corresponding to 27% of total energy consumption as illustrated in Figure 1.

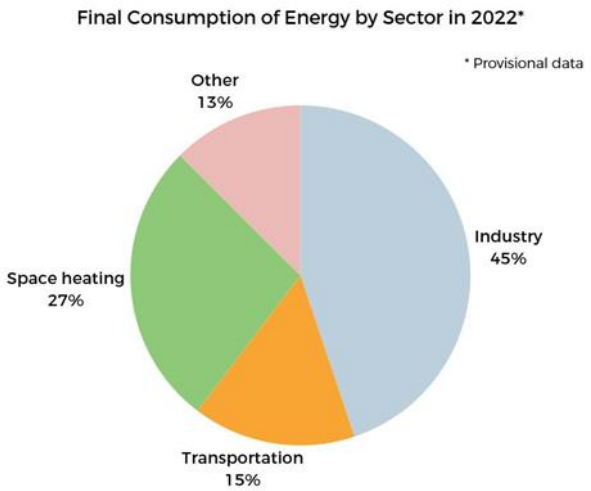

Figure 1. Finland's Final Energy Consumption share in each sector in 2022 [7]

One energy efficiency measure is to utilize industrial excess heat to heat buildings. Utilization of industrial waste heat reduces primary energy consumption as the by-product of industry is used as the heating source of houses, resulting in carbon reduction [8]. However, since many industrial processes operate year-round whereas the demand for heating of buildings is seasonal, energy storage is required to store the heat for a long time, months or even years and then supply it when it is needed. In 2014, the IEA announced that utilizing Industrial Waste Heat (IWH) with Thermal Energy Storage (TES) plays a major role in decarbonization of the energy system because of the temporal and geographical decoupling of supply and demand of heat [9].

There are three primary types of TES based on the method used to store heat, including sensible, latent, and thermochemical heat storage. Amongst these, latent heat storage stands out due to its relatively high energy density and successful commercialization. Latent TES utilizes the latent heat of the material during its phase change; therefore, the material's temperature does not change during charging and discharging, but rather the material melts, crystallizes, or evaporates. One such material is Erythritol which is a sugar alcohol that can store heat while being melted and release it when crystallized. It has a high energy density compared to other phase change materials, but it suffers from undesired crystallization. Therefore, it is not capable of storing heat for more than days. However, a research team at Aalto University has developed a cold-crystallization material, one of which consists of a matrix of erythritol in a cross-linked sodium-polyacrylate (ErNa), a sugar alcohol with polymer, to provide stability and long-term heat storage. Within this material, they achieved a maximum of 9 months of heat storage at temperatures between 0 to 10 °C. As it is capable of storing heat for a long period of time, it can be suitable to be implemented in buildings.

In Finland, the majority of detached houses located in rural areas rely on electricity for their space heating, which leads to high energy costs for the houses. On the other hand, there is considerable heat being released to the environment from industrial processes. If the waste heat can be transported from industry to these houses to satisfy their heating demands, it would have a great impact on energy efficiency.

This master's thesis aims to evaluate utilization of Aalto University's innovative thermal storage technology to efficiently store and distribute waste heat from industrial sources to detached residences in remote locations. Various models for delivering industrial waste heat to detached houses via this novel thermal storage are proposed and their technoeconomic feasibility is investigated.

1.2 Aim and Scope

This master's thesis, which is part of an Academy of Finland project, aims to evaluate the optimal integration of a novel long-term heat storage material which is a cold crystallization material in the building and industrial systems. The work investigates the technical and economic feasibility of storing industrial waste heat and utilizing it for the heating of buildings. The first aim is to discover which industry sectors are more suitable to be integrated with the mentioned heat storages, because these storage materials have specific working temperature intervals. The second goal is to propose different models regarding how the heat can be

extracted from industry, transferred to a detached family house and supplied to the building. The third goal is to estimate the costs within different configuration systems to evaluate how competitive they can be in the market in comparison with supply of heat with ground-source heat pumps and direct electricity.

1.3 Research Questions

In this thesis, the following questions have been answered:

- Which types of industrial waste heat have the potential to be integrated with the novel PCM storage?
- How can the industrial excess heat be recovered, transferred to the single-family house apartments in the countryside, and supplied to the building by Cold-crystallization thermal storage?
- Are the proposed storage models and case studies cost-effective?
- How competitive can they be with other common heating systems of detached houses?

2
Theoretical Background

2.1 Current State of Heat Consumption and Industrial Waste Heat in Finland

EU industries consume 3200 TWh of energy per year which accounts for more than a quarter of the EU's total energy consumption [10]. Metal, chemical, paper, food and non-metallic industries are responsible for almost two-thirds of this energy consumption. In Finland, 45% of the total final energy consumption belongs to industrial processes as shown in Figure 1. The total potential waste heat in all industries in Finland is estimated to be approximately 6 TWh per year [5]. More than half of Finland's waste heat arises from pulp, paper and print industry, 13% from iron and steel industry, and 10% from chemical and petrochemical industry as can be seen in Figure 2 [11].

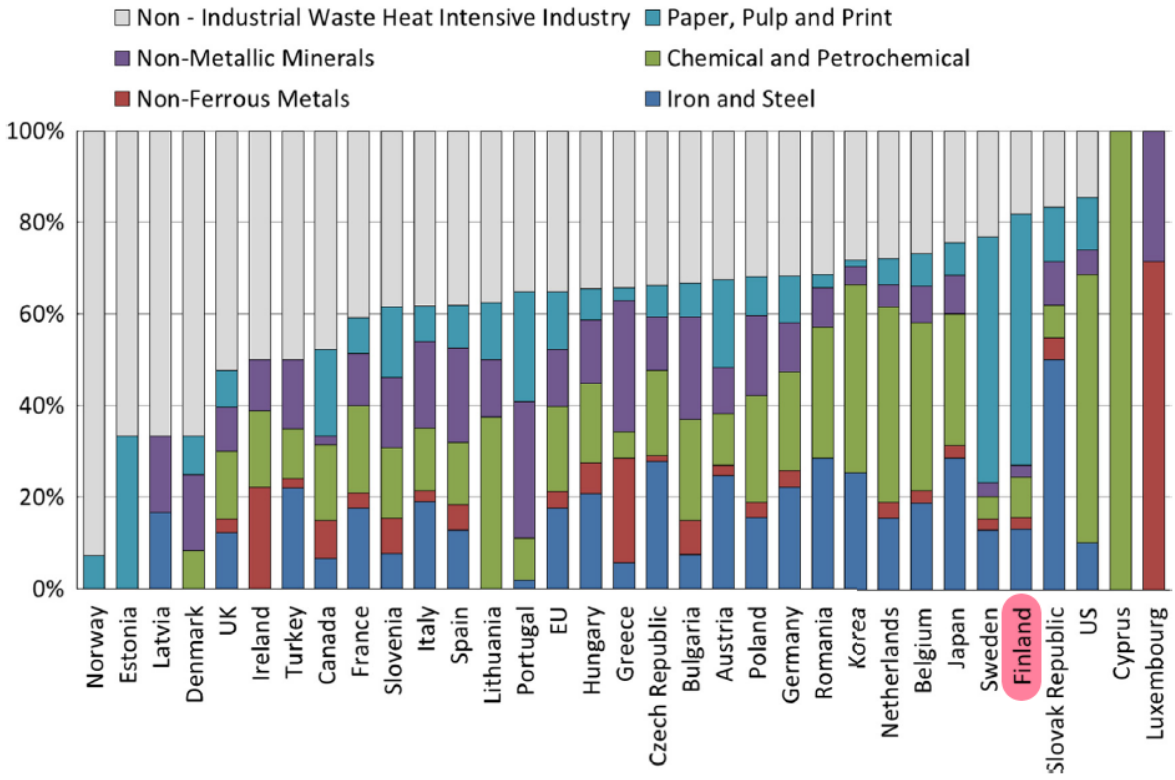

Figure 2. Percentage of Industrial Waste Heat in industries

In Figure 3, it can be observed that the highest waste heat temperature range occurs at the metal industry which is mainly between 500-1000 °C, while for the pulp and paper industry and chemical industry, this range is 100-200 °C and below 100 °C, respectively [5]. The waste heat

is normally in the form of steam, condensation heat, exhaust gas, wastewater, coolant water, flue gas and outgoing air [12].

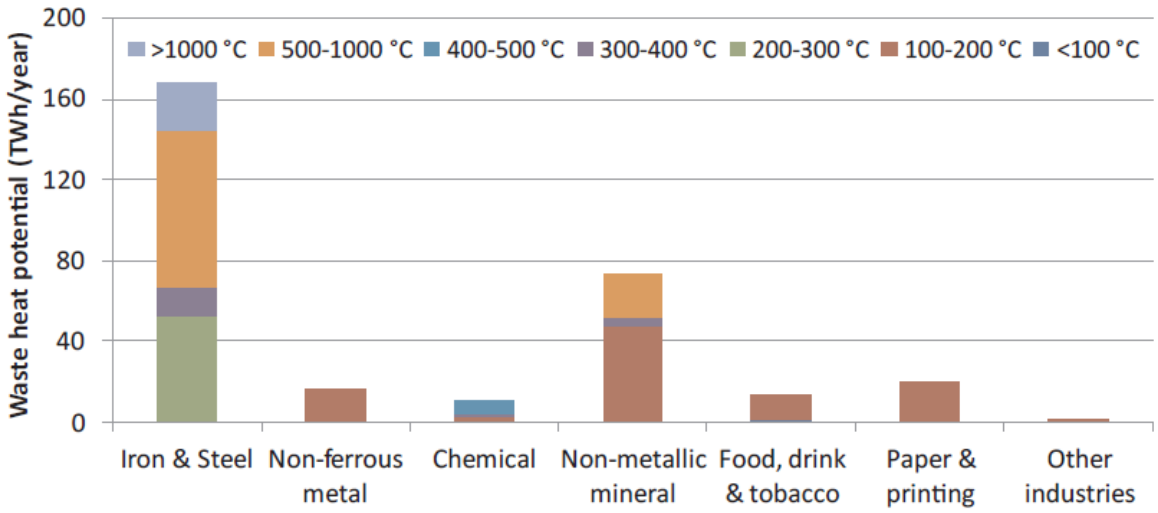

Figure 3. Waste heat potential in EU for each industrial sector within their temperature levels in 2015

In Finnish industry, one third of the primary energy consumption, electricity and heat, is not recovered and is therefore released to the surroundings [13]. Approximately 70% of the EU's industrial energy consumption is in the form of heating, while the remaining 30% is in the form of electricity [14]. Heating is utilized for process heating and industrial site space heating. Process heating spans a broad spectrum of temperatures across different industries, with the metal industry reaching temperatures as high as 1000 °C. For some industries such as machinery, the heating demand is mostly for space heating [5].

The excess heat from an industry should be cooled in order to minimize its negative impact on the environment. It goes through cooling towers, heat exchangers and some fans to be cooled and ready to be exhausted either to the atmosphere or nearby water bodies. All these facilities consume some energy to cool down the heat, and therefore they are responsible for some energy costs and emissions. By effectively utilizing and recovering the IWH, not only do the emissions reduce but also the consumption of fossil fuels as the primary resource is reduced. The IWH can be recovered and used to supply the heat for other processes at the industrial site. However, for this purpose, heat exchangers should be installed. In 1970, at the University of Manchester, a systematic tool called Pinch Analysis was developed to estimate the maximum possible energy recovery within the industrial processes, as well as the minimum hot and cold utilities.

Most of processes and industries still have some heat that cannot be recovered internally within other processes. This heat can be utilized for space heating of the industry during winter or delivered to other sectors. Transfer of IWH to other locations can be done thanks to the Thermal Energy Storage (TES). In the following, different TESs are discussed and the selected one is explained in detail.

There are different waste heat exploitation technologies that can make the waste heat usable such as heat-to-power with organic Rankine cycle, heat-to-cooling with thermally driven

chillers and heat pumps. When the temperature of the waste heat is lower than utilization temperature, it can be upgraded to reach the desired temperature using heat pumps. Industrial (high temperature) heat pumps are a promising technology that can elevate the waste heat temperature currently up to almost 150 °C [15], [16]; however, some research is being done to increase this temperature for further application [17]. Their feasible temperature lift is between 30 and 50 °C, thus heat pumps are mainly able to be integrated with low-temperature industrial waste heat with a maximum temperature of 120 °C [18].

2.2 Buildings' Heating Systems

Globally, buildings are responsible for 30% of greenhouse gas emissions and 40% of the total energy consumption [19]. The relatively high proportion of emission release and energy consumption in the residential sector arises from reliance on fossil fuels for providing energy, low energy efficiency in buildings, and insufficient insulation levels in many houses. In the EU, half of the electricity consumption belongs to residential and tertiary sectors. Space heating and water heating account for 22% and 9% of this electricity consumption respectively [20]. Due to the geographical location of Nordic countries such as Finland, space heating demand accounts for a great portion of energy consumption. The proportion of energy use in Finnish dwellings attributed to space and water heating is 82%, as illustrated in Figure 4.

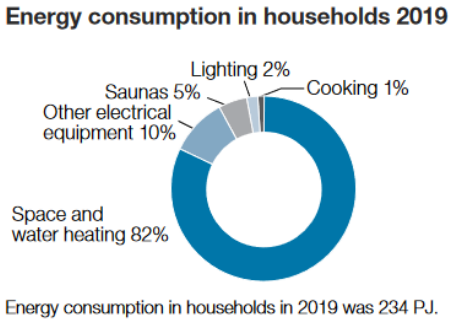

Figure 4. Finnish households' energy consumption

Normally, the indoor temperature of houses in Finland is 21 °C and houses have triple-glazed windows to improve insulation and reduce the heat loss [21]. In populated areas, heat is supplied efficiently by district heating, the central heating network where its heating comes from combined heat and power plants. On the other hand, detached buildings located in sparsely populated areas are not connected to the district heating system. In Finland, 89% of residential buildings are detached houses [22] with the majority of them providing heating through electricity [23]. The definition of detached house is a house that does not share a wall with another house. In detached houses, heating system comprises of heat generation, storage, and delivery to heated space as well as the control system. Heat can either be directed to inside the house or stored right after being transferred from the power generator. Examples of heat generators include electric heaters, boilers, and heat pumps that generate heat from other sources of energy. Fossil fuel heaters emit greenhouse gases which are not environmentally friendly and conflict with the current policies regarding the reduction of emissions. Electric heaters and heat pumps that use electricity for providing space heating are sensitive to electricity prices and it impacts the energy costs of houses during every fluctuation and during

high demand. The generated heat is delivered mainly by means of fluids such as water and air, through fans, heat exchangers, and pipes placed under the floor. Heat storage is used in some heating systems, such as solar heating and wood pellet heating, where heat is stored in an accumulator.

The share of most common heating systems in Finland, including district heating, electric heating, heat pumps, ground source heat pumps, furnace, and wood heating, is displayed for both urban and rural areas in Figure 5. It is evident that Electric heating is the prevailing technology in rural regions, accounting for 40% of all heating systems. Geothermal heat pumps come in second place, with a share of 33%, while heat pumps hold almost 8% of the rural market.

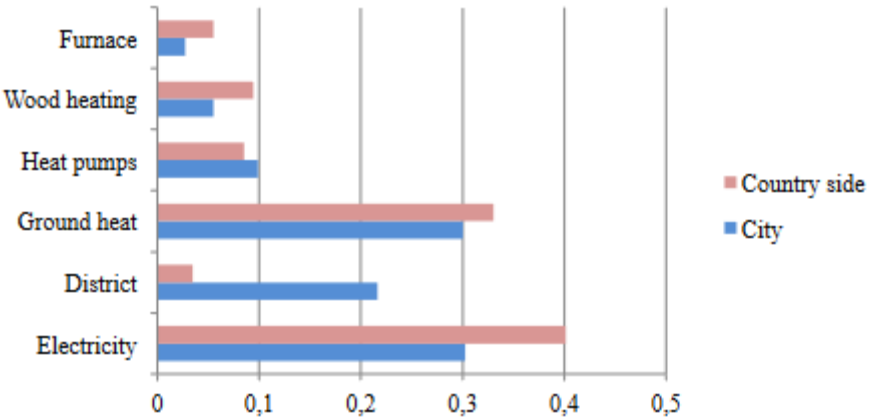

Figure 5. Heating systems share in cities and countryside in Finland [24]

The efficiency of electric heaters is almost 100%, meaning that the heating demand is equal to the electricity consumption. Globally, and especially in Europe, the electricity price has increased due to an increase in fuel costs and a transition towards renewable energy sources. For instance, due to reliance of power plants on natural gas imported from Russia, the average electricity price in Finland in 2022 was two times higher than in 2021. To reduce the impact of this electricity fluctuation on society and for decarbonization of energy systems, remote houses' heating can be supplied by more efficient heating equipment such as heat pumps.

Heat pumps are classified in different categories based on their heating source and sink. The most efficient ones for buildings' heating are Air to Air and Ground-source heat pumps. Air-to-air heat pumps utilize the heat of outdoors to heat up the indoor environment. When investing in heat pumps, not only can they provide heating, but also cooling during the summer. The primary drawback of air-to-air heat pumps is their efficiency decline to almost 1 when the outdoor temperature reaches a certain point known as the "balance point." In most air-to-air heat pumps, the balance point is around -20°C [25], resulting in the heat pump operating solely as an electric heater, with only the compressor powering the heating function. In Nordic countries, particularly in the northern regions, when the outdoor temperature drops to -30 °C, a heat pump may not be able to supply enough heat, resulting in the indoor temperature falling below the comfort level. However, ground-source heat pumps maintain their efficiency as they rely on the temperature of the ground. Nevertheless, their cost is higher due to expenses

associated with drilling the ground, installation and piping costs, and the elevated price of the heat pump. Moreover, the decision regarding installing geothermal heat pumps is affected by the soil type and size of the available site.

According to data on living conditions in Europe supplied by Eurostat, homes in Finland are in very good condition when it comes to insulation and heating systems, and just 0.2% of Finns reside in flats that are in poor condition [26]. A total of 6% of single-family homes have low energy efficiency, according to energy performance certificates and one quarter of the total emissions arise from heating of these houses [26]. Following the energy crises of the 1970s, Finland has consistently enhanced the energy efficiency of newly constructed buildings, largely attributed to the implementation of stricter building regulations. As a result, the mean energy consumption of buildings constructed in the 1960s is 240 kWh/m^2, whereas for buildings completed in the 2010s, it is one-third of this value, equivalent to 85 kWh/m^2 [27]. The construction of new structures in the 2010s represents 26% of the total stock of single-family and semi-detached houses [28].

As buildings are one of the biggest energy consumers, it has been essential to improve their energy efficiency. In 1991, the Passive House concept was developed and implemented in Germany. Since then, the standard of passive houses has been developed mostly in Central Europe and adjusted for implementation in Nordic countries. For instance, in Sweden, the heating power requirement (energy per period of time) has been defined as between 10-14 W/m^2 [29]. Meanwhile in Finland, the country has been divided into three sections including south, middle, and north, to define the maximum energy requirement of passive houses. In the south, the maximum space heating demand is 20 kWh/m^{2}a, and for primary energy this value should not exceed 130 kWh/m^{2}a. For the middle and south, heating demand is 5 kWh/m^{2}a and higher [29]. Passive house refers to a low energy building where heat loss has been significantly reduced, and space heating mainly comes from heat radiation form the occupants themselves, lightning and appliances, so the need for external heating supply is considerably lower than normal houses. These houses are well insulated and have a heat recovery system for ventilation and smart heating system. The aim of this type of house is to avoid the need for conventional heating systems and utilize renewable energy sources. Thus, they provide the opportunity to utilize heat storage in the residential sector.

2.3 Thermal Energy Storage

Renewable energy production, such as solar and wind, are seasonal, with peaks and drops at different times of the year. In Nordic countries, there is a high demand for heating during the winter when solar energy is scarce. Conversely, during the summer, solar energy is abundant but the demand for heating is low. Also, the quantity of wind energy varies throughout the year due to natural fluctuations. During periods of high heating demand, the available wind energy may not be sufficient to meet the demand. Energy storage is therefore required to address this mismatch between production and demand and to store excess energy during low demands for utilization during high peaks. Moreover, energy storage enhances the reliability of the system and provides added flexibility to it.

Thermal energy storages can be categorized in different ways but according to the form of energy that is charged and discharged, there are three different main categories including sensible, latent and thermochemical storages. In sensible TES, heat is stored in the material within its heat capacity, therefore the material's temperature increases. Common sensible TESs include hot/chilled water tanks, underground TES and concrete TES [30]. The problem with these types of TES is their relatively low energy density which results in big volumes as well as their considerable heat loss over time. However, they are cheap and reliable [31]. In Latent TES, Phase Changer Material (PCM) is used where its phase changes during charging and discharging. Inorganic salts and paraffins are some of these PCM materials [30]. They have higher energy storage, so they are capable of storing a large amount of heat in a relatively small volume [32], [33]. Their weaknesses however are their low thermal conductivity, higher costs, high corrosivity as well as heat losses if heat is stored for a long time [33]–[35]. Latent TES technology has been commercialized for a few materials and temperature ranges, but it is mostly still under development. Lastly, Thermochemical TES stores heat in a form of chemical reaction that occurs in the material mixture such as silica gel + water and zeolite + water [30]. This TES type has significantly higher energy density as well as lower heat loss thus they can perform as a long-term TES. However, their capital cost is relatively high, and the technology is complex so mainly they are in laboratory scale and underdevelopment [31].

For near future, Latent TES seems to be utilized commercially and numerous numbers of research is being carried out about enhancing this technology. Sugar alcohols, paraffins and hydrates have been the focus of a lot of attention.

2.3.1 Latent Heat Storage

As mentioned earlier, Latent TES is an attractive technology because of its relatively high energy density, and it releases heat mainly at a constant temperature level. Several phase change materials (PCMs) have been successfully brought to the commercial market and most of them utilize both the latent heat and sensible heat for storage. However, a significant number of PCMs continue to face various obstacles pertaining to their material behavior such as long-term stability, and thermal conductivity [34].

One category of PCMs are sugar alcohols such as Erythritol which have a high melting enthalpy of 339 kJ/kg and melting temperature of 118 °C. They have a substantial supercooling degree, which is the difference in temperature between their melting point and the temperature at which they remain in a supercooled state. Supercooling is a state that material is in a liquid phase while being below the melting temperature [36]. Supercooling is unfavorable in traditional short-term TES systems, as it makes the phase change difficult to initiate and therefore causes a delay in the release of heat [37]. However, supercooling can offer benefits in the context of long-term TES. If the PCM remains in a supercooled state, meaning it is in a metastable condition where the latent heat of melting can be stored without any loss for a long period of time [38]. Supercooling has been deployed in small scale TESs since 1895, with heating pads being the most widely used commercial product that utilized this phenomenon [38].

Although sugar alcohols have a significant potential for undergoing supercooling, they alone cannot consistently retain thermal energy in the supercooled state due to unintentional

crystallization. In large applications, when TES volume increases, the likelihood of premature crystallization increases, resulting a substantially shorter storage time [39], [40]. The following paragraph describes one of the developed PCM materials that proven to be able to successfully store heat for several months in kg scale.

2.3.2 Cold-Crystallization Thermal Energy Storage

Sugar alcohols are susceptible to significant supercooling, and when they cool down even further, they may vitrify. Polymers and cross-linking agents are examples of additives that can modify the storage material's vitrification, cold-crystallization, and supercooling characteristics and brings stability to the crystallization [41]. At Aalto University some research and experiments have been conducted with the aim of achieving long-term stability of TES utilizing sugar alcohols, mainly erythritol cross-linked in polymers including sodium polyacrylate and polyvinyl alcohol [42], [43].

In recent trials conducted by Konsta Turunen, a doctoral researcher, at Aalto University, erythritol in a cross-linked sodium-polyacrylate (ErNa) has successfully achieved long-term heat storage at three different scales tested up to 6.7 kg of material [41]. In ErNa TES, supercooling, glass transition and cold crystallization were utilized, therefore it has been named as Cold Crystallization Material (CCM). In the charging process, material is melted when being heated, then it undergoes supercooling close to the glass transition temperature. Glass transition means utilizing extreme supercooling that results in formation of amorphous and glassy solid from vitrification of liquid. When supercooling goes on until reaching very low temperature close to glass transition temperature, there is a substantial decrease in molecular motion. Over time, the movement gradually decelerates to the point where the material undergoes vitrification, resulting in its transformation into an amorphous solid state. In this state, the molecules exhibit a low energy level, resulting in a significant energy barrier for the process of crystallization [44]. Following the designated storage period, the material undergoes a heating process, mentioned as reheating, to reach a specific temperature known as the cold-crystallization temperature, which serves as the trigger for initiating the discharge process. As the temperature of the material rises, there is an increase in molecular motion. In due course, molecules acquire a sufficient level of energy to surpass the energy threshold required for the process of crystallization resulting in the material undergoing crystallization and subsequently releasing the latent heat that was trapped within. During the process of crystallization, the release of heat causes the temperature of the material to rise towards its melting point. The process in which crystallization occurs at temperatures lower than melting temperature is known as cold crystallization [41]. The working principle of CCM TES explained above is illustrated in Figure 6.

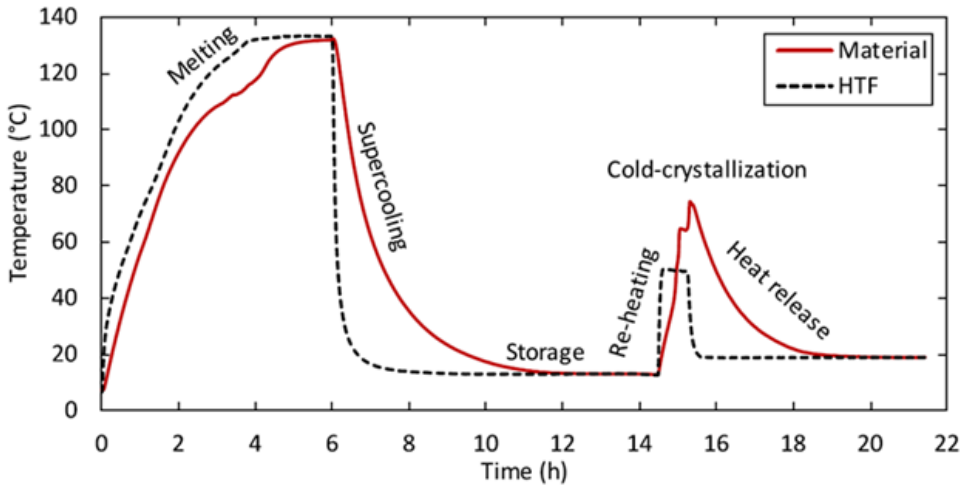

Figure 6. Working principle and each stage of CCM TES [41]

The ErNa TES has been tested at different scales for characterizing its thermophysical properties at different temperatures. All these experiments have been carried out by Konsta Turunen at Aalto University. In the first experiment, 15 mg-25 mg of material was put to analyze and achieve cold-crystallization rate [41]. In the prototype, testing of 6 kg of material within two different heat exchange arrangement were done to observe the effect of heat transfer rate on the operational parameters [41]. One drawback of CCM is its relatively low thermal conductivity, as a result suitable design of the heat exchangers plays a significant role in storage efficiency [45].

One potential method to enhance heat transfer involves the utilization of metal fins that can be affixed to the system where latent heat storage plays as an active storage meaning the storage tank is filled with PCM while heat transfer media flows inside the tubes. Another method of heat exchange commonly known as encapsulated PCM is when PCM is put into number of capsules and the storage tank is filled with the heat transfer media [46]. Therefore, in the tested prototype, in one TES unit (marked as unit 1 in Figure 7), finned tube heat exchanger was used, and the container was filled with 6.72 kg of ErNa-80 (80% erythritol, 20% sodium polyacrylate) and the other TES unit (marked as unit 2 in Figure 7) utilized tubes which were filled with 6,31 kg of ErNa-80 [41]. The main advantage of the second storage is that if nucleation occurs in one of the tubes during the cooling process, it will result in the complete crystallization solely within that specific tube, while the remaining ErNa tubes would remain unaffected. The thermal fluid was heated up in an electric heater to be prepared for charging the storage. For supercooling, circulating fluid flowed in a heat exchanger that was connected to a tap water system. During the storage period, the storage system was placed in a refrigerated room to stay at the storage temperature [41]. A schematic of the prototype system built for testing ErNa TES is provided in Figure 7.

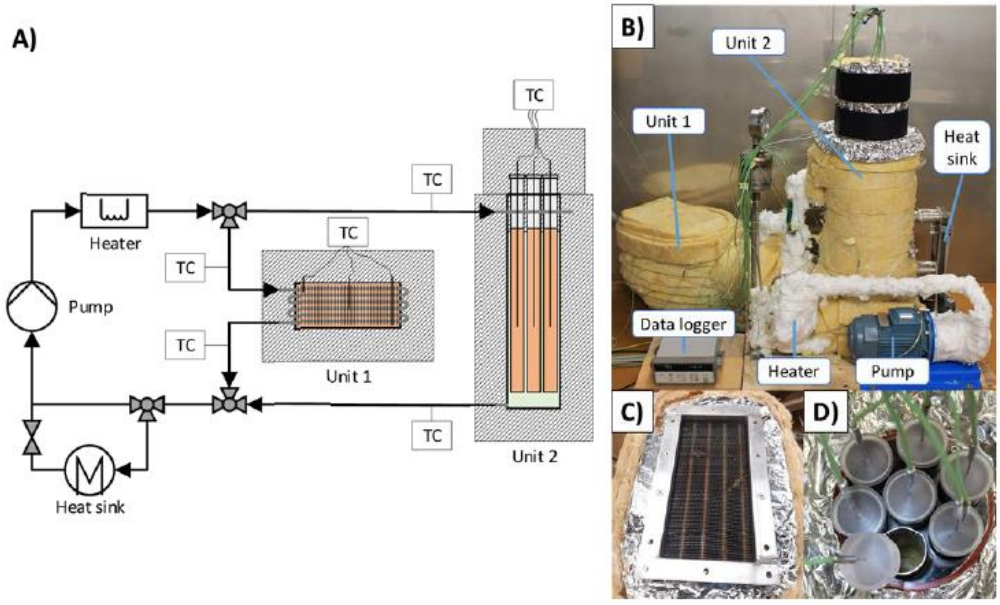

Figure 7. Prototype system tested for ErNa TES [41]

Results achieved from the prototype indicated higher storage efficiency for the TES within finned tube heat exchanger [41]. Enthalpy- temperature diagram of the tested protype during a full cycle for both heat storages comprising finned tube heat exchanger and encapsulated heat exchanger that discharge heat until 50 °C, are provided in Figure 8. It can be clearly observed that the ratio of discharging heat in comparison to the charging heat is far higher for finned tube heat exchanger. It should be noted that the efficiency of ErNa TES is dependent on the final application temperature. In the experiment when discharging temperature of 30 °C was utilized, TES with finned tube HX yielded efficiency of 28% when only final discharging heat is utilized whereas, TES with encapsulated HX had efficiency of 18%. However, when supercooling heat at temperature of 30 °C is utilized for heating application as well, efficiency of storage with the finned tube HX escalates to 77% [41].

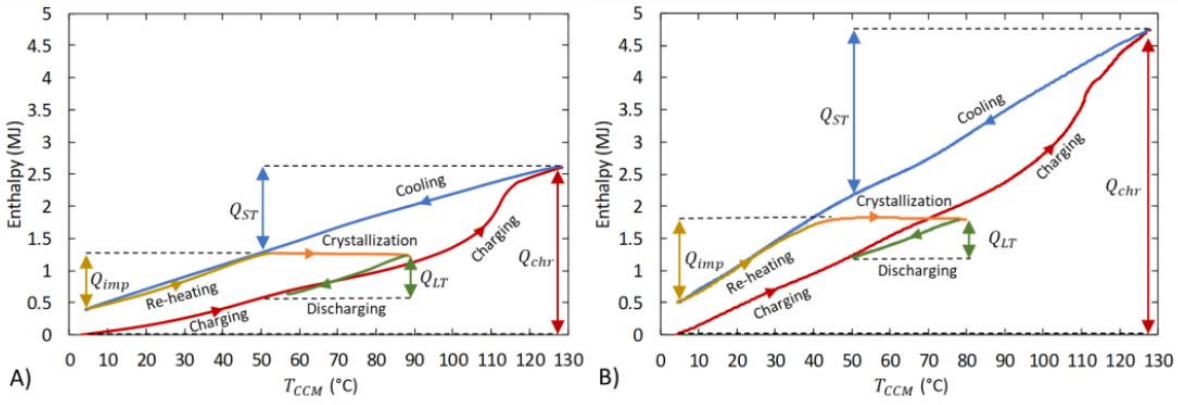

Figure 8. Enthalpy-temperature diagram of ErNa stored at 4 °C in A) Storage unit with finned tube heat exchanger and B) Storage unit with tubes filled in ErNa immersed in heat transfer fluid [41]

Some of the thermophysical properties of ErNa-80 achieved during prototype testing are provided in Table 1. ErNa-80's volumetric melting enthalpy is approximately 240 MJ/m^3,

which is consistent with the average values observed in short-term TES applications using phase change materials [41].

Table 1. Thermophysical characteristics of ErNa-80 measured in kg scale [41]

Parameter	Value	Unit
Density	1460 at 25 °C 1430 at 120 °C	kg/m^3
Specific Heat Capacity	1.6 at 20 °C (Solid) 2.5 at 120 °C (Liquid)	kJ/kgK
Melting Temperature	111	°C
Melting Enthalpy	166	J/g
Cold Crystallization Temperature	49	°C
Cold crystallization Enthalpy	136	J/g

The relation between cold crystallization enthalpy (ΔH_{cc}) and melting enthalpy (ΔH_m) reported by Konsta Turunen [41] are illustrated in Eq. 1. Where $C_{p,l}$ and $C_{p,s}$ are specific heat capacity of CCM in the liquid and solid phase respectively, T_m is the melting temperature and T_{cc} is the cold crystallization temperature.

$$\Delta H_{cc} = \Delta H_m - \int_{T_{cc}}^{T_m} \left(C_{p,l} - C_{p,s} \right) dT \quad (1)$$

In the context of CCM TES, it is recommended that the charging temperature exceeds the melting temperature of the PCM. Conversely, the discharging temperature is contingent upon the temperature requirements of the specific application utilizing the released heat. Hence, energy storage density of a specific material varies in different applications and is not a single value [41]. When the prototype was tested, a critical cooling rate in the range of 0.1 °C/min and 0.6 °C/min was established when material is cooled from the final charging temperature to the storage temperature [41]. If supercooling happens slower than this rate, there is a relatively high chance of unwanted crystallization.

ErNa-80 TES successfully demonstrated up to 9 months of storage when the TES was maintained between temperature of 0-10 °C [41]. Since the discharging temperature can be in any temperature below 90 °C, it has the potential to provide house's heating demand.

2.4 Mobilized Thermal Energy Storage & Previous Studies

Mobilized thermal energy storage is a technology that facilitates the transport of heat from one location to another. It has the potential to fulfill the heating demand of buildings located in sparsely populated areas and thereby increase energy efficiency, decrease greenhouse gas emissions and utilization of fossil-based sources. The system includes a thermal storage, a heat exchanger, and a transport media. The transport media can be a truck, a ship, or a train depending on the heat source and heat sink locations. In many studies, a heat transfer fluid such as oil collects heat from the source, transfers it to the storage and finally release it to the end-user [47]. Sensible heat storages are not optimal for mobile thermal storage due to low energy

density and significant heat losses. Consequently, their size becomes excessively large, making transportation between locations challenging.

Previous research has mostly focused on two container models: direct contact heat exchanging and indirect heat exchanging. In direct heat exchanging, heat transfer media is mixed with the heat storage material. To utilize this technique, the PCM must be insoluble in the transfer media, and a considerable density difference between them is required to enable separation. An economic analysis was conducted for an erythritol heat storage in Sweden in which direct heat exchanging was used for charging and discharging. In this case study, thermal oil was heated at the industrial site and then entered the storage to directly transfer its heat content to erythritol. Results showed that it takes a considerable amount of time for the storage to be fully charged, due to the use of direct contact and the low thermal conductivity of the PCM material [48].

Trans-Heat Container (THC) is a German Japanese project to effectively use unused waste of the industry in containers. The storage investigated in Germany had Sodium Acetate Trihydrate (SAT) as the phase change material with a melting temperature of 58 °C and heat of fusion of 230 kJ/kg. The storage utilized direct contact for heating and melting the PCMs by injecting heat transfer fluid to the TES through pipes. [49]. One advantage of direct contact heat exchange is its high heat transfer rate and performance. For charging, the heat source should ideally have a temperature over 90 °C but not lower than 70 °C and the end user should have a heating demand at less than 50 °C. So, the applications can be water heating and space heating. The storage facility that was tested in Germany weighted 30 tonnes. In Japan, the same storage material was tested but due to heat demand, infrastructure, and climate difference between these two counties, the Japanese storage unit weighted 24 tonnes [50].

Another mobilized heat storage that was tested in Japan utilized Erythritol as the PCM material whose phase transformation temperature is 118 °C and melting enthalpy is 340 kJ/kg. The optimal heating source temperature is 150 °C and the minimum temperature is 130 °C. The user's demand temperature should be lower than 110 °C. In this storage case, a modular approach was employed, where a container weighing 10 tonnes was constructed by combining four individual storage units. This storage type underwent testing to assess its suitability for central heating and hot water applications, as well as its potential for cooling purposes, achieved through the utilization of an absorption refrigerator [50].

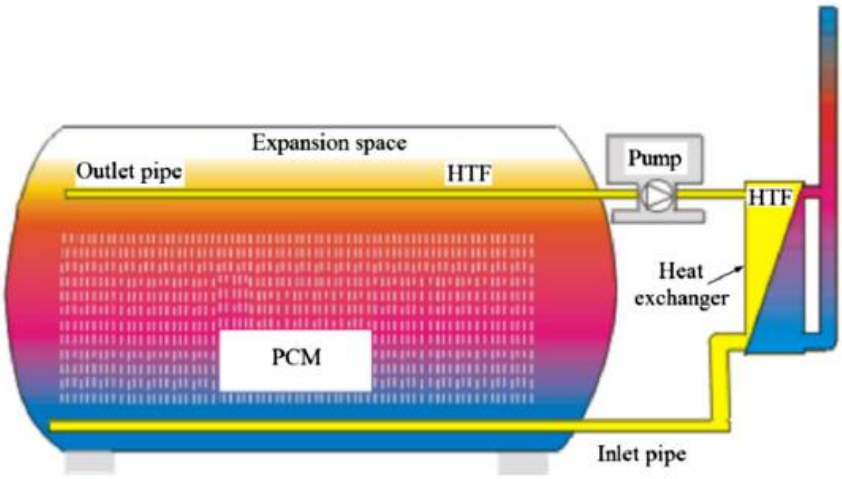

Figure 9. TransHeat's Direct contact M-TES [49]

In indirect heat exchanging, heat transfer media transfers its heat to the storage while flowing through immersed pipes inside the storage container. The heat transfer rate in this model depends on the contact area and material's thermal conductivity. The Alfred Schneider [51] company in Germany designed a thermal storage using fins made of high thermal conductivity metal in the heat exchanger to increase the heat transfer area. The storage is 20 ft container holding 22 tonnes of SAT and possessing the heat capacity of 2400 kWh.

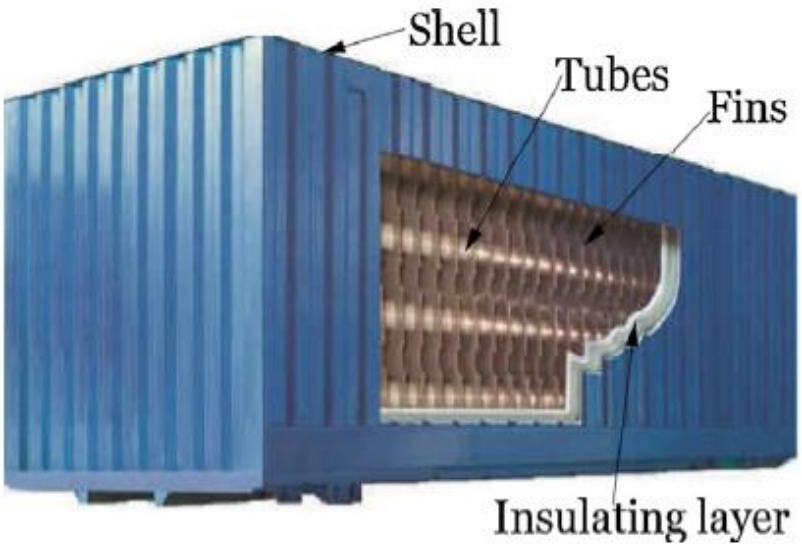

Figure 10. Alfred Schneidar M-TES container [51]

In the city of Surrey in British Columbia (Canada) a district energy network has been implemented that operates using a combination of natural gas boilers and geothermal exchange for providing hot water for both space and domestic hot water heating to residential and commercial buildings. However, the municipality plans to transition to low-carbon energy sources through the use of a district energy network. They are also considering the storage and usage of industrial waste heat using a mobilized TES system as an attractive alternative energy source. In 2019, the City of Surrey, in partnership with the Pacific Institute for Climate

Solutions and Canmet Energy, initiated a project to create a prototype for the storage. The project lasted for three years [52]. They proposed a transportable storage whose material is thermochemical liquid sorption. A study [53] investigated the economic and environmental aspect of this M-TES transported via either diesel truck, renewable natural gas fired truck or electric truck. They studied the effect of distance of the heat source from the district energy network as well including 15, 30 and 45 km.

Furthermore, two companies in Poland, Enetech sp.z.o.o. [54] and Neo Bio Energy [55] have commercialized mobilized thermal energy storage utilizing PCM materials charged by the waste heat. Enetech sp.z.o.o provides two storages installed in parallel, that are able to store 7 GJ of heat in 24 tonnes of storage media. When one of the storages is being charged at the industry, the other one is being discharged to provide heat to a building. When it is completely discharged, the fully charged one is delivered and installed to secure supply of heat. Neo Bio Energy has not provided detailed information about the material and sizes of storages it offers but rather a simple statement to the effect that it is capable of storing waste heat of Combined Heat and Power plants.

As can be seen there have been numerous studies on Erythritol M-TES systems. Erythritol is an organic PCM with high melting enthalpy making it an efficient and low volume latent thermal storage. One issue associated with pure erythritol is its tendency to crystallization making this thermal storage unable to store the heat for months. Therefore, regular transportation is required to transfer the heat from the source to the sink. S. Guo et al. [56] conducted a case study where erythritol TES is transported regularly between the industrial site and building because of its weakness in keeping the heat for long time. In their research, they investigated the impact of number of trips between heat source and end-user on the economic analysis up to eight trips per day.

3
Methodology

3.1 Heating Demand of Detached House

For this case study, a detached house with a floor area of 100 m^2 located in the north of Finland near the city of Oulu, was selected as the end user of transported heat. It was assumed that the house is a passive building to ease the calculation by having lower amount of heating demand and, as a result, smaller storage volume. The average annual heating need of a passive house located in Oulu is estimated to be 25 kWh/m^2a [57]. However, the average heating energy consumption of a normal building built after 2010 is 89 kWh/m^2a. This value increases according to the house construction time reaching 190 kWh/m^2a for those built between 1980-1989 [27]. As mentioned in Section 2.2, still major detached houses in rural areas rely on electricity for their heating need and it has been assumed that the studied house also utilizes direct electric heating.

3.2 Potential Industries

As mentioned in Section 2.3.2, the CCM storage charging temperature is restricted by its melting temperature as well as the onset temperature of thermal degradation. For ErNa, the melting temperature is 110 °C and the onset temperature of thermal degradation is 150 °C. Therefore, the optimal charging temperature is between 120 °C and 130 °C. If CCM storage is supposed to be charged by the excess heat of the industry, the chosen industry should have waste heat temperature above 120 °C. To determine what is the industry's unused heat amount and its temperature, pinch analysis can be used.

Potential industries are:

- Pulp and paper industry since almost half of the waste heat in Finland arises from this sector and its waste heat temperature is reported to be in in the range of 100-200 °C.
- Iron and steel plant as the waste heat temperature is mostly above 200 °C. In terms of the amount of waste heat in Finland, it is placed in the second seat after pulp and paper comprising 15% of total waste heat.

3.2.1 Pinch Analysis

Pinch analysis, also referred to as process integration or pinch technology, is a method used to minimize energy consumption in industrial processes. It involves determining the minimum amount of energy required while ensuring thermodynamic feasibility, and subsequently identifying the most efficient energy supply methods and heat recovery systems.

Processes at the industry consist of different streams that can be classified as hot and cold streams based on whether they need to be heated up or cooled down. Hot stream is the flow that needs to be cooled down for achieving lower temperature and therefore it represents

cooling demand while cold stream represents heating demand as it desires to reach higher temperature. These two streams can be drawn in a diagram of temperature-heat load to indicate how much heating and cooling the processes require (externally), if hot and cold streams could have exchanged heat internally between themselves. Industries install high-capacity heaters and coolers.

Pinch Analysis is used to determine energy targets, which identify the energy demand gap between real industrial processes and the optimal system. A minimal temperature difference, ΔT_{min}, is taken into consideration while drawing the composite curves. The smallest temperature difference between the hot and cold streams that can be accepted in a heat exchanger is defined as ΔT_{min} and the value is based upon economic factors (i.e., the trade-off between the capital cost of heat exchangers and the cost of fuel). The pinch temperature, which establishes the boundaries of the heat source and heat sink regions in a pinch analysis, is the temperature at which there is no heat flow. At the pinch point, no heat flow occurs. Heating is required above the pinch as the area above the pinch acts as a heat sink, while the area below acts as a heat source that must be cooled down by an external cooling system. The heat source for the PCM TES is essentially excess heat that cannot be utilized in industrial processes and must be disposed of by cooling.

The Grand Composite Curve (GCC) is a graphical representation of the temperature-enthalpy relationship in the stream network. It illustrates the changes in heat supply and demand during the operation. The GCC is formed by combining all the hot and cold streams of the process at various temperature intervals. In this curve, the temperatures are modified to obtain shifted temperatures, where the hot streams are reduced by $\Delta T_{min}/2$ and the cold streams are increased by $\Delta T_{min}/2$. The GCC curve has the benefit of indicating the temperature at which heating and cooling demands arise. This implies that it will be simpler to identify opportunities for waste heat utilization and heat integration. An example of grand composite curve is shown in Figure 11.The important point about GCC curve is that it does not represent the actual waste heat of the mill but rather the industrial plant where maximum energy recovery is implemented in it. Therefore, the actual waste heat of the mill is higher than the number GCC curve shows since internal heat recovery at the mill has not been optimized.

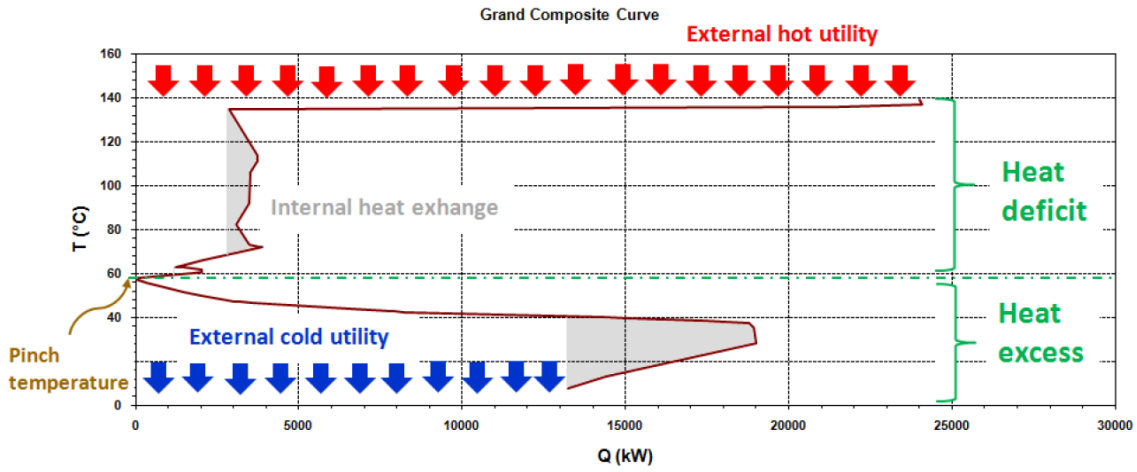

Figure 11. Example of GCC [58]

3.2.2 Iron and Steel Plant

Iron and steel industry is the most energy-intensive sector in Finland. It has a great amount of waste heat, and its temperature is high as well, making it a suitable option for utilizing its waste heat for CCM TES. To gain knowledge about heat sink at the iron and steel plant as well as its temperature range, pinch analysis of this industry should be studied. In this thesis, the pinch analysis done for an integrated steel plant located in Luleå, Sweden has been taken as the reference mill [59].

The primary components of the steel factory include of a Coke plant, a Blast Furnace, two Basic Oxygen Furnaces converters, Ladle metallurgy, and two Slab casters [59]. Coke is produced through dry distillation of coal within the coke unit. 75% (weight basis) of the coal is converted to coke and the rest is raw gas with high energy content. This raw gas is transported to the gas purification facility, where it undergoes a cleaning process. Next, in the Blast furnace where iron ore pellets and coke are put as an input, hot metal is produced alongside the generation of BF gas as a secondary product. The process of steel production involves the conversion of hot metal into steel through the utilization of two Basic Oxygen Furnace (BOF) converters, resulting in the generation of BOF gas as a secondary product. Following the ladle treatment process, the steel undergoes casting into steel slabs using two slab casters. The cast slabs undergo the process of rolling to be transformed into strip material. In this plant, process of converting cast slabs to strip material is done in some other company far from the plant industrial site.

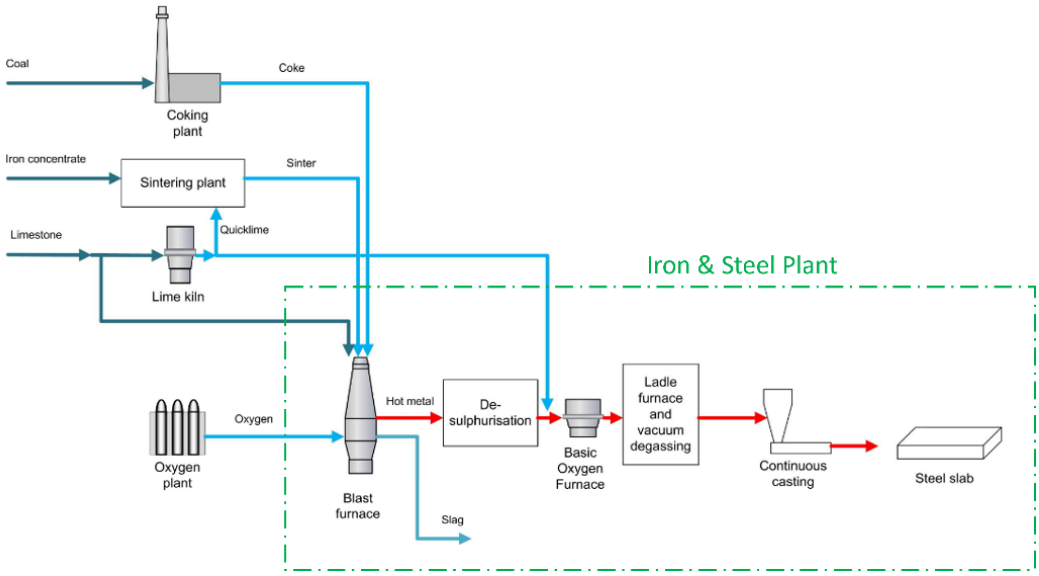

Figure 12. Process at Iron and Steel manufacturing industry

In this thesis, pinch analysis of the blast furnace and the steel plant were studied and taken as the potential industry to be integrated with thermal storage as temperature levels in this section is the highest. Moreover, these facilities are normally located in short distance from one another and thus can be taken as a one process area [59]. As reported in [59], the pinch temperature of the combined blast furnace and steel plant is approximately 200 °C. Below this temperature is the heat source which means heat cannot be used at the industrial process and therefore it is

wasted. The Grand Composite Curve of iron and steel industry (presented in Figure 13) was achieved considering ΔT_{min}=10 °K [59]. As can be seen, the heat sink amount (Q) is flat in a wide temperature range from 60 °C to 160 °C, holding 3 MW of heat. Below 60 °C, it increases drastically in a small range of temperature.

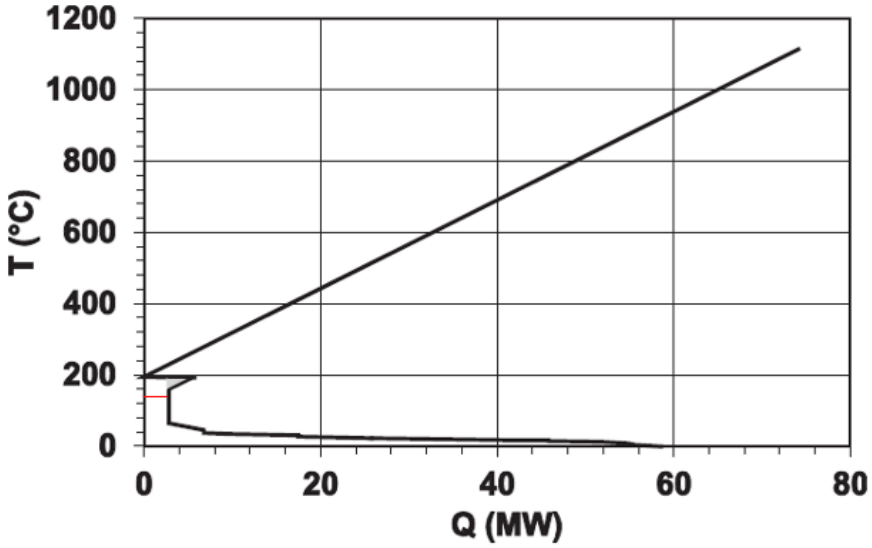

Figure 13. Grand Composite Curve of Iron and Steel industry

As discussed in Section 2.3.2, during charging of the CCM storage, the storage temperature should reach between 120 °C and 130 °C. Also, for preventing thermal degradation, charging temperature should be below 150 °C. Thus, it has been assumed excess heat at temperature of 145 °C would charge the storage. From the GCC curve, it can be observed that at this temperature level, the available heat sink is 3 MW.

In this plant, high and medium pressure steam along with hot water is used as the hot utility of blast furnace and steel plant while for the cold utility, cooling water is utilized [59]. Since this iron and steel plant is located near sea, it is utilizing cooling water to remove the excess heat. However, in some plants located far from the natural waters, a cooling tower may be used as the cold utility. As a result, utilizing the unused heat in those factories results in considerable cost saving when lowering the load of the cooling tower.

Iron and steel plant was chosen as the top suitable industry for charging CCM TES with its excess heat, however in the following, pinch analysis of another industry with high potential for this application will be investigated.

3.2.3 Pulp & Paper Industry

In Finland, Pulp and Paper industry is among the leading industries worldwide that comprise more than half of all industrial waste heat. Mechanical pulping is one of the oldest methods of pulp productions due to its simplicity and low capital cost. However, there are some drawbacks associated to it including its high electricity consumption as well as the requirement to have high-quality wood. There have been some developments to improve this method such as Thermomechanical Pulping (TMP). TMP is the most common mechanical pulp production

technology due to its high ratio of produced pulp to the used raw wood and sufficient paper strength. TMP is mainly used for newspaper and magazine production. Due to a decline in demand for these print materials, many TMP mills are being shut down. However, as my research team had access to data on a TMP mill, I chose to investigate whether this specific type of pulp and paper production could be integrated with ErNa TES.

Major electricity consumption of TMP, as high as 80% of it, arises from the refining process where transformation of wood chips to fibers is done by mechanical motors [60]. At first, chips exiting the chipper are fed into the refiner which consist of a stationary disc and rotating disc operating with electric motor. Dilution water that is injected to the refiner along with the operation of plates crush the wood chips and produce pulp out of them. The output of refiner is pulp mixed with steam which is generated from moisture content of the chips as well as from dilution water evaporation. Next pulp is separated from the steam in the cyclone from which steam is utilized to meet the heat requirement in the drying section of paper mill [61].

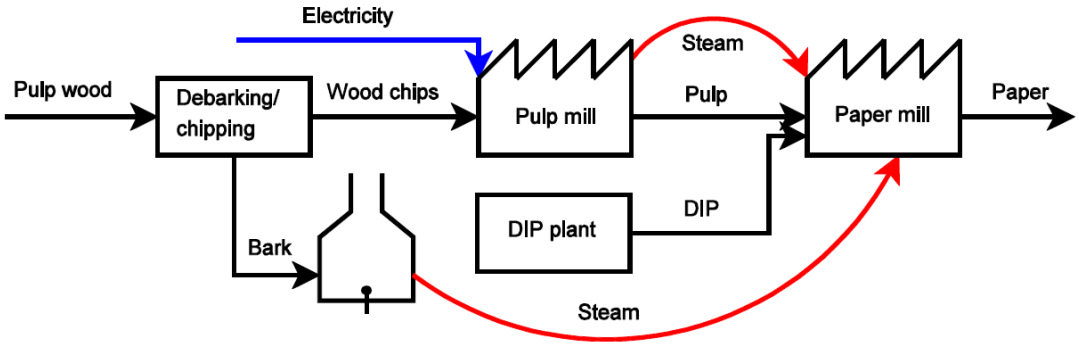

Figure 14. Schematic process in Thermomechanical Pulping including pulp and paper mill and de-inked pulp plant

A pinch analysis done for a Swedish TMP and paper mill comprising three TMP lines, two de-inked pulp (DIP) and three paper mills as the general schematic is provided in Figure 14 [62]. In the de-inked pulp plant, ink of paper fibers produced from recycled papers is removed. Pinch Analysis result indicated that the pinch is approximately in the range of 53 °C and 72 °C based on two different pinch analysis methods (Heat Load Model (HLMPP) and Detailed pinch analysis) and assuming individual minimum temperature difference [62]. The GCC curve of the studied TMP mill is shown in Figure 15. Heat sink in the industry is in temperature levels below pinch temperature, and for TMP mill, this level is below approximately 53-72 °C.

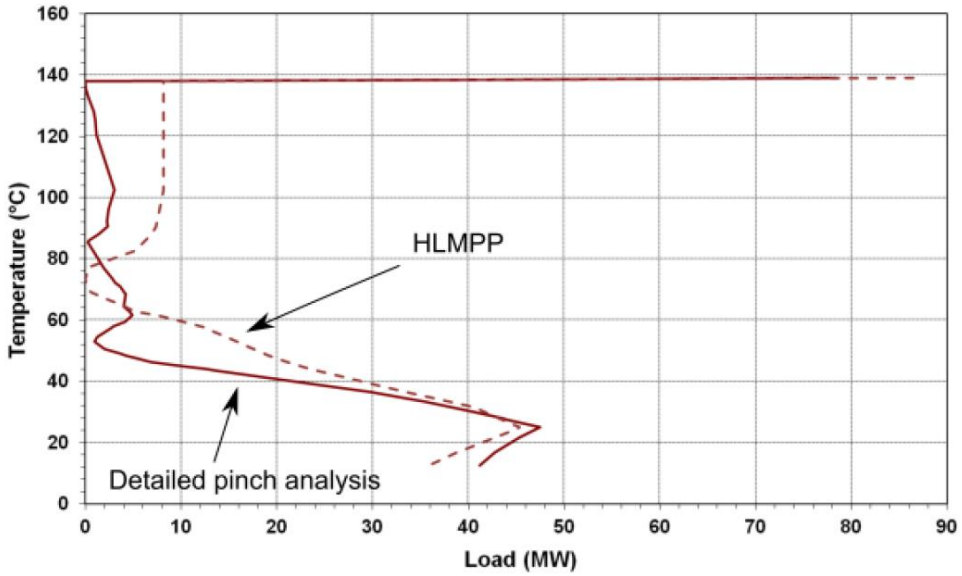

Figure 15. Grand Composite Curve of Thermomechanical Pulp and Paper

For utilizing excess heat from the TMP mill for charging the ErNa storage, industrial heat pump should be included in the system since for charging the TES, heat at minimum temperature of 110 °C is required. As shown in the pinch analysis, at the excess heat from the TMP mill is at much lower temperature levels. To increase the temperature of excess heat from the process so that it can be used for charging the ErNa TES, an industrial heat pump is necessary. The schematic of the system, Figure 16, indicates how the unused excess process heat goes through in the industrial heat pump (the evaporator section) and after its increase in heat pump's compressor, the high temperature heat from the heat pump's condenser side is transferred for charging the TES.

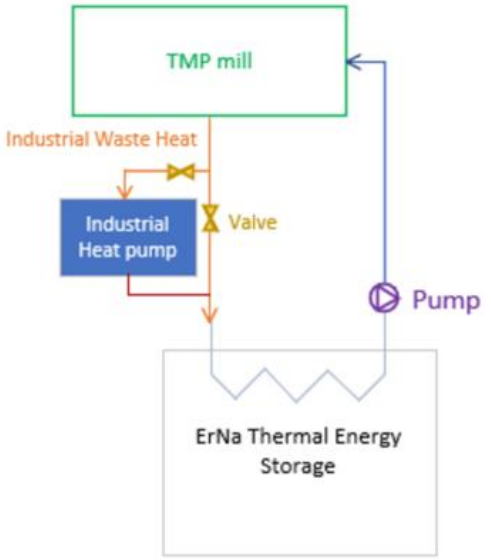

Figure 16. Schematic of charging ErNa heat storage with industrial waste heat of thermomechanical pulp mill

The investment cost of industrial heat pump is quite high, typically in the range of 250-900 €/kW [16]. Therefore, to reduce the cost and increase the profitability of the whole storage

system, it was decided to choose the unused heat of iron and steel plant for transportation to the house.

In future studies, if it was decided to transfer the heat of TMP mill to the house, the investment cost of heat pump as well as the electricity consumption of it should be considered in the economic assessment. It should be noted that electricity prices at the industry are lower because of lower tax rate. It has been reported that in 2021, the average electricity price for industry in Finland was 67.6 €/MWh [63] while the value for households was 87 €/MWh.

3.3 Storage Models

In this study, a cylindrical tank was selected as a suitable storage unit due to its convenient transportability and ease of relocation. The storage tank is assumed to have a constant ratio between its height and its cross-sectional area across all storage models and units. The material of the storage unit is stainless steel due to its high thermal conductivity.

As discussed earlier, the arrangement of a heat exchanger has a direct influence on the quantity of heat that is charged, discharged, reheated and supercooled. ErNa-80 TES prototype set-up indicated enhanced energy efficiency by using a finned tube heat exchanger, which greatly improved thermal conductivity. Therefore, this study assumes the utilization of a finned tube heat exchanger within the storage tank. The key distinction between the storage unit in this study and the prototype is the temperature at which the heat is discharged. In the case of space heating for a dwelling, a discharge temperature of 30 °C can be sufficient [41]. Decreasing the discharging heat temperature enhances storage efficiency by increasing the discharge heat [38]. The heat exchanger that is considered and determined in each storage model has copper fins with steel tubes. Some properties of these two materials that were utilized for achieving results are listed in Table 2.

Table 2. Some properties of Steel and Copper

Parameter	Value	Unit
Density of Steel	7750	kg/m^3
Specific heat capacity of Steel	500	J/kgK
Density of Copper	8960	kg/m^3

3.3.1 Storage Model 1: Mobilized ErNa TES(s)

3.3.1.1 One-time Transportation

ErNa, used as the cold crystallization material thermal storage, exhibits exceptional latent heat storage efficiency, maintaining its effectiveness for up to nine months when stored within a temperature range of 0 to 10 °C. Consequently, it holds the potential to store the annual heating requirements of a house, especially when charged during the warmer months when space heating demands are minimal.

The primary benefit of cold-crystallization material storage is its ability to store latent heat over extended periods, whereas sensible heat remains usable only for a short duration, typically a matter of hours. When charging the heat storage system during the summer, it must be followed

by a supercooling process; otherwise, the stored heat gradually dissipates to the surroundings, leading to premature crystallization. The required amount of ErNa needed to fulfill the annual heating needs of a house can be calculated according to Eq. 2:

$$V_{CCM} = \frac{E_{th,house}}{\Delta H_{cc}} \quad (2)$$

Where V_{CCM} is the required volume of the cold crystallization material for supplying the heat (m^3), $E_{th,house}$ is the annual heating demand of the house (kWh) and ΔH_{cc} is the volumetric cold crystallization enthalpy, which is the amount of energy released during crystallization of material per volume of the material (kWh/m^3_{ccm}).

The CCM should not fill all the volume of the tank because there should be some space for placing heat exchanger inside the container. As discussed in [41], CCM can occupy maximum 80% of the TES and the rest of the volume would be kept for heat exchanger and safety considerations. Therefore, it has been assumed $V_{CCM}/V_{cont} = 0.8$ where V_{cont} is the storage tank volume (m^3) and can be achieved simply.

Volumetric energy density of ErNa has been reported as 200 MJ/ m^3. This number quantifies the total amount of energy that the storage system may receive as an input, including both sensible heat and latent heat. The heat that can reach to the storage depends on the thermal conductivity of container. Therefore, Eq. 3 determines the amount of charging heat per volume of the container.

$$Energy\ Density = \frac{E_{charge}}{V_{Cont}} \quad (3)$$

Where E_{charge} is the total charging heat (kWh). Figure 8A displayed a graph illustrating the variation in enthalpy at each stage of the ErNa-80 storage system's operation, from charging to discharging with the use of a finned tube heat exchanger. Thus, by extending the findings from this prototype to the larger storage system needed to fulfill the heating needs of the house, the enthalpy changes at each stage of the storage can be calculated.

<u>Stage 1:</u> Charging at the Iron and Steel Plant

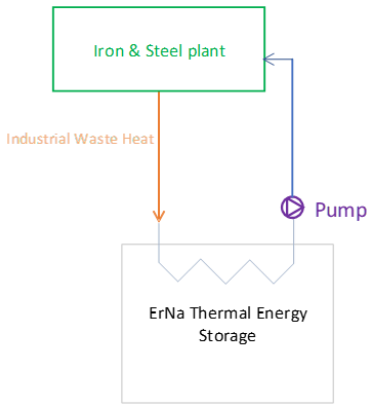

Figure 17. Schematic of Charging ErNa TES at the industry

As mentioned in Section 2.3.2, the recommended charging temperature range is from 110 °C (the temperature at which the substance melts) to 150 °C (the temperature at which thermal degradation begins). Given that the pinch temperature of the iron and steel mill is 200 °C, it is a favorable combination to integrate this industry with ErNa storage. The sizing of the heat exchanger is crucial for determining the appropriate temperature to feed into the storage. A greater temperature differential between the initial heat input and the ultimate temperature of the storage, results in a reduced requirement for heat transfer area in order to exchange an equivalent quantity of heat. In order to achieve a storage temperature of 130 °C after fully charged, a higher temperature of 145 °C was chosen for the steel plant to account for any extra heat. According to Figure 13, temperature of 145 °C corresponds to a heat flow rate of 3000 kW. It is presumed that the heat exchanger within the TES is capable of transferring all this heat flow rate. Given the use of heat exchangers in the industry for cooling surplus heat using cooling water, it is presumed that in this model, only one heat exchanger is positioned within the TES to store the heat within the TES material. The formula used to determine the size of heat exchangers is indicated by Eq. 4.

$$A = \frac{Q}{U \Delta T_{LM}} \tag{4}$$

Where Q is the heat flow rate inside the heat exchanger (W), U is the overall heat transfer coefficient (W/m^{2}K) and ΔT_{LM} is the logarithmic mean temperature difference between hot and cold fluid. The overall heat transfer coefficient is a function of the convective heat transfer of cold and hot fluids as presented in Eq. 5.

$$\frac{1}{U} = \frac{1}{h_h} + \frac{1}{h_c} \tag{5}$$

Where h_h and h_c are the convective heat transfer coefficient of hot and cold fluid (W/m^{2}K), in this case industrial waste heat and ErNa respectively. This analysis assumes that the industrial waste heat stream used to charge the storage is in the form of steam, with a convective heat transfer coefficient of 10000 W/m^{2}K [64]. To simplify matters, the heat transfer coefficient of ErNa was considered to be equivalent to that of pure erythritol, which is 398 MW/m^{2}K [65]. ΔT_{LM} for countercurrent flow is calculated according to Eq. 6.

$$\Delta T_{LM} = \frac{\left(T_{h,in} - T_{c,out}\right) - \left(T_{h,out} - T_{c,in}\right)}{\ln\left(\frac{T_{h,in} - T_{c,out}}{T_{h,out} - T_{c,in}}\right)} \tag{6}$$

Where $T_{h,in}$ and $T_{h,out}$ are inlet and outlet temperature of hot fluid and $T_{c,in}$ and $T_{c,out}$ are inlet and outlet temperature of cold fluid, respectively. During charging of the ErNa heat storage, $T_{h,in}$ is the temperature of industrial excess heat stream flowing directly in the tube of heat exchanger while $T_{c,in}$ is the initial temperature of ErNa when charging begins. $T_{h,out}$ is the

temperature that industrial heat reaches after giving its heat to the CCM and $T_{c,out}$ is the final temperature of ErNa after being completely charged.

Finned tube heat exchangers are installed within the storage units of all storage models to facilitate heat transfer and allowing all the heat gains and losses. The tubes extend vertically along the entire height of the storage tank. Figure 18 displays the chosen finned tube heat exchanger together with its dimensions.

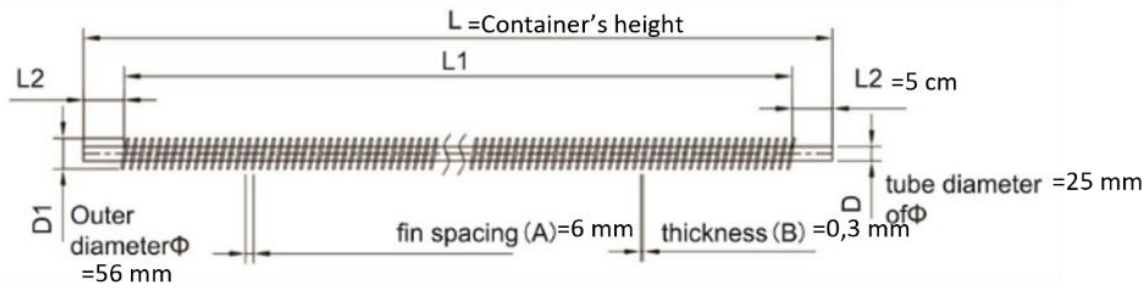

Figure 18. Selected Finned Tube

The finned tube heat exchanger enhances the heat transfer surface area in comparison to a conventional shell and tube heat exchanger. With conventional heat exchangers, the heat transfer area is limited to the lateral surface area of the tubes. However, with finned tubes, the additional surface area of the fins is also taken into account. The heat transfer area of the finned tube is expressed by Eq. 7.

$$A_{finned-tube} = \pi DL + \frac{\pi}{4}(D_1^2 - D^2) \times n_{fin} \quad 7$$

Where D is the tube's diameter (m), D_1 is the outer diameter of fins (m), L is the length of tube (m) and n_{fin} is number of fins on the tube. The number of fins on the tube can be calculated according to Eq. 8.

$$n_{fin} = \frac{L_1}{a} \quad 8$$

Where L_1 is the length of the tube that has fins and a is the space between each two fins. The number of finned-tubes required to meet the necessary heat transfer area in the storage unit can be simply determined by Eq. 9.

$$n_{finned-tube} = \frac{A}{A_{finned-tube}} \quad 9$$

The 3-D model of storage unit with heat exchanger placed in it is provided in Figure 19. In all storage models, it has been assumed all heat power available at the industry at 145 °C (3000 kW) is utilized for charging. When instead of one single TES unit, multiple TES units are charged simultaneously, this heat power is divided by the number of TES units.

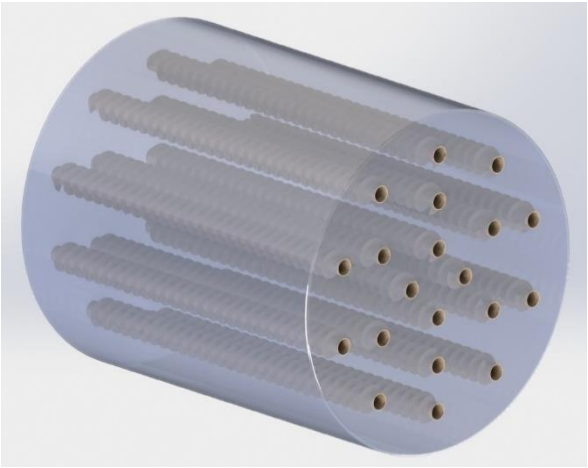

Figure 19. 3-D model of the Storage unit with its heat exchanger

Stage 2: Supercooling

In order to achieve long-term storage, it is necessary to cool ErNa to a temperature that is close to its glass transition temperature. As a result, in this procedure, most of the acquired sensible heat would be lost. In order to maximize energy efficiency and minimize cooling costs, it has been determined that the heat is directed towards industries requiring heating within the temperature range that requires supercooling (from 130 °C to 5 °C). Food industry is one of the sectors which has the heating demand at low temperatures.

Beer production is a highly energy intensive process, with 59% of the energy consumed being in the form of heat [66]. Finland ranks 21st in consumption of beer per capita with an annual intake of 72 liters making it among the most widely consumed beverages [67]. There are local breweries throughout Finland. Beer brewing procedures require a heat source that operates at a reasonably high temperature. Schematic of processes done in brewery is presented in Figure 20. At the beginning, malt and water are mixed and then they are combined with the mixture of rice and steam in the mash converter. In the process of combining, low pressure (LP) steam is used to increase the temperature to 78 °C. In Lautertun, wort is separated from the solid mash and once again steam is used as the hot utility to increase the wort temperature to 90 °C. The clarified wort undergoes an energy intensive boiling process with steam in the wort kettle. After being clarified in whirlpool, it is cooled down to 13 °C by cooling water to be prepared for subsequent fermentation stage.

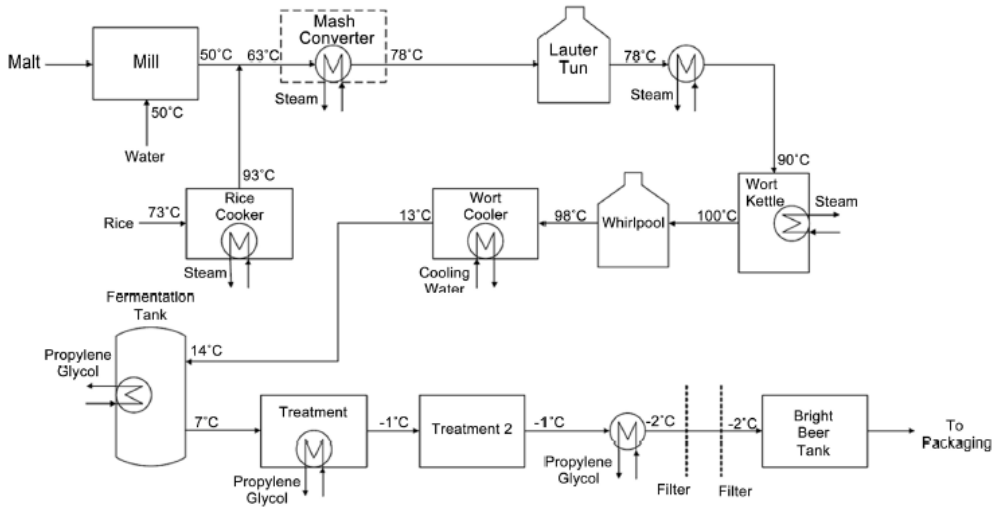

Figure 20. Brewing Process [68]

A Pinch analysis conducted for a brewery has revealed that the pinch temperature is 68 °C [68] and heat demand, which is above the pinch, falls within the temperature range of 68 °C to 110 °C (shifted). Hence, a portion of the heat generated during supercooling can be effectively used as the brewery's hot utility. The brewery process GCC for $\Delta T_{min} = 10°C$ is shown in Figure 21 from [68]. ErNa TES as the industry's hot utility is marked in the diagram along with the GCC of the brewery. It can be seen that according to the size of the heat exchanger placed in the TES, supercooling heat of ErNa TES is able to meet a portion of the brewery's heat power requirement, about 963 kW. The remaining heat power must be supplied by the hot utility of the brewery plant. For transferring the heat of the ErNa TES to the brewery, it was assumed that water flows inside the tube of storage's HX and absorbs the heat. According to Figure 21, the temperature of the thermal energy storage (TES) decreases from 130 °C to 73 °C during the heat exchange process.

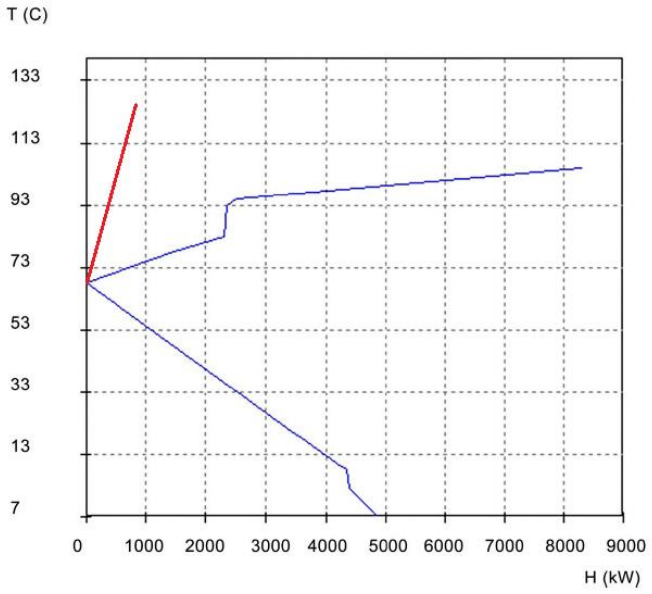

Figure 21. Grand Composite Curve of Brewery drawn in blue along with marking the ErNa Storage as its hot utility drawn in red

Nevertheless, despite transferring the supercooling heat from the CCM to the brewery, the process of supercooling is not fully achieved as ErNa temperature is much higher than glass transition temperature. An industry that requires low temperature heat is the dairy sector. A pinch analysis was conducted for the milk processing section at a dairy factory in Iceland, revealing a pinch temperature of 4 °C [69].

In the milk processing section, the process begins with the transfer of stored raw milk in batches to a buffer tank. From there, it is directed to the regeneration section, where it undergoes a controlled heating process. This heating serves multiple purposes, including the separation of whole milk, light milk, and skimmed milk, achieved by carefully managing the cream content. After homogenization, the milk undergoes a two-step heating process. First, it is heated through recovered heat in the split regeneration, and then it is further heated to pasteurization temperature (76°C), this time using hot water. The milk then proceeds through a holding tube, ensuring full pasteurization. Following pasteurization, the sequence continues as the milk is cooled to 8°C within the regeneration system by the incoming homogenized milk. The final step involves further cooling, taking the milk to a temperature of -3°C, accomplished using a glycol mix [69]. The schematic of all the processes is presented in Figure 22.

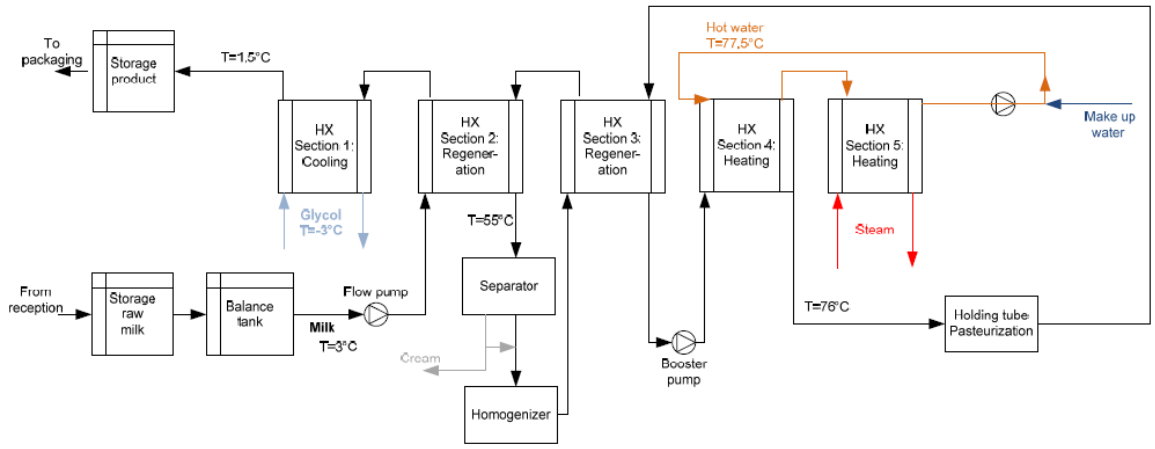

Figure 22. Processes in the Milk Processing [69]

The GCC of the milk processing along with the curve where CCM storage acts as the hot utility is presented in Figure 23 . It was explained that when supplying the heat of brewery with the supercooling heat of the ErNa storage, the ErNa reaches temperature of 73 °C. Very good insulation for storage and thus negligible heat loss and temperature drop while travelling from brewery site to the diary plant were assumed. Upon arrival at the dairy facility, heat at temperature of 73 °C can be supplied. By taking into account ΔT_{min}=2 °C [69], the TES's supercooling heat can cover 86 kW of heat. The remaining heat requirement of 27 kW is still dependent on external hot water.

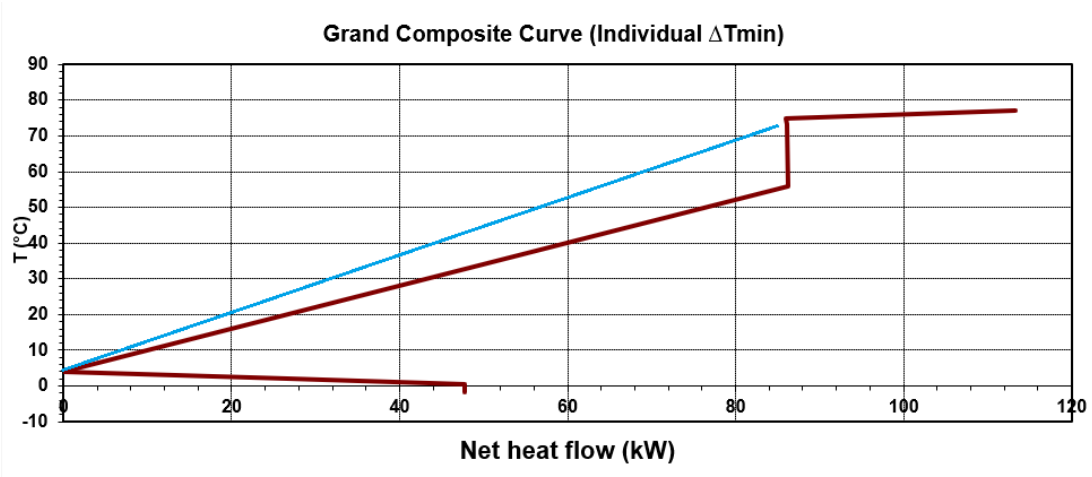

Figure 23. Grand Composite Curve of milk processing along with marking the CCM Storage as its hot utility [69]

Similar to utilizing the ErNa supercooling heat in brewery, in milk processing, water flows inside the heat storage's heat exchanger. At the dairy plant, TES's temperature drops from 73 °C to 5 °C while providing 86 kW of the milk processing plant's heating need. Following the heat exchange process, TES is ready to be transferred to the residential site. The temperature change during transit was assumed to be negligible, resulting in the material retaining a temperature of 5 °C upon arrival at the house.

Stage 3: Storage

To maintain long-term stability during the storage phase, it is essential to keep the CCM within a temperature range of 0 to 10°C. When the material is charged during the summer and discharged during cold months, it must be stored at very low temperatures for extended periods. Creating a refrigerated space for the CCM TES can be excessively costly. As a cost-effective alternative, one feasible approach for maintaining the storage at the designated temperature range is to place the storage underground. In Finland, at depths ranging from 10 to 150 meters underground, the ground temperature typically ranges between 2 and 6°C, depending on the specific location. In northern Finland, near the city of Oulu, the temperature within this depth range remains consistently about 3-4°C [70].

Stage 4: Reheating

Reheating is performed to trigger the crystallization and discharge of the TES. Therefore, it should be carried out immediately prior to the start of the building heating demand. Unfortunately, it is not feasible to transport the TES back to the industry for reheating using industrial waste heat due to the crystallization and heat release that occurs once the reheating is complete. Additionally, a portion of the heat would be lost during the transfer of the TES back to the house. In order to mitigate this problem, it is necessary to perform the reheating at the building site. It has been decided to reheat the TES with direct electricity heating as in the studied remote house, there is no other heating source installed. In the storage tank, heating element should be placed by which reheating can take place.

Household's electricity voltage is 220 V, and assuming maximum current dedicated for reheating is 25 A, then the maximum electricity power with which CCM material can be heated up is 5.5 kW. When one large TES unit is placed to supply the entire annual heating of the house, the demand for reheating is significant. Therefore, it takes days to complete the reheating process. To address this issue and reduce the time and perhaps the cost of reheating, the impact of dividing the storage into multiple units was investigated, as will be discussed in the Results Section. The higher the number of TES units, the shorter the time for reheating each unit. This makes it possible to do the majority of reheating during the night when electricity prices are very low, sometimes even below zero.

Stage 5: Discharging

Discharging of heat starts when crystallization begins. In other words, latent heat that was stored in the material starts to be released when crystallization begins. The sizing of the CCM TES volume was done in a way that released heat fulfills the annual heating demand of the house. Fortunately, when heat at low temperature is needed, discharge of heat can be done gradually and therefore release of heat can theoretically take place for months. For transferring the heat of CCM storage to inside the house, the water that flows inside the house's radiators flows inside the finned tube heat exchanger inside storage. For space heating, it has been assumed the temperature of 30 °C is needed for outlet water from HX. As in the building there are some heat exchangers installed, it has been assumed no more heat exchangers will be placed in the building and the existing ones are adequate for this model.

In Figure 24, schematic of the storage model 1 has been displayed starting from transportation of the fully charged ErNa TES from iron and steel plant to the brewery and dairy plant for completing supercooling and ultimately to the end-user, a detached house, for discharge.

Figure 24. Schematic of storage model 1

3.3.1.2 Multiple Transportation Rounds

One case study for transferring the surplus heat of industry to buildings is to perform charging the ErNa TES at the iron and steel plant several times during a year. This approach results in a decreased amount of ErNa material and a reduced storage tank scale. It can be assumed that the first charging is done during beginning of June when there is no heating demand at the building. A few months later, when all the stored heat is utilized for house's heating, the storage is taken out for the second round of charging and returned to the house after being charged at the iron and steel mill, as illustrated in Figure 25. This procedure can continue depending on

the storage size. With smaller TES size, the frequency of commuting between the industry and the house increases.

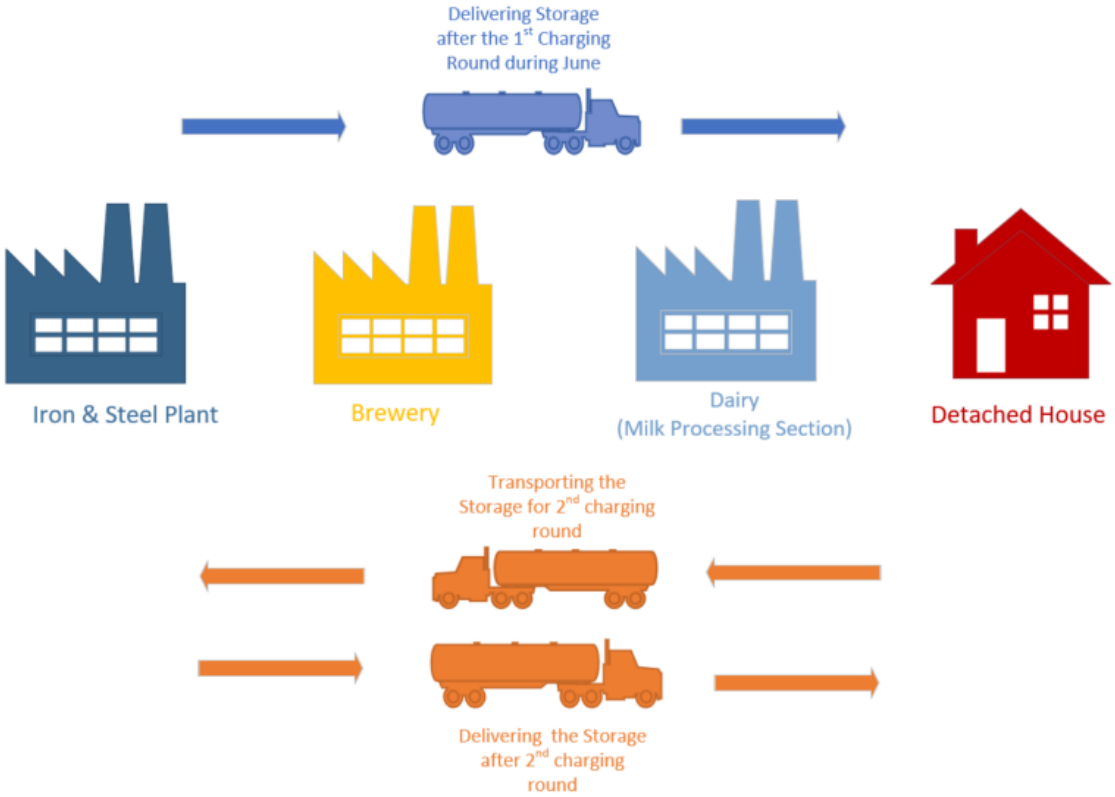

Figure 25. Multiple Transportation round model

One advantage of this case study is that when number of trips increases, there is a higher likelihood of selling heat to brewery and dairy facility because they might not purchase heat once a year while they still heavily rely on their own hot utilities. Reheating is also performed several times a year and takes shorter time to be completed in each cycle. This impacts the reheating cost with electricity as the price of electricity varies in different months.

3.3.2 Storage Model 2: Cascade ErNa TES(s)

The major issue within storage model 1 is the extensive use of electricity for reheating ErNa TES. Furthermore, the assumption of completing the supercooling at other industries, such as brewery and milk processing, may not be very practical as they do not receive a continuous supply of heat and still rely on their own hot utility. Therefore, it is unlikely that they would be interested in purchasing this heat. Therefore, in this section, new mobilized heat storage model is proposed. The schematic of storage model 2 is presented in Figure 26 and the model will be explained in detail in the following.

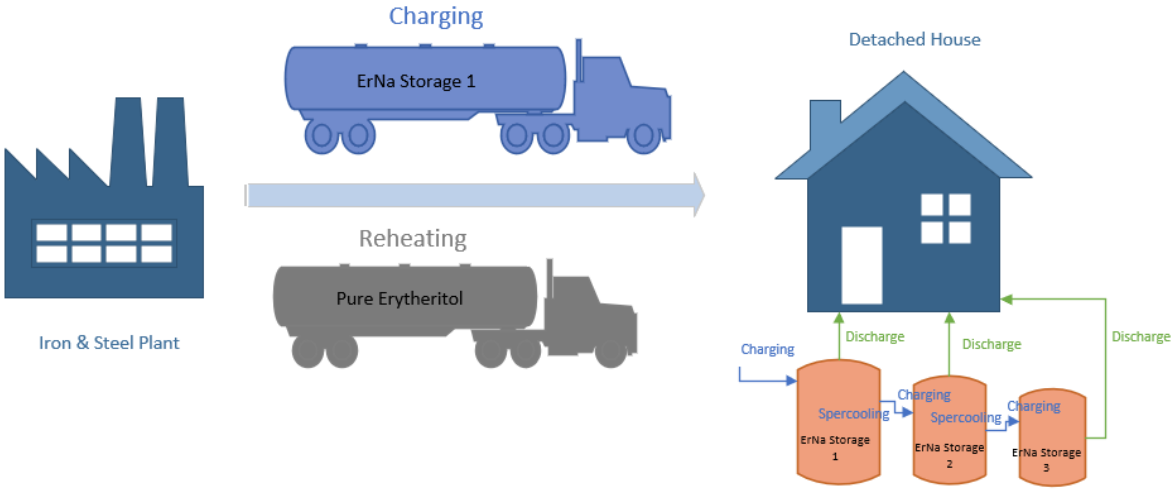

Figure 26. Schematic of the whole model for cascade ErNa TES system (storage model 2)

Stage 1&2: Charging & Supercooling

This model consists of multiple ErNa units interconnected by pipes, allowing the supercooling heat from one unit to be transferred and used to charge the subsequent unit in a continuous manner as shown in Figure 26. The ErNa storages are placed underground and the biggest one (Storage 1) is charged at the industry and has the capacity for delivering the heat which is sufficient for charging other ErNa units. It has been assumed that ErNa heat storage 1 reaches a temperature of 150 °C, which is the highest charging temperature that ErNa can undergo (below thermal degradation). Storage 1 is transported directly to the house and releases its supercooling heat to storage unit 2 via the heat transfer fluid. It has been assumed storage unit 2 charges to 135 °C and storage unit 3 reaches 123 °C when completely charged. This procedure continues until all units are fully charged. For sizing the heat exchanger, it has been assumed during charging process of TES unit 2 and 3, there is a temperature difference of 5 °C between inlet fluid (hot side) and final temperature of TES (cold side), and a temperature difference of 2.5 °C between the outlet fluid and initial temperature of TES. The Charging heat of each unit except unit 1 can be calculated according to Eq. 10.

$$E_{charge,i} = E_{supercool,i-1} \tag{10}$$

Where index i is the storage number. The discharging heat of all units, after crystallization, should be equal to the annual heating demand of the house as shown in Eq. 11.

$$\sum_{i=1}^{n} E_{discharge,i} = E_{th,house} \tag{11}$$

Moreover, the charging heat of each units is equal to the supercooling heat of previous unit as expressed in Eq. 12.

$$E_{charge,i} = E_{supercool,i-1} \tag{12}$$

Based on the data obtained from Figure 8, for the ErNa prototype Unit A (which includes an ErNa TES with a finned tube heat exchanger), it can be determined that the ratio of supercooled

heat to the charging heat is approximately 0.83. If we assume that this ratio remains constant for all units regardless of their size, then Eq. 13. can be implemented for each unit.

$$\frac{E_{supercool,i}}{E_{charge,i}} = 0.83 \tag{13}$$

By combining Eq. 10-13, Eq. 14 is achieved from which the heat that needs to be put in TES unit 1 (the transportable unit) from waste heat is obtained.

$$E_{charge,1} = \frac{\sum_{i=1}^{n} E_{charge,i} - E_{th,house}}{\left(1 - 0.83^{n}\right)} \tag{14}$$

After obtaining charging heat of ErNa TES unit 1, the supercooling heat of unit 1 is achieved from Eq. 13. Eq. 10 can then be used to calculate the charging heat of unit 2 based on supercooling heat of unit 1. This procedure continues until all the heating values are acquired. Similar to Section 3.3.1, the volume and mass of ErNa and volume of storage tank can be calculated according to heat gains and losses in each ErNa unit. In Section 4.3, a case study wherein three ErNa storage units supply the heat of the house has been brought and discussed in detail.

When the fully charged storage 1 is connected to the piping network at the building site, water from the water tank is pressured by the pump and flows through the heat exchanger of ErNa storage 1. During this process, valves 2 and 6 are closed and valves 5 and 1 are open. The flowing water extracts heat from ErNa storage 1 and transfers it to ErNa storage 2. The opening of valve 3 permits the circulation of cold water back to the storage, resulting in a continuous flow throughout the system until ErNa TES 1 reaches complete supercooling and ErNa TES 2 is fully charged. During the next stage, ErNa storage 2 undergoes supercooling, resulting in the transfer of its heat to ErNa storage 3. In order to achieve this, valve 3 is shut while valves 4 and 7 are opened, facilitating the cascade heat transfer and water circulation for the purpose of transmitting heat until the entire heat exchange process is completed. For supercooling the last unit, ErNa TES 3, water is circulated to finish the supercooling process. Afterwards, the hot water is stored in a water tank, where it releases its heat either to the ground or is discharged from the system through a drain valve.

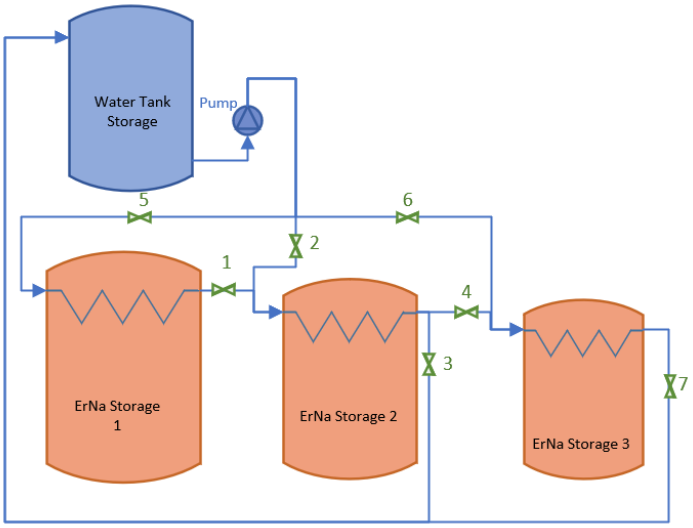

Figure 27. Charging and Supercooling of Cascade ErNa TES model

To enable using one single heat exchanger placed in each TES unit for both charging and supercooling, the ratio of logarithmic temperature difference between the hot and cold sides during charging to that of supercooling needs to be 0.83, according to Eq. 13. Hence, during the supercooling stage, the temperature difference between the inlet fluid (cold side) and the final temperature of TES (hot side) has been assumed to be 3 °C. As a result, temperature difference of 7 °C was achieved between the outlet fluid and the initial temperature of TES.

The charging time of each unit, which is equivalent to the supercooling time of the previous unit, is set to the maximum time that supercooling can take place without occurrence of crystallization in it. It was reported that the critical cooling rate in ErNa storage with finned tube heat exchanger is in the range of 0.04-0.9 °C/min, with the recommended value of 0.3 °C/min [41]. Therefore, supercooling time of 6.7 hours has been assumed in this study. Within this time and the energy required for each TES unit's supercooling, the heat transfer rate can be achieved, and finally by assuming convective heat transfer coefficient of water approximately 6000 W/m^{2}K [71], the required heat transfer area for HXs of ErNa TES unit 2 and 3 was determined.

For determining the required flowrate of the circulating fluid, in this case water, we identified the maximum heat transfer rate during charging and supercooling, as well as the temperature difference experienced by water during this process. Using the specific heat capacity of water (4186 kJ/kgK), we were able to obtain the mass flow rate, which was found to be 0.53 kg/s based on our assumptions. To enable providing this flow rate during the supercooling period, 8.5 tonnes of water should be placed in the water tank.

Stage 3, 4 & 5: Storage, Reheating & Discharging

Similar to storage model 1, all ErNa TESs are kept underground to maintain low temperatures. Prior to the onset of the house's heating demand, reheating is required. For storage model 2, the ErNa TESs reheating was assumed to be accomplished with excess process heat from an industrial plant instead of using direct electric heating. For transporting the heat to the house,

charging and transporting pure erythritol TES was assumed. The decision to choose this PCM TES was based on its cost-effectiveness compared to ErNa, its high energy density and ability to retain heat during transportation from the industry to the household. In pure erythritol TES, when storage is discharged, both latent heat and sensible heat are simultaneously released. Therefore, for determining the required amount of erythritol, Eq. 15 was used.

$$E_{reheat} = m_{Er}\left[C_{p,Er(l)}(T_{m,Er} - T_i) + L_{f,Er} + C_{p,Er(s)}(T_f - T_{m,Er})\right] + m_{Er}C_{p,tank}(T_f - T_i) \quad 15$$

In which $C_{p,Er(l)}$ is erythritol's specific heat in the liquid phase (kJ/kgK), $T_{m,Er}$ is erythritol's melting temperature (°C), $L_{f,Er}$ is the latent heat of fusion (kJ/kg), $C_{p,Er(s)}$ is erythritol's specific heat in solid phase (kJ/kgK), T_i is the storage temperature before charging (°C), T_f is the storage temperature after being fully charged (°C), and $C_{p,tank}$ is the specific heat capacity of storage tank's material (kJ/kgK), in this study stainless steel. Eq. 15 indicates that part of the heat that is put as the input is stored in the steel storage tank. The heat stored in the steel tank is significantly smaller than the heat stored in the PCM material due to its lower specific heat capacity and lower mass. It is noteworthy that during the discharge of erythritol TES, the heat stored in the tank is also released for reheating the ErNa storages. This study neglects the heat loss of the storage tank resulting from the temperature difference with its surroundings. Some properties of Erythritol are listed in Table 3.

Table 3. Thermophysical Properties of Erythritol [46], [56]

Parameter	**Value**	**Unit**
Density	1420 at 20 °C 1300 at 120 °C	kg/m^3
Specific Heat Capacity	1.35 at 20 °C (Solid) 2.7 at 140 °C (Liquid)	kJ/kgK
Melting temperature	118	°C
Melting Enthalpy	339	kJ/kg

When erythritol TES arrives at the residential site, it is connected to all ErNa storages via pipelines and pressurized water transfers erythritol's stored heat to ErNa storages. As shown in Figure 28, erythritol TES is placed after the water tank and water passes through the erythritol TES's heat exchanger, where it is heated before flowing through all ErNa storage units' heat exchangers. This process continues until all ErNa TESs reach the cold crystallization temperature of approximately 50 °C. The reheating process of the smallest ErNa storage is completed earlier than the other two; consequently, valve 3 is closed to stop the flow of water in ErNa storage 3. In the same manner, valve 2 is closed when ErNa TES unit 2 is fully charged. Upon full reheating of all three units, the pump is shut down, and each unit releases the heat to the house whilst being crystallized.

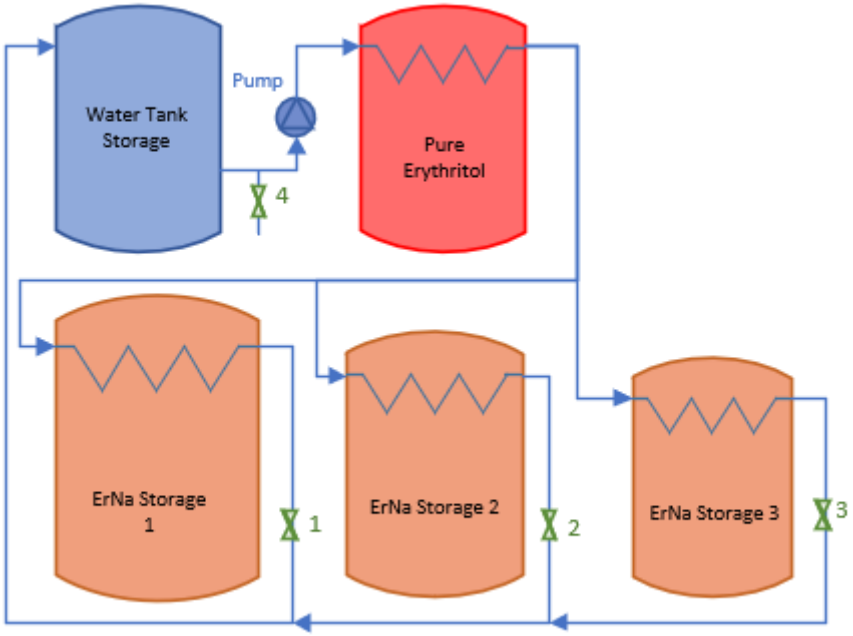

Figure 28. Reheating system of storage model 2

3.4 Possible Locations for Implementing Storage Models

This section presents potential places for implementing the proposed storage models. In Raahe, a city on the west coast of Finland, the SSAB Company has a steel plant. The factory is an area of about 500 hectares in size and their main products are hot-rolled sheets and coil products. Two blast furnaces produce pig iron, which is refined into steel in a steel smelter. Molten steel is used to make steel blanks, which are rolled into products in a hot rolling mill. The factory area also has a coke plant, a power plant, its own harbor and one of Finland's largest laboratory facilities [72].

Valio, Finland’s largest dairy producer, has a production site in Oulu. At this site, raw milk is processed into milk, ice cream and sour milk products. Raw milk mainly comes to the factory from dairy farms in Oulu's surroundings, on average within a radius of 100 kilometers. In the north, the milk is collected for the factory along the Oulujoki river. Annually, the factory processes over 70 million kilograms of raw milk into processed products [73]. Moreover, there are many local breweries all around the Finland and in Oulu there are also some breweries. Näilo Brewing Co and Sonnisaari Panimo are small craft breweries that can be potential customers for storage model 1.

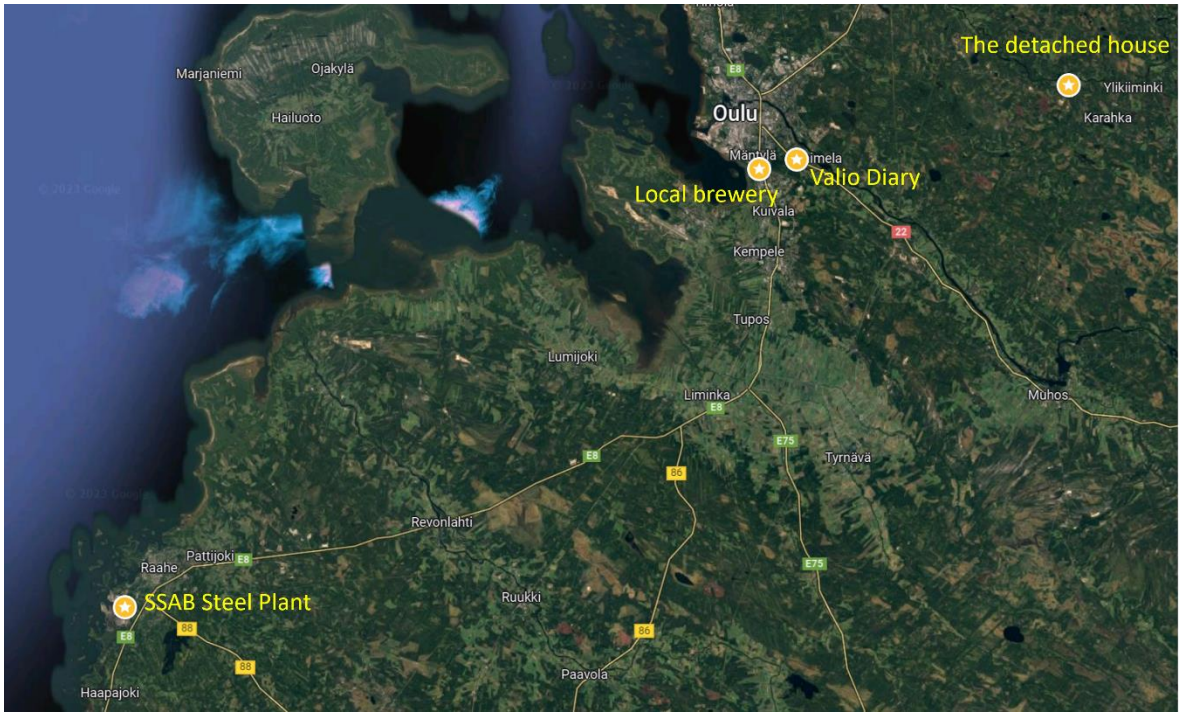

Figure 29. Location of potential industries for charging ErNa and selling out the heat of supercooling

In Figure 29, the location of SSAB steel plant, Valio dairy factory, the local breweries are marked. The detached house location is hypothetical; however, it is situated in Vesala, a suburb in close proximity to Oulu. The driving distance from steel plant to brewery, dairy plant and eventually to the detached house is about 110 km. It is important to note that the data utilized for calculations to obtain results are not specific to these factories, but rather derived from literature sources.

3.5 Economic Assessment

In order to assess the cost efficiency of a technology, certain metrics can be employed. Typically, costs can be categorized into two primary types: capital costs, also known as CAPEX, and operational and maintenance (O&M) costs, also referred to as OPEX. Capital costs refer to the initial investment required for purchasing equipment and installation. On the other hand, O&M costs are recurring expenses incurred over the lifespan of the equipment, which might fluctuate over time, such as electricity and fuel costs.

The capital costs in this research study include the expenses for the storage tank, PCM material, heat exchanger, and the cost of placing the storage underground. These costs are incurred at the beginning and are only paid once over the lifespan of the storage system. Conversely, the expenses related to transportation and reheating of CCM storage using electricity are classified as operation and maintenance expenditures. These costs are incurred on an annual basis and might fluctuate depending on economic factors such as inflation. Nevertheless, they are regarded as fixed in this analysis within the operational timeframe of the storage system.

By collecting excess heat from industrial processes to charge the TES, the industrial cold utility responsible for dissipating this excess heat is reduced, resulting in energy cost savings for the

industry. At most iron and steel facilities in Finland, such as Raahe SSAB, excess heat is dissipated by natural cooling water. There is a general guideline that states the cold utility cost at the industrial site is roughly one-tenth of its hot utility cost. Within an iron and steel mill, the production of medium and high-pressure steam serves as the primary source of heat, resulting in a cold utility cost that is just one-tenth of the expense incurred for medium and high-pressure steam. Assuming that steam is generated through the combustion of natural gas and the boiler's efficiency is 80%, the cost saved for supplying cold utility can be calculated using Eq. 16.

$$C_{iron\&steel,saving} = 0.1\frac{C_{gas}}{\eta_{boiler}} E_{charge} \quad 16$$

Where C_{gas} is the price of natural gas (€/kWh), η_{boiler} is boiler's efficiency and E_{charge} is the quantity of thermal energy extracted from the surplus heat generated by the iron and steel plant, which is then used to charge the heat storage system (kWh).

The same approach can be extended to encompass the reduction of energy expenses in both the brewery and milk processing sectors. However, in these two industries, the cost reductions are associated with the hot utility, namely by utilizing heat storage as the hot utility instead of steam and hot water. To obtain energy savings in the brewery and dairy plant, the coefficient 0.1 in Eq. 16 should be excluded to achieve energy savings in the brewery and dairy factory as presented in Eq. 17.

$$C_{brewery/diary,saving} = \frac{C_{gas}}{\eta_{boiler}} E_{supercool} \quad 17$$

Where $E_{supercool}$ is the amount of supercooling heat used in each industry (brewery and milk processing). It should be noted that energy savings in these three industries are expressed in terms of revenue.

Another source of income for this system is the money that the household puts in for the heating of the house. Prior to the installation of ErNa heat storage at the property, for the household owner must pay the cost of direct electric heating. The highest amount that they are willing to spend for the new heating system is equal to the direct electric heating expense. This thesis considers the electricity prices of the year 2021. To simplify the calculations in this section, the monthly electricity costs provided in Appendix 1 have been used to calculate the revenue collected from the house.

Capital costs can be converted to annualized cost by assuming that they have been borrowed over a specific duration, which corresponds to the lifespan of the system, at a fixed interest rate. The annualized capital cost can be achieved as described in Eq. 18.

$$Annualized\ capital\ cost = Capital\ cost \times r \quad 18$$

Where r is the annuity factor which is a function of interest rate and lifetime, and can be calculated according to Eq. 19, where i is the interest rate (%) and t is the lifetime (years).

$$r = \frac{i(1+i)^t}{(1+i)^t - 1} \quad (19)$$

To assess the economic performance and profitability of an investment, various indicators are available, such as the Net Present Value (NPV). The NPV is a measure of profitability that considers discounted cash flows of both the CAPEX and OPEX, using a discount rate over the technology's lifetime. Put simply, money invested in a technology today is more valuable than the same amount of money invested in the future, where it could have earned interest. The calculation of a technology's net present value involves summing the present values of all its related cash flows, as presented in Eq. 20.

$$NPV = \sum_{t=0}^{t} \frac{F_t}{(1+i)^t} \quad (20)$$

Where F_t is the net cash flow in year t, and i is discount/interest rate. If an investment is made in year 0, immediately prior to the implementation of the technology, and no cash flow occurs until year 1, then the NPV can be calculated according to Eq. 21.

$$NPV = \sum_{t=1}^{t} \frac{F_t}{(1+i)^t} - I_0 \quad (21)$$

Where I_0 is the investment or capital cost. Given the assumption that the cash flow, defined as the annual revenue minus costs, remains constant throughout the research, the calculation of NPV can be further simplified using the annuity factor (r) and expressed as Eq. 22.

$$NPV = \frac{F}{r} - I_0 \quad (22)$$

The study has included the calculation of the Levelized Cost of Energy (LCOE) as an additional economic measure to facilitate the comparison of the ErNa TES system with other heating technologies used in remote houses. LCOE represents the amount that the energy provider should charge clients in order to recover the initial investment along with the specified interest rate. The formula for LCOE is represented by Eq. 23.

$$LCOE = \frac{total\ present\ costs(€)}{total\ present\ usable\ energy(kWh)} \quad (23)$$

Total present costs and total present usable energy can be converted to future values by utilizing interest rate similar to the process used for calculating present value. Furthermore, as a result of a consistent level of usable energy and OPEX in each year, LCOE can be further simplified and turns into Eq. 24.

$$LCOE = \frac{I_0 - \frac{annual\ OPEX}{r}}{\frac{annual\ usable\ energy}{r}} \quad (24)$$

The usable energy refers to the total annual amount of heat released from the ErNa storage system, during both supercooling and discharging, which is then used for heating purposes in various applications, including residential heating and heating in brewery and milk processing industry in storage model 1.

The financial parameters and their corresponding values used for the economic analysis of this thesis are provided in Table 4. The transportation cost was collected from a research paper that conducted economic assessment for a mobilized TES, and it includes labor, fuel, and truck costs [56].

Table 4. Economic Parameters

Parameter [Reference]	**Unit**	**Value**
Lifetime [56]	years	20
Interest rate [48]	-	6%
Industrial Waste Heat Price	€	0
Erythritol Price [74]	€/kg	0.47
Sodium Polyacrylate [75]	€/kg	0.9
Transportation Cost [56]	€/km/33 tonne	1.08
Natural Gas Price [76]	€/MWh	10
Finned Tube [77]	€/m	4.79
Stainless Steel Sheet Price [78]	€/kg	0.94
Excavation cost for placing ErNa storage underground	€/m^3	15
Pump for the Cascade TES [79]	k€	1.5

4
Results

In this section, the results corresponding to the storage models are provided and discussed. In Table 5, the thermal energy gain and loss in each stage of the ErNa TES which can satisfy the heating demand of a 100 m^2 passive house near the city of Oulu are listed. The discharging heat is equal to the annual heating requirement of the house and other values including required charging heat, supercooling heat and reheating have been determined by utilizing Eq. 2-3.

Table 5. Heat gain or loss of the ErNa storage unit (s) capable of providing heat demand of the passive house in Oulu

Parameter	**Unit**	**Value**
Total Charging Heat (E_{charge})	kWh	5823
Total Supercooling Heat ($E_{supercool}$)	kWh	4833
Total Reheating (E_{reheat})	kWh	1810
Total Discharging Heat	kWh	2500

When ErNa TES is used for a detached house whose input heat comes from the surplus heat of an iron and steel plant, it leads to reduced cooling water requirements, resulting in savings for the cold utility of the iron and steel plant. This saving is achieved simply by using Eq. 16 in Section 3.5. In addition, the house will pay for supplying its heating demand from the ErNa TES. As mentioned in Section 3.5, the household will pay maximum the amount that they used to pay annually for their heating through direct electricity. Therefore, based on the house's monthly heating demand and monthly electricity price in 2021, the house revenue from heating was estimated. Revenue from household and cold utility saving at iron and steel plant are provided in Table 6 and are the same for both proposed storage models. For storage model 1, an additional revenue will be obtained by selling the supercooling heat to a brewery and milk processing, as provided in Table 6. Although the revenue from selling this heat is not that significant but by utilizing the heat of supercooling in other industries instead of wasting it, increases the energy efficiency, lowers the fossil fuel consumption for generating steam and ultimately has a positive environmental impact. The low revenue from the house, which is 246 €, can be attributed to the fact that the assumed house is a passive house with lower heating demand and electricity consumption compared to a typical house. In addition, the savings on cold utilities at the iron and steel plant are insignificant since the assumed mill uses low-cost cold water.

Table 6. Annual Revenue for all storage models (both storage model 1 & 2)

Annual Revenue	Unit	Value
Revenue from household	€/a	246
Cold Utility Saving of Iron & Steel Plant	€/a	7
Revenue from brewery and dairy plant (For Storage model 1)	€/a	58

4.1 Results of One-time Transportation of Storage Model 1

To fulfil the heating requirements of a single-family house by charging ErNa TES using industrial waste heat once a year in the industry and then transporting it to the residence, a single large ErNa TES unit or multiple smaller TES units can be utilized. The benefit of having multiple TES units lies in the flexibility it provides to the system, allowing for a shorter period of reheating with electricity mainly after midnight, typically from 11 pm to 7 am, when electricity prices are significantly lower. When ErNa storage is divided into multiple units and all of them are charged at the industry, the thermal energy gain and loss in each stage, which were provided in Table 5, are divided by the number of TES units. Furthermore, as they are charged simultaneously at the industry, the input heat flow rate of each TES unit is equal to the available heat power at the iron and steel plant divided by the number of units.

The volume of ErNa and tank storage is calculated using Eq. 3. For the scenario where one storage unit was used, a tank wall thickness of 5 mm was assumed. As the number of units increased to five and then ten units, the thickness changed proportionally. The rationale for adopting different tank wall thickness for each case study is that the weight of ErNa inside the units changes significantly, which is illustrated in Table 4. As a result, the strength of the storage tank may be reduced when the ErNa material inside of it depletes. To calculate the required wall thickness of the tank, mechanical design is necessary. However, this study has assumed some reasonable values for the TES tank thickness.

According to Eq 4-9, the required heat transfer area and quantity of finned tubes within the TES unit were attained for each scenario and are specified in Table 7. Utilizing the number of HX tubes and their respective sizes, the mass of the heat exchanger was calculated. As previously mentioned, the heat exchanger consists of steel tubes and copper fins. Estimating the mass of the heat exchanger is vital in calculating transportation costs, which depend on both the distance travelled and the weight carried.

Table 7. Technical properties of ErNa TES (s) in storage model 1 for one-time transportation

Parameter	Number of Storage Units			Unit
	1	5	10	
ErNa Volume in each Storage Unit	45.3	9.1	4.5	m^3
ErNa Mass in each Storage Unit	64.8	13	6.5	tonne
Storage Tank Volume	56.7	11.3	5.7	m^3
Wall thickness of Storage Units	5	4	3.5	mm

Parameter	Number of Storage Units			Unit
	1	5	10	
Size of Each Storage Tank	Φ4x4.5	Φ2.7x2	Φ2.2x1.4	m
Storage Tank Mass of Each Unit	3.2	0.9	0.49	tonne
Number of Finned Tubes in each Unit	4	2	2	-
Heat Exchanger Mass in Each Unit	34.7	7.4	5	kg
Total Charging time	1.9	1.9	1.9	hours

As outlined in Section 3.5, the CAPEX of this system encompasses the cost of ErNa material and the storage tank, the heat exchanger expenses, and the cost of excavating the land for placing the TES (s) underground. The capital cost of the storage tank was estimated based on the market value of similar tanks currently available for sale. From the cost of raw stainless steel listed in Table 4, and the mass of the material used in comparable tank shapes, the proportion of additional expenses, including the manufacturing cost of the tank was calculated. The final cost for producing the tank is almost 4 times higher than the cost of the steel used in them. Notably, we obtained a comparable price for a similar tank from a seller on Alibaba.com [80]. The same approach was used for estimating the capital cost of storage tanks. The tank storage price is affected by its wall thickness, therefore the values achieved for capital cost of TES might be quite different from a real case.

For the cost assessment of ErNa, the analysis assumes the utilization of ErNa-80 as the material mobilized in the thermal energy storage (TES) system. This material comprises 80% erythritol and 20% sodium polyacrylate. The cost of ErNa material in each storage model was then computed using data provided in Table 4. The expense of the finned tube heat exchanger was procured from an Alibab.com supplier, the price of which is noted in Table 4. The cost was based on the quantity and length of tubes used. The cost of excavating the ground to place the TES units is directly proportional to the size of the excavation. The value provided in Table 4 was used to derive this cost.

The diagram in Figure 30 displays the capital costs for each scenario. The major portion of the CAPEX, about 74%, is attributed to the ErNa material in the first scenario (one TES unit), preceded by the storage tank cost. On the other hand, the HX cost and excavation cost are negligible. As the number of TES units increases, the storage tank cost rises, consequently leading to an increase in capital cost from 49.8 k€ for one TES unit to 56.4 k€ for ten TES units.

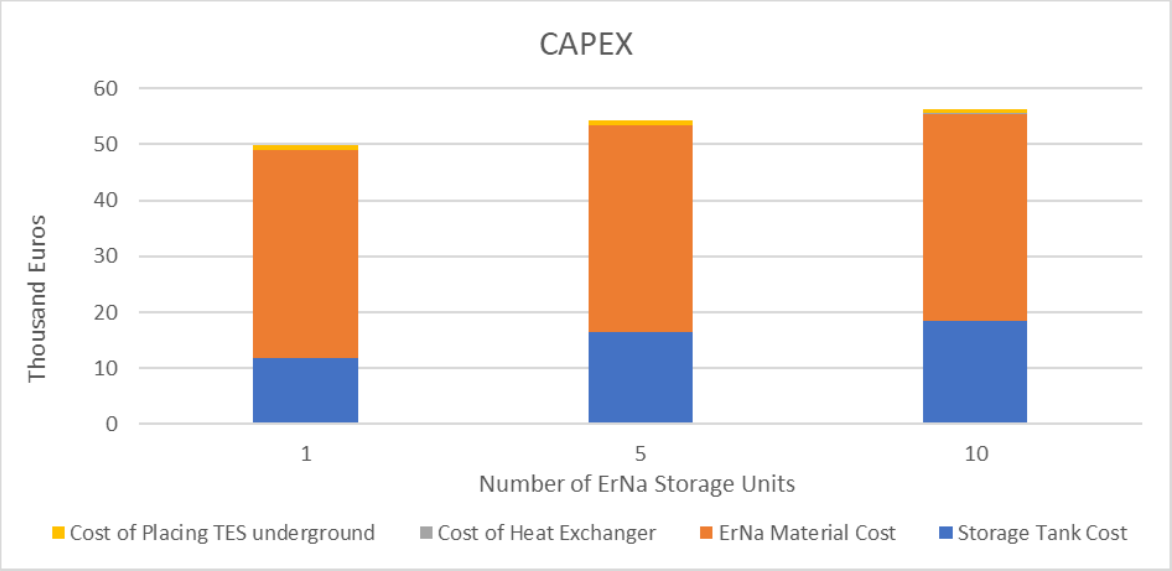

Figure 30. Capital cost diagram for one round transition of ErNa TES in storage model 1 comprising one, five and ten TES units

As detailed in Section 3.5, OPEX in storage model 1 comprise reheating cost with electricity and transportation costs. There are also other OPEX such as labor cost that has not been taken into account in this study. Regarding reheating cost with electricity, the data related to household electricity prices in 2021 in Finland was used. When there is only one storage unit, reheating is done once a year, lasting for nearly 14 days. As heating demand for houses typically begins in September, it is assumed that reheating is carried out at the beginning of the month. During the daytime in this period, the average household electricity price was 114 €/MWh, whereas during the night (from 11 pm to 7 am) the price dropped to 69 €/MWh. It is possible to carry out a significant portion of the reheating process during the night when electricity prices are lower.

A key assumption made in this case study is that the probability of crystallization is relatively low until the temperature reaches 30 °C. Thus, the reheating can be paused when the electricity price increases and resumed when it drops until ErNa reaches 30°C. It has been assumed the storage is well insulated which minimizes the heat loss during the reheating pause. In this study, heat loss has been considered negligible. Via this technique, the majority of reheating occurs during the low-priced electricity period at night. However, reheating cannot be paused when ErNa's temperature goes above 30°C and must continue even when the electricity price is high. When multiple ErNa storage units are in use, the reheating process of the next unit begins when one unit approaches full discharge. Table 8 displays the timetables for reheating in each scenario, with the associated electricity prices for both day and night.

Table 8. Reheating periods with average electricity prices during day and night for one, five, and ten TES units in storage model 1

Number of Units	Reheating Initiating Day	Average Electricity Price during day (€/MWh)	Average Electricity Price during night (€/MWh)
1	1 September	114	69
5	1 September	114	69
	18 November	100	37
	20 December	325	65
	24 January	90	63
	1 March	61	47
10	1 September	114	69
	22 October	85	35
	16 November	125	37
	4 December	225	125
	20 December	325	65
	10 January	75	59
	24 January	90	63
	13 February	90	74
	1 March	61	47
	22 March	65	47

The reheating cost with electricity was determined based on the prices listed in Table 8 and the amount of energy required for reheating in each time. The transportation cost in each scenario is influenced by the weight of the TES(s) due to the load weight limitations of trucks. The weight of TES (s) includes the ErNa material, storage tank, and the HX weights. Given that the driving distance is approximately 110 km, transportation can be conveniently obtained using the values specified in Table 4.

Figure 31 shows a diagram of all OPEX for each scenario, similar to CAPEX. The revenue of the system for each scenario is shown as negative values in the diagram. The revenue in this model consists of the revenue from the supply of heat to the house, the supply of some heat to the brewery and milk processing plant, and the cold utility savings of the steelworks. The revenue is the same regardless of the number of storage units. Figure 31 demonstrates a clear correlation between the growth in the number of TES units and the decrease in OPEX, resulting in an improvement in the annual cash flow. One ErNa TES has annual operating expense of 443 €, while dividing the TES into ten smaller units, lowers the cost to 365 €. The diagram displays the net OPEX for each scenario, which is calculated by subtracting the revenue from the OPEX. Prior to the installation of the ErNa TES, the net OPEX was equivalent to the direct electric heating cost of the house, which was 246 €. Detailed CAPEX and OPEX values can be found in Appendix 2.

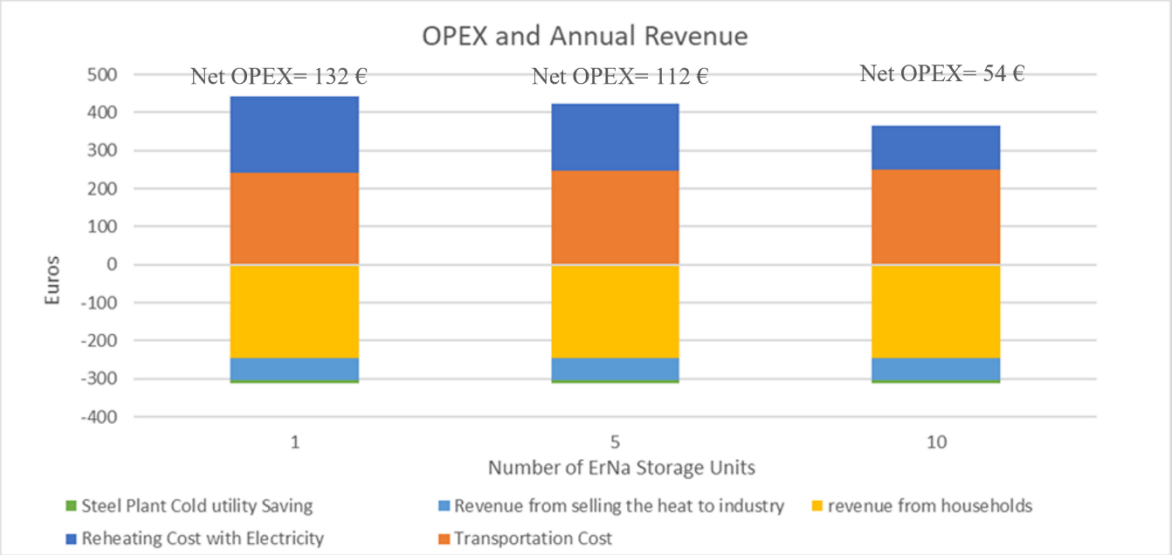

Figure 31. OPEX and annual revenue diagram for one round transition of ErNa TES in storage model 1 comprising one, five and ten TES units

In order to identify the scenario with the highest economic performance among these three options, it is necessary to calculate the NPV. A greater quantity of TES units resulted in reduced OPEX but increased CAPEX, making it challenging to determine the most favorable option. The NPV and LCOE of the mobilized ErNa storage for one, five, and ten ErNa TES units were determined using Eq. 22 & 24. The results are indicated in Figure 32. It is clear that using a single unit of ErNa TES results in a reduced LCOE of 0.59 €/kWh and a higher NPV of -51.3 k€. Thus, using a single unit leads to improved economic performance. Although the annual cash flow is more negative in one TES unit system (-132 €), the smaller initial investment results in a higher NPV.

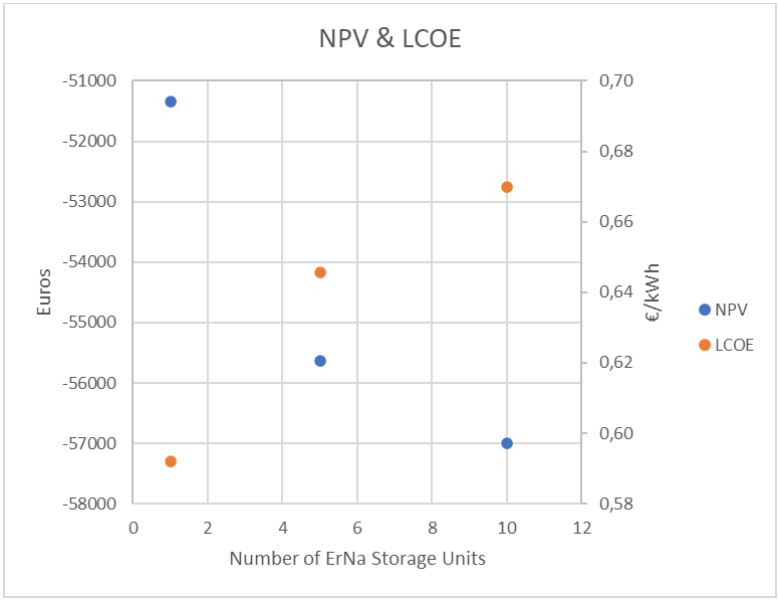

Figure 32. NPV and LCOE for one round transition of storage model 1 comprising one, five and ten TES units

4.2 Results of Multiple Transportation Rounds of Storage model 1

As in the one round transportation of ErNa TES, one single TES unit demonstrated superior economic performance, one large-size TES unit is assumed to be transported multiple rounds in this scenario. Up to four trips between the iron and steel mill and the detached dwelling were considered. The heat gain and loss in each stage including charging heat at the iron and steel plant industry, supercooling at the brewery and milk processing, reheating with electricity and discharging to the house in each transportation cycle can be easily achieved just by diving the values listed in Table 5, by number of commuting rounds.

Table 9. Charging and Reheating time for transportation rounds (maximum four times per year)

Number of Charging rounds	Charging Date	Reheating Date
Once	June	2 September
Twice	June-10 Jan	2 Sept-10 Jan
Three times	June-13 Dec-6 Feb	2 Sept- 13 Dec-6 Feb
Four times	June-28 Nov-10 Jan-21 Feb	2 Sept-28 Nov-10 Jan-21 Feb

The sizing of TES, which includes the storage tank and ErNa, was performed using a process similar to that used for one-time transit. In addition, the HX in the TES system is specifically designed to match the heat dissipation capacity of the iron and steel plant at the charging temperature. This allows for the efficient utilization of the entire 3000 kW heat output generated by the steel plant in each charging round. Table 10 presents the technical characteristics of the TES and HX for a maximum of four charging cycles in the industry.

Table 10. Technical Properties of storage model 1 in multiple Transportation rounds

Parameter	Number of Charging Rounds				Unit
	1	2	3	4	
ErNa Volume in each Storage Unit	45.3	22.7	18.9	11.3	m^3
ErNa Mass	64.8	32.4	21.6	16.2	ton
Storage Tank Volume	56.7	28.3	15.1	14.2	m^3
Thickness of Storage Unit Walls	5	4	3.7	3.5	mm
Size of Each Storage Tank	Φ4x4.5	Φ3.4x3.2	Φ3x2.6	Φ2.8x2.3	m
Storage Tank Mass	3.2	1.6	1.1	0.9	ton
Number of Finned Tubes in each Unit	4	4	4	4	

Parameter	Number of Charging Rounds				Unit
	1	2	3	4	
Heat Exchanger Mass in Each Unit	34.7	34.7	34.7	34.7	kg
Charging time	1.9	1.9	1.9	1.9	hours

Regarding capital expenses, these were calculated according to the same procedure as that used for the one-time transportation scenario. These costs are displayed in Figure 33 and detailed in Appendix 2. It is obvious that when the number of charging rounds rises, there is a significant decrease in CAPEX due to the reduction in size of the ErNa material and storage tank. When ErNa TES is transported and charged at the industry four times per year, the capital cost drops drastically from 49.8 k€ to 12.8 k€ since one-fourth of ErNa material is sufficient to meet the yearly heating demand of the house.

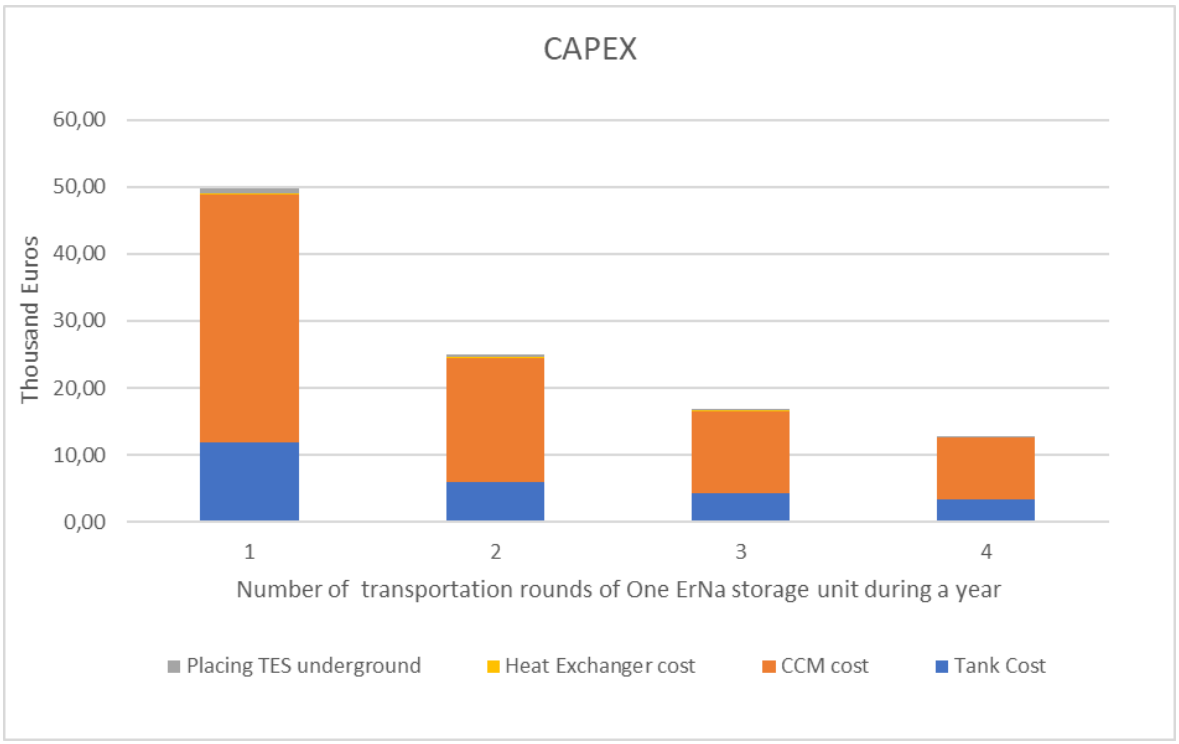

Figure 33. Capital cost of multiple round transit of one single ErNa TES unit in storage model 1 for up to four rounds

The OPEX was calculated similarly to OPEX for the one round transportation of ErNa. However, in this case study, transportation cost depends on both the number of transportation rounds and the weight of the TES unit. Reheating cost depends on the timing of the reheating and the electricity price during that period. Two and three cycles of charging per year results in performing the reheating during periods with high electricity prices in Jan, Dec and Feb, as listed in Table 9. If the schedule for complete reheating had avoided peak prices, the OPEX for two and three charging cycles would have decreased. Furthermore, the revenue and cost savings remain unchanged for multiple transportation rounds of TES, as the price of the heat sold to the house, brewery, and milk processing aligns with the energy and is consistent. In

Figure 34 and in Appendix 2, the achieved OPEX and revenue for each transportation cycle scenario are presented. It is clear that the greatest operating expenditure is linked to three rounds of TES charging (589 €) followed by two rounds of charging (576 €), while the lowest expense is associated with one round of TES transportation (costing 443 €). The diagram incorporates the Net OPEX for each scenario, facilitating a straightforward comparison with the Net OPEX of the house when it was heated using electricity, which amounted to 246 €.

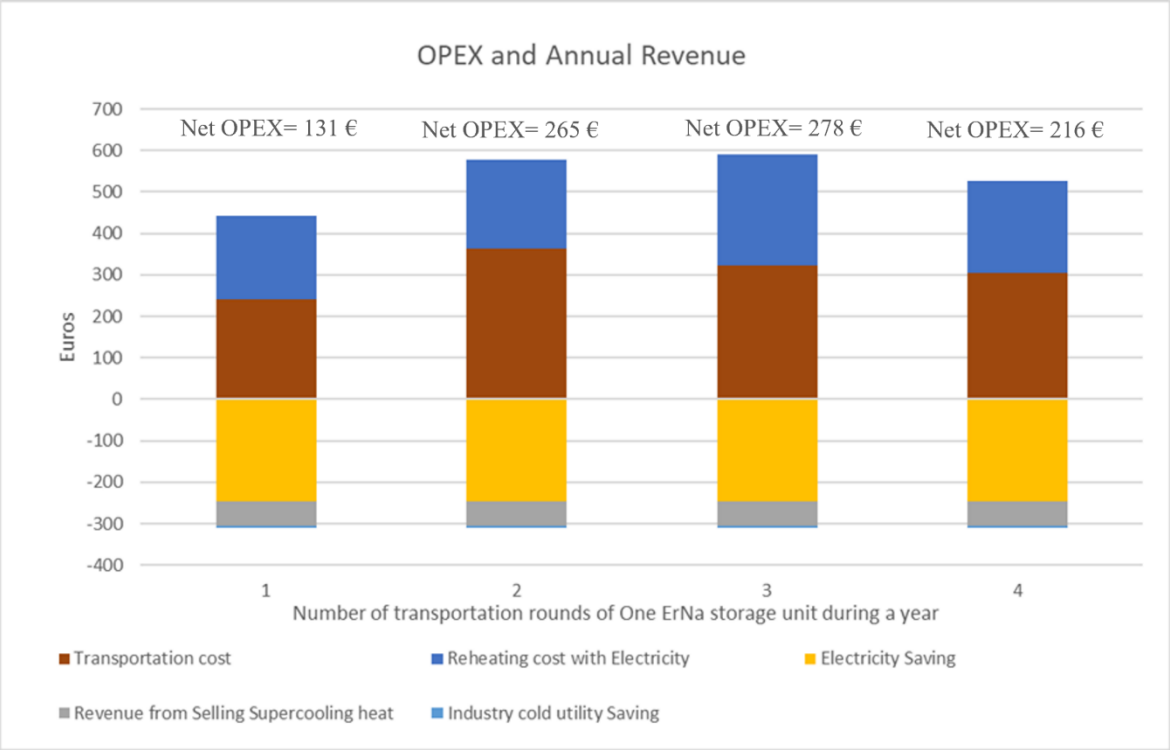

Figure 34. OPEX and annual revenue of multiple round transportation of one single ErNa TES unit in storage model 1

When the ErNa TES system is designed to meet the entire annual heating demand of a house by a single charging at the industry and a single transportation round, the initial investment cost is the highest. However, it results in the lowest OPEX and ultimately leads to the largest annual cash flow. The economic performance of four-time transportation was superior due to its ability to produce the lowest LCOE of 0.15 €/kWh and the highest NPV. It is evident that NPV grows when there is a higher number of trips between the house and the industry. This increase is significant, ranging from -51.3 k€ to -15.3 k€ when charging cycles are increased from one to four.

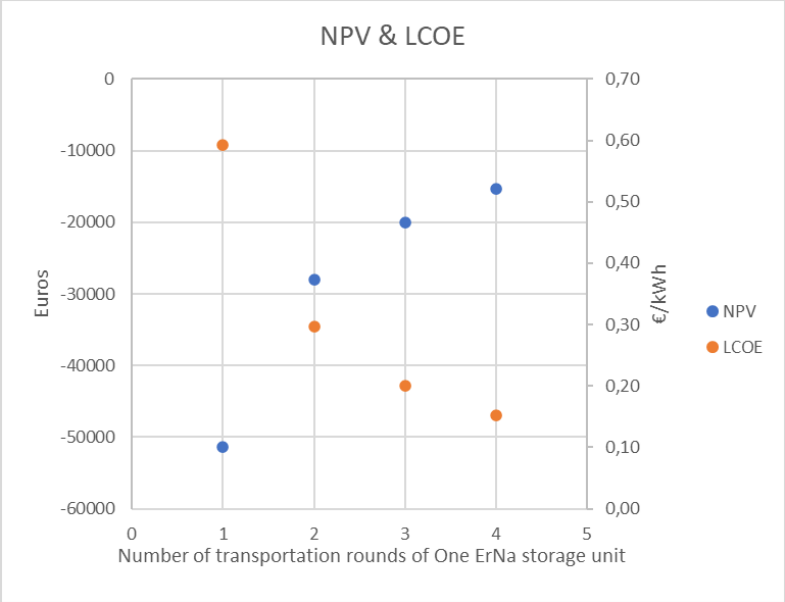

Figure 35. NPV and LCOE for multiple round transition of ErNa TES in storage model 1 up to four rounds

4.3 Results of Storage Model 2

This section presents the outcomes related to storage model 2, where ErNa TES is divided into three units, with the largest one (ErNa Storage 1) being charged by the industrial surplus heat. The charging heat of unit 1 and the corresponding volume needed for the ErNa TES unit 1 were calculated using Eq. 14. The sizing of ErNa TES units 2 and 3 was determined based on the amount of heat they receive from the prior unit, as specified in Eq. 12-13. Similar to previous storage model, it has been assumed all the available heat flow rate at the iron and steel plant industry is utilized, therefore HX of ErNa TES unit 1 is sized using Eq. 4-9. The heat transfer area of ErNa TES unit 2 and 3 were achieved by taking into consideration the critical supercooling rate of ErNa discussed in Section 2.3.2. The technical properties of this model including size of all three ErNa TES units are presented in Table 11.

Table 11. Technical Properties of ErNa TESs in model 2

Number of ErNa Storage Units = 3				
Parameter	ErNa Storage Unit 1 (Mobilized)	ErNa Storage Unit 2	ErNa Storage Unit 3	Unit
Charging Heat	2312	1919	1593	kWh
ErNa mass	25.7	21.4	17.7	ton
ErNa Storage Tank Volume	22.5	18.7	15.5	m^3
Size of ErNa Storage Tank	Φ3.2x2.8	Φ3x2.6	Φ2,9x2.4	m
Mass of Storage Tank	1.4	1.2	1.1	ton
Time for charging	0.8	6.7	6.7	hours

Number of ErNa Storage Units = 3				
Parameter	ErNa Storage Unit 1 (Mobilized)	ErNa Storage Unit 2	ErNa Storage Unit 3	Unit
Time for Supercooling	6.7	6.7	6.7	hours
Number of Finned Tube	7	15	14	-
Heat Exchanger Mass	36.8	71.2	60	kg

As stated in Section 3.3.2, reheating in model 2 is accomplished by utilizing the industrial waste heat, which is transported by pure erythritol TES to the ErNa storage units located at the dwelling site. Eq. 15 was used to determine the necessary erythritol and TES size and similar to HX of ErNa TES unit 1, erythritol TES's HX is sized to utilize the entire heat flow rate available at the steel mill. The technical specifications of erythritol TES for the purpose of reheating are presented in Table 12.

Table 12. Technical properties of erythritol storage which transports the heat from industry to ErNa storages for their reheating

Parameter	**Value**	**Unit**
Pure Erythritol Mass	12.6	ton
Pure Erythritol Tank Volume	10.8	m^3
Pure Erythritol Tank Size	Φ2.6x2	m
Mass of Erythritol Storage Tank	0.6	ton
Number of Finned Tube in Erythritol Storage Tank	6	-

In storage model 2, in addition to ErNa TESs, other equipment such as erythritol TES, a pump for circulating heat transfer fluid, piping, and valves have been included. This addition to the existing ErNa TESs equipment results in a much higher capital cost compared to storage model 1 as can be seen in Figure 36. Storage model 2 CAPEX escalates to 62 k€.

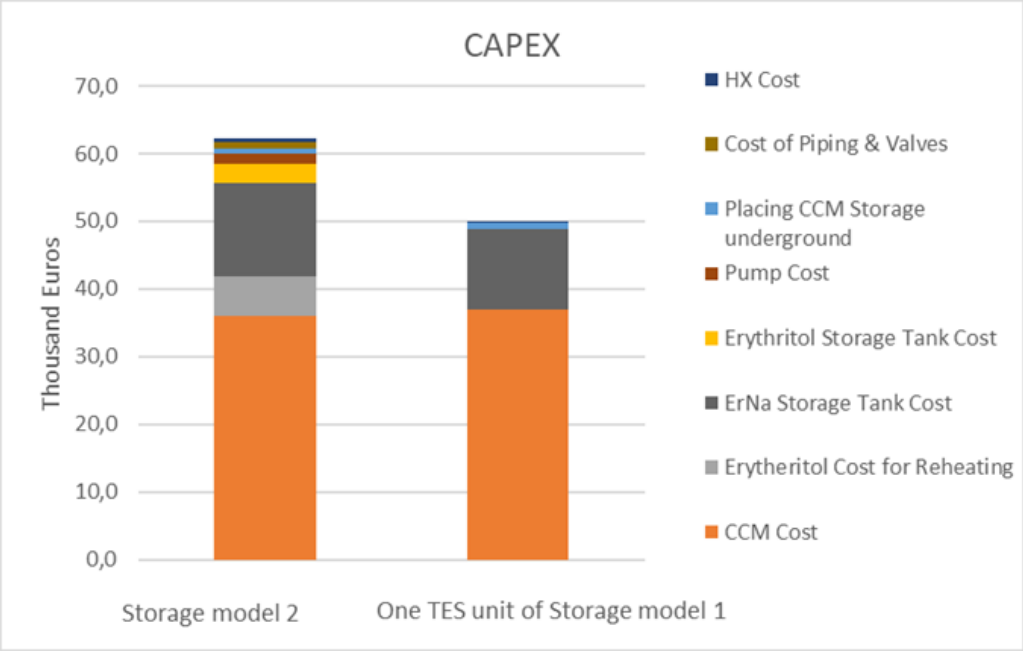

Figure 36. CAPEX of once charged storage model 2 in comparison to one unit of storage model 1 charged once a year

In storage model 2, only the transportation cost of ErNa TES unit 1 and erythritol TES is considered as operating expenses (OPEX). The revenue generated from selling the supercooling heat is not included, as the supercooling heat of all ErNa TES units is used to charge other units, except for the last unit whose supercooling heat is assumed to be wasted. The OPEX and revenue are displayed in Figure 37 and in Appendix 2. The revenue collected from household overcomes the transportation cost leaving a positive annual cash flow of 144 €. This indicates that the capital expenditure is being recovered each year. However, it is necessary to ascertain whether the entire initial investment is recouped within the system's lifespan. By utilizing OPEX, CAPEX, annual revenue, interest rate and lifetime, NPV of -61 k€ and LCOE of 0.74 €/kWh were achieved indicating that storage model 2 cannot generate profitability by the end of system’s lifetime. In Table 13, annual cash flow, NPV and LCOE of storage models 1 and 2 are presented for comparison.

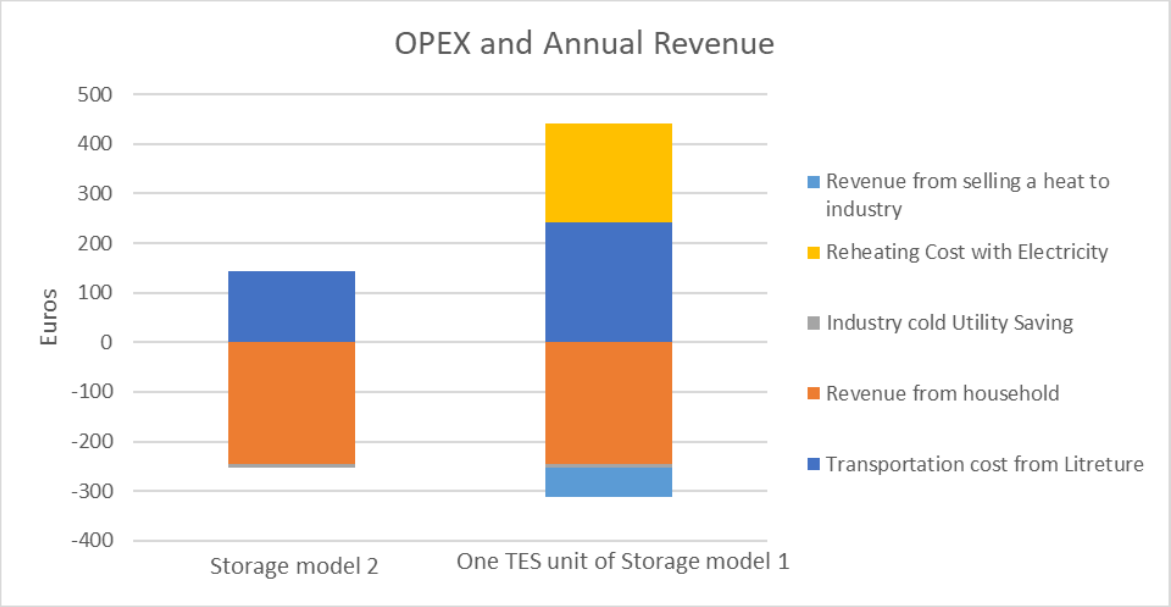

Figure 37. OPEX and Annual Revenue of once charged storage model 2 in comparison to one unit of storage model 1 charged once a year

Table 13. NPV & LCOE for One time transportation of model 2 in comparison to that of model 1

Parameter	**Storage model 2 Charged Once a year**	**Storage model 1 Charged Once a year**	**Unit**
Annual Cash Flow	109	-131	€
LCOE	0.74	0.59	€/kWh
NPV	-61	-51.3	k€

5
Discussion

5.1 Economic Performance of Both Two Storage Models

In this thesis, different methods of transporting heat from industry to the house and providing the heat by ErNa thermal storage which is a long-term latent heat storage have been proposed and studied. Techno-economic analysis was conducted for each of the proposed models and case studies to identify how profitable they are.

In storage model 1, all ErNa TES (s) are charged at the industry and transported to the house. In case study 1, the effect of number of TES units on economic performance was investigated. Adoption of small TESs facilitates transportation and placing them underground in residential areas, resulting in reduced labor expenses and enhanced system flexibility. Three different storage numbers including one single unit, five and ten ErNa TES units were studied. Based on the economic evaluation, the unit with the lowest transportation cost was a single large-size TES unit, while the highest cost was associated to ten units according to assumptions made for storage tank dimensions. When it comes to reheating cost, the highest one belonged to one TES units and the lowest one to ten units. Increasing the number of units does not guarantee a drop in reheating cost, as the cost is influenced by the price of electricity at the time of reheating. In order to minimize the cost of reheating using electricity, it is advisable to construct an intelligent system that can start the reheating process during periods of low power costs and suspend it when the price of electricity increases. Therefore, these led to possessing the highest OPEX by utilizing one single ErNa TES unit followed by five and ten TES units. Conversely, when a single ErNa TES unit transfers the heat all at once and supplies it to the house, the CAPEX is minimized because of the reduced cost of a storage tank for a single unit compared to several smaller units. Thus, the NPV of a single unit of ErNa TES was the highest however negative equal to -51.3 k€. The LCOE of one ErNa TES unit is around 0.59 €/kWh, significantly exceeding the average household electricity price of 0.09 €/kWh.

Furthermore, the impact of the number of transportation rounds between industry and the house on the profitability of storage model 1 was investigated. When heat is transferred to the house more frequently, the size of the storage unit is reduced, resulting in a lower CAPEX associated with the ErNa material and the storage tank. While it may appear reasonable that transportation expenses would rise in conjunction with more frequent commuting, the cost of transportation is dependent upon both the distance traveled and the weight of the cargo being transported. As the frequency of transportation trips between the house and the industry for TES increases, the storage volume and weight decrease. Thus, it was seen that despite two or three rounds of transportation, the reduction in carried weight was insufficient to compensate for the increased transit distance, resulting in greater transportation costs. When examining transportation conducted four times, the cost of transportation decreased in comparison to two and three

rounds of transportation. This indicates that the reduction in storage weight is offsetting the rise in commuting distance. The cumulative OPEX for four rounds of transportation remains higher than that of a single transportation event. However, the CAPEX for the four rounds is significantly lower, leading to an improved NPV of -15.3 k€ and reduced LCOE of 0.15 €/kWh. This case study indicates that increasing frequency of ErNa TES charging cycles in the industry significantly enhances the economic efficiency of the system, making it comparable to the average electricity price.

The second storage model involved the development and analysis of a distinct configuration system named as Cascade TESs. This model brings annual positive cash flow of around 144 € due to not utilizing electricity for completing reheating but rather transporting the industrial surplus heat for ErNa TESs. Nevertheless, as a result of including additional equipment in this particular model, the capital cost was much greater in comparison to storage model 1. This posed a challenge in attaining profitability within the projected 20-year lifespan of the system and resulted in a higher LCOE of 0.74 €/kWh compared to storage model 1.

5.2 Effect of Number of Transportation Rounds on Storage model 2

Reducing the amount of ErNa material has a major impact on the economic performance of the ErNa TES as was observed in charging the storage model 1 multiple times throughout a year. In this section, the effect of increasing the number of transportation rounds from industry to the house in storage model 2 is investigated. In Figure 38, the effect of increasing charging and transportation round on NPV and LCOE for both storage models are shown in a single diagram for comparison. When transportation round increases to 4 times, LCOE of storage model 2 drops to 0.26 €/kWh and its NPV grows to -21.4 k€. It is visible due to high capital cost of storage model 2, storage model 1 possesses better economic efficiency when it is transported more frequently.

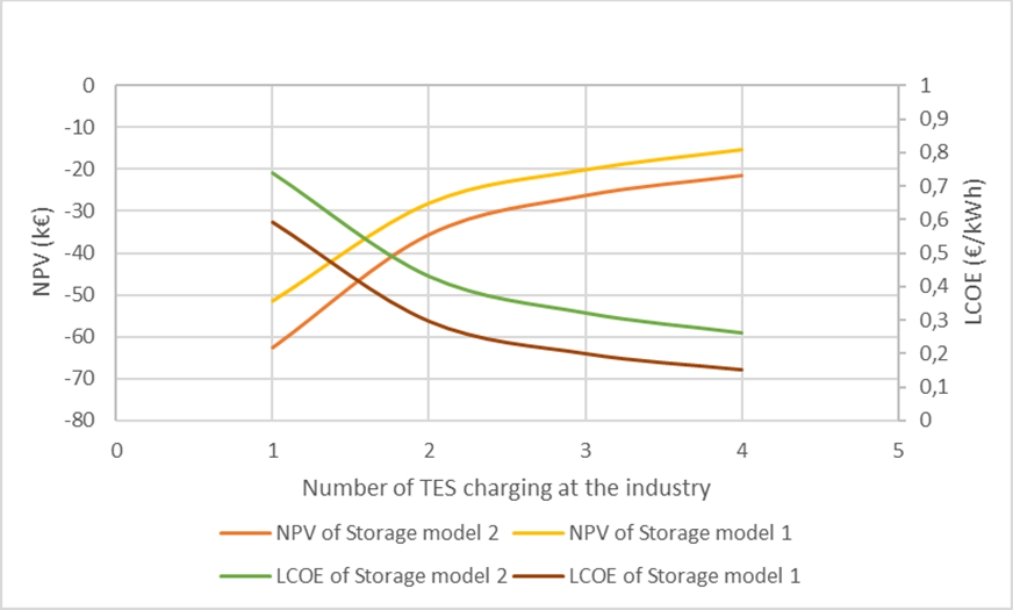

Figure 38. NPV & LCOE of storage model 1 & 2 in different transportation rounds up to four trips

5.3 Effect of Distance of Detached House from the Industry

The distance between the house and the industry is a metric that affects the annual cash flow, as well as LCOE and NPV. An investigation was conducted to examine the impact of distance on the optimal economic outcome of storage models 1 and 2, with the TES being charged four times per year. Figure 39 displays the diagram of NPV-distance. A reduced travel distance leads to increased NPV and improved economic performance. It is clear that when the distance decreases to 5 km, NPV increases in a linear manner from -15.3 k€ to -12 k€ for storage model 1, and from -21.4 k€ to -19.3 k€ for storage model 2. This suggests that distance does not have a substantial effect on profitability, and the main obstacle to achieving a positive NPV is the high capital cost of ErNa material.

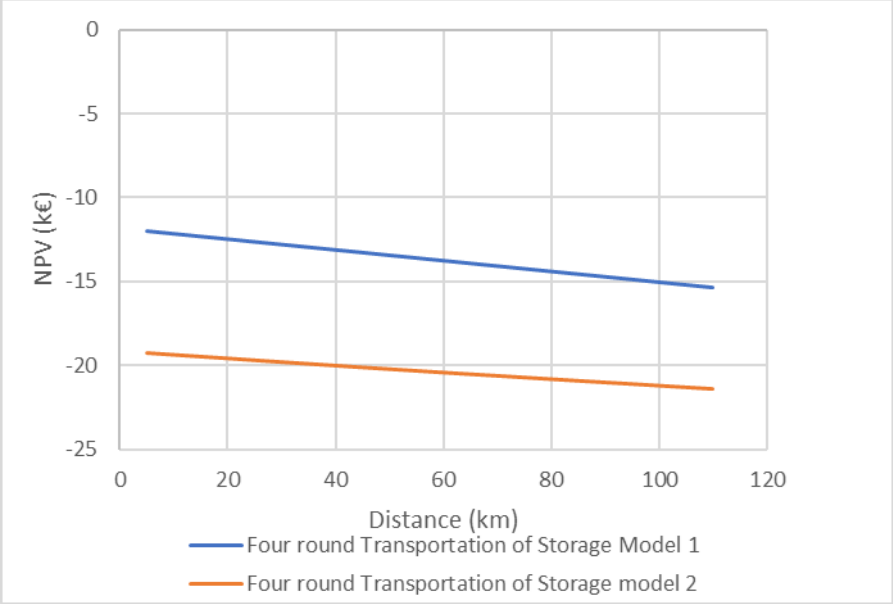

Figure 39. NPV-Distance diagram for ErNa TES model 1 & 2 commuting four times a year

5.4 Comparison with Other Common Heating Systems

In this section, the achieved results from economic analysis of ErNa storage models are compared with air source and ground source heat pumps. There are also other types of heat pumps, including exhaust air heat pumps and air-to-water heat pumps. Exhaust air heat pumps have higher efficiency as they utilize the heat from the exhaust air to heat the supply air. However, the European Heat Pump Association has reported that Finland has not made major investments in exhaust air heat pumps and air to water heat pumps [81]. Therefore, their economic performance has not been studied in this thesis.

5.4.1 Air source Heat Pump (ASHP)

Heat pump's coefficient of performance (COP) is a measure for achieving efficiency of heat pumps. It is defined as the heat pump's useful heat to the input energy. In case of air source heat pumps where electricity is used to compress the working fluid to transfer the heat from hot reservoir to the heat sink, the input energy is electricity. Thus, COP can be simply formulized as Eq. 25.

$$COP = \frac{Q_{cond}}{Electricity} \quad (25)$$

Where Q_{cond} is the heat supplied to condenser or heat sink. When air source heat pump is supplying heat to the house, the condenser heat is the house heating demand. COP is also proportional to the temperature difference between the evaporator and condenser. Evaporator in heat pumps extracts heat from the hot source, while condenser gives out that heat to the cold source. Air source heat pumps transfers the heat from the outside environment to inside the house, therefore, evaporator is in contact with the surrounding while the condenser is in touch with the inside the house.

The COP of an air source heat pumps is influenced by the outside temperature or in other words the temperature difference between heat source and heat sink. Figure 40 displays a graph that is provided by a vendor illustrating the correlation between the actual COP of a heat pump and the outdoor temperature when it is used for space heating. As can be observed when outside temperature reaches around -20 °C, the COP of heat pump drops to almost 1 and therefore air heat pump behaves similarly to direct electric heating system. It is important to note that the COP of the latest ASHPs reach 1 at temperatures around -35°C. To achieve electricity consumption by air heat pump, monthly heating demand of the house and average monthly electricity price of year 2021 were used. Thanks to the COP values derived from Figure 40 by utilizing monthly temperature from Figure A1.4 in Appendix 1, along with the monthly heating demand of the house, which represents Q_{cond}, provided in Figure A1.3 in Appendix 1, monthly electricity consumption of heat pump for an entire year was achieved. As a reminder, the annual heating demand of the house was assumed to be 25 kWh/m^2, resulting in lower electricity consumption compared to a normal house with an annual heating demand of 85 kWh/m^2.

The costs associated with an air heat pump include the price of the heat pump itself, as well as the installation to the heating and ventilation system of the house. Installation and equipment cost both are categorized as the CAPEX and for this study, they were collected from k-Rauta, a well-known retail chain in Finland. However, electricity consumption cost is the OPEX of air heat pump. Yearly maintenance cost has been neglected in this study. The values are presented in Table 14. As the chosen house is a passive building, it requires a smaller capacity and less expensive heat pump compared to a typical house. Therefore, the overall CAPEX of a heat pump for a typical house would be higher since a larger capacity HP needs to be installed.

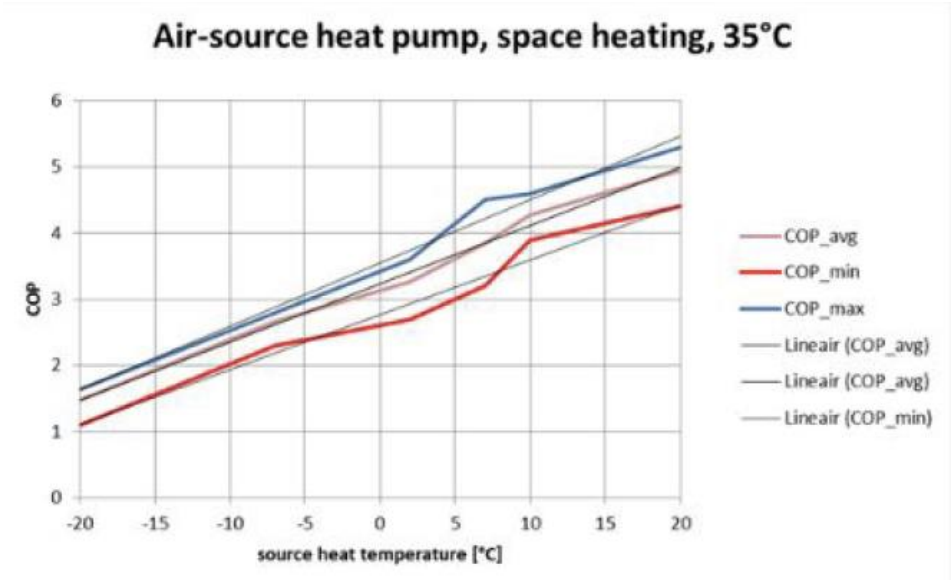

Figure 40. Air source heat pump performance curve [25]

Table 14. Cost associated to the air source heat pump (ASHP) placed for heating of a passive house in Oulu

CAPEX	**Value**	**Unit**
Air source HP Electricity Cost	81	€/year
OPEX [Reference]	**Value**	**Unit**
Air source HP Price [82]	869	€
Air source HP installation Cost [82]	799	€

Table 15. Economic Assessment of air source heat pump placed for heating of a passive house in Oulu

Parameter [Reference]	**Value**	**Unit**
Lifespan [83]	15	years
Interest rate	5%	-
Annual Cash Flow	165	€/a
NPV	53	€
LCOE	0.03	€/kWh

Table 15 presents the assumed interest rate and lifespan along with calculated annual cash flow, NPV and LCOE. It is very clear that ASHP is profitable to be installed as a positive NPV and LCOE of 0.03 €/kWh are generated.

5.4.2 Ground source Heat Pump (GSHP)

Geothermal heat pump is another heating system that has high potential to be implemented in detached houses. This system takes advantage of relatively constant temperature of the underground to heat up or cool down the house. To implement this heating system, wells need to be drilled in the ground to implement the boreholes for circulation of thermal fluid for changing heat to or from the ground. Unlike air source heat pump, geothermal heat pumps are

not influenced much by the outside temperature and the COP is typically between 3 and 6. However, the investment cost of this type of heat pump is much higher than air heat pumps, which makes it challenging to implement in all houses.

For this study, a ground source heat pump with a capacity of 5.5 kW [84] was chosen, which is one of the smallest models available in the Finnish market and its COP was reported to be 4.1. Formulas for obtaining electricity consumption of ground source heat pump are similar to air source heat pump as Eq. 25.

The installation cost of GSHP includes ground loop installation as well as excavation and drilling cost. Therefore, it is influenced by the soil type of the residential site, the available area of the land to decide whether to implement horizontal or vertical looping and so on. Therefore, the installation cost provided in Table 16 is a rough estimation and can vary significantly house by house and location by location.

Table 16. Cost associated to the ground source heat pump placed for heating of a passive house in Oulu

OPEX	**Value**	**Unit**
Ground source HP Electricity Cost	41	€
CAPEX	**Value**	**Unit**
Ground source HP Price	7250	€
Ground source HP installation Cost	7000	€

The assumed lifespan and interest rate for the GSHP as well as calculated NPV and LCOE are provided in Table 17. According to the chosen GSHP and electricity saving of the house when GSHP is utilized, negative NPV of -11.6 k€ and LCOE of 0.38 €/kWh are generated. LCOE is significantly higher than the average electricity price of 0.09 €/kWh.

Table 17. Economic Assessment of ground source heat pump placed for heating of a passive house in Oulu

Parameter [Reference]	**Value**	**Unit**
Lifespan [85]	25	years
Interest rate	5%	-
Annual Cash Flow	205	€/a
NPV	-11.6	k€
LCOE	0.38	€/kWh

6

Conclusion

This work presented a techno-economic analysis of a mobilized long-term latent thermal energy storage (TES) system that meets the space heating requirements of a passive single-family house located in a remote area near the city of Oulu. In this work, Cold Crystallization Material (CCM) heat storage is utilized for transferring industrial waste heat to the house for its heating purpose. When the CCM TES is fully charged, it should be subjected to supercooling, a process in which it is cooled while remaining in its liquid phase. To maintain the stored heat, ideally the material should be kept at a temperature between 0 to 10 °C. Finally, to release the latent heat, the temperature of the material must be increased to the cold crystallization temperature to initiate crystallization and heat release.

In this thesis, unused heat from an iron and steel plant was identified as the most suitable thermal input for the CCM TES, and erythritol in a cross-linked sodium polyacrylate matrix (ErNa) was chosen as the CCM. Two models were proposed for transferring and providing heating of a detached house. In model 1, all required ErNa materials are charged at the industrial site, transported to other industries for executing supercooling, transported to the house for storage, reheated with electricity during periods of low prices, and finally releasing their heat to the house.

In model 1, the economic performance of using a single large-size ErNa TES unit or multiple number of smaller units which are charged all at the same time and once a year but discharged one by one were investigated. One large TES yielded the highest economic performance with a levelized cost of energy supply (LCOE) of 0.59 €/kWh and Net Present Value (NPV) of -51.3 k€. Furthermore, in model 1, the impact of transferring one TES for multiple cycles between the industry and the house during a year was studied. The results indicated that performing up to four trips between these two sites, causes NPV to increase to -15.3 k€ and LCOE to drop to 0.15 €/kWh which is comparable to the average electricity price (0.09 €/kWh). The main issue within model 1 is utilization of electricity for reheating of the TES which results in negative annual net income in all the case studies.

In model 2, a single ErNa TES unit is charged at the industrial site, transported to the house where other ErNa TES units are located, supercooled by transferring its heat for charging the next ErNa TES unit in sequence, reheated through transported heat from the industry by pure erythritol TES, and discharged its heat to the house. When ErNa TES in this model is charged once a year, LCOE of 0.74 €/kWh and NPV of -61 k€ were achieved. However, when the ErNa TES in this model travels multiple rounds between the industry and house for charging, i.e., four times, LCOE drops to 0.26 €/kWh and NPV increases to -21.3 k€. The strength of model 2 is the elimination of electricity usage for heating which results in achieving positive annual

income. However, due to possessing higher CAPEX in comparison with model 1, LCOE is higher which makes model 2 less cost-effective.

The economic evaluation of these two models was compared with other heating systems utilized in detached houses, including air-source heat pumps (ASHP) and ground-source heat pumps (GSHP), for the same house. ASHP yields a positive NPV and has LCOE of 0.03 €/kWh which is below the electricity price. The economic evaluation demonstrated that GSHP has better economic performance than the two suggested ErNa TES models. Nonetheless, when ErNa TES in model 1 is charged and transported four times each year and the house is located less than 5 km away from the industry, ErNa TES can rival GSHP in terms of their NPV, which is approximately -11 k€, even though GSHP brings positive annual cash flow.

The major barrier to achieving profitability in this study is the high capital cost associated with ErNa material. In models 1 and 2, ErNa material costs account for 74% and 70% of the total capital cost, respectively. Therefore, the reason for better economic performance with a higher number of commutes between the industry and the site was rooted in the reduction amount of ErNa material. It is clear that relying solely on the discharge of latent heat from CCM for a single house's heating demands makes economic profitability challenging to achieve, as significant amount of CCM is required. However, it is regrettable that the released sensible heat during CCM TES's supercooling may not be practical to utilize for one single-family house, as that heat needs to be discharged over a period of hours, and a single house does not require a significant amount of heat all at once.

For future studies, it is suggested to evaluate the economic performance of CCM TES in rural areas where houses are connected to each other by a piping network, such as low temperature district heating. This could enable the supply of a considerable amount of released supercooling heat to the piping network for the heating of multiple houses in the countryside. Even when supercooling takes place during the summer, it could be utilized for the tap water heating network. Thus, the revenue collected from all the houses may be high enough to recover the capital cost over the lifespan of the storage system. Another potential future study could be conducting an economic assessment for storage model 2 when the water tank, which is heated up by supercooling of CCM TES, supplies part of the house's heating and possibly CCM TES's reheating. This strategy also results in a lower demand for CCM material for providing a house's heating.

References

[1] Intergovernmental Panel on Climate Change (IPCC), *Climate Change 2021 – The Physical Science Basis: Working Group I Contribution to the Sixth Assessment Report of the Intergovernmental Panel on Climate Change*. Cambridge: Cambridge University Press, 2023. doi: DOI: 10.1017/9781009157896.

[2] "Net Zero by 2050 – Analysis - IEA." Accessed: Oct. 28, 2023. [Online]. Available: https://www.iea.org/reports/net-zero-by-2050

[3] "Renewables 2021 – Analysis - IEA." Accessed: Oct. 18, 2023. [Online]. Available: https://www.iea.org/reports/renewables-2021

[4] "Heating - IEA." Accessed: Oct. 28, 2023. [Online]. Available: https://www.iea.org/energy-system/buildings/heating

[5] M. Papapetrou, G. Kosmadakis, A. Cipollina, U. La Commare, and G. Micale, "Industrial waste heat: Estimation of the technically available resource in the EU per industrial sector, temperature level and country," *Appl Therm Eng*, vol. 138, pp. 207–216, 2018, doi: https://doi.org/10.1016/j.applthermaleng.2018.04.043.

[6] "Waste not, gain big: Reusing industrial heat energy or selling it for a profit | SUSPIRE Project | Results in brief | H2020 | CORDIS | European Commission." Accessed: Oct. 18, 2023. [Online]. Available: https://cordis.europa.eu/article/id/421989-waste-not-gain-big-reusing-industrial-heat-energy-or-selling-it-for-a-profit

[7] "Overall electricity consumption decreased by 6 per cent and wind power production was at a record high in 2022 - Statistics Finland." Accessed: Oct. 18, 2023. [Online]. Available: https://stat.fi/en/publication/cl8lmyfdcqgc70dukvv6dsrdd

[8] R. Law, A. Harvey, and D. Reay, "Opportunities for low-grade heat recovery in the UK food processing industry," *Appl Therm Eng*, vol. 53, no. 2, pp. 188–196, 2013, doi: https://doi.org/10.1016/j.applthermaleng.2012.03.024.

[9] "Improving industrial waste heat recovery – Analysis - IEA." Accessed: Nov. 02, 2023. [Online]. Available: https://www.iea.org/articles/improving-industrial-waste-heat-recovery

[10] "Energy statistics - an overview - Statistics Explained." Accessed: Oct. 28, 2023. [Online]. Available: https://ec.europa.eu/eurostat/statistics-explained/index.php?title=Energy_statistics_-_an_overview#Energy_intensity

[11] L. Miró, S. Brückner, and L. F. Cabeza, "Mapping and discussing Industrial Waste Heat (IWH) potentials for different countries," *Renewable and Sustainable Energy Reviews*, vol. 51, pp. 847–855, 2015, doi: https://doi.org/10.1016/j.rser.2015.06.035.

[12] YIT (Teollisuus- ja verkkopalvelut Oy), "Teollisuuden ylijäämälämmön hyödyntäminen kaukolämmityksessä (Utilization of industrial excess heat in district heating, in Finnish)," 2010.

[13] "TUOTANNON HUKKALÄMPÖ HYÖDYKSI".

[14] “Energy Efficiency Database | Data & Indicators | ODYSSEE.” Accessed: Nov. 03, 2023. [Online]. Available: https://www.indicators.odyssee-mure.eu/energy-efficiency-database.html

[15] M. Chamoun, R. Rulliere, P. Haberschill, and J.-L. Peureux, “Experimental and numerical investigations of a new high temperature heat pump for industrial heat recovery using water as refrigerant,” *International Journal of Refrigeration*, vol. 44, pp. 177–188, 2014, doi: https://doi.org/10.1016/j.ijrefrig.2014.04.019.

[16] C. Arpagaus, F. Bless, M. Uhlmann, J. Schiffmann, and S. S. Bertsch, “High temperature heat pumps: Market overview, state of the art, research status, refrigerants, and application potentials,” *Energy*, vol. 152, pp. 985–1010, 2018, doi: https://doi.org/10.1016/j.energy.2018.03.166.

[17] D. M. van de Bor and C. A. Infante Ferreira, “Quick selection of industrial heat pump types including the impact of thermodynamic losses,” *Energy*, vol. 53, pp. 312–322, 2013, doi: https://doi.org/10.1016/j.energy.2013.02.065.

[18] C. Kondou and S. Koyama, “Thermodynamic assessment of high-temperature heat pumps using Low-GWP HFO refrigerants for heat recovery,” *International Journal of Refrigeration*, vol. 53, pp. 126–141, 2015, doi: https://doi.org/10.1016/j.ijrefrig.2014.09.018.

[19] “AR4 Climate Change 2007: Synthesis Report — IPCC.” Accessed: Oct. 19, 2023. [Online]. Available: https://www.ipcc.ch/report/ar4/syr/

[20] P. Bertoldi and B. Atanasiu, “Electricity consumption and efficiency trends in the enlarged European Union,” *IES–JRC. European Union*, 2007.

[21] “Housing in Finland.” Accessed: Oct. 19, 2023. [Online]. Available: https://www.infofinland.fi/en/housing/housing-in-finland

[22] “Energy consumption in households - Statistics Finland.” Accessed: Oct. 28, 2023. [Online]. Available: https://stat.fi/en/statistics/asen

[23] “Statistics Finland - Buildings and Free-time Residences 2020.” Accessed: Oct. 28, 2023. [Online]. Available: https://www.stat.fi/til/rakke/2020/rakke_2020_2021-05-27_tie_001_en.html

[24] K. ’Savolainen, “Living in Detached Houses in Finland,” 2014.

[25] “Marijke” “Menkveld,” “De systeemkosten van warmte voor woningen,” Utrecht, 2015.

[26] “Long-term renovation strategy 2020-2050 FINLAND.”

[27] T. ’Soimakallio, S. ’Lehtilä, A. ’Similä, L. ’Honkatukia, J. ’Hildén, M. ’Rehunen, A. ’Saikku, L. ’Salo, M. ’Savolahti, S. ’Tuominen, P. ’Vainio, T. ’Koljonen, *Pitkän aikavälin kokonaispäästökehitys*. Prime Minister’s Office Finland, 2019.

[28] “Energy performance certificate register,” 2018.

[29] T. Dzhigit, J. Dürr, J. Tuunanen, and M. Luoma, “Passive houses in Finland,” *Stroitel’stvo Unikal’nyh Zdanij i Sooruzenij*, no. 13, p. 12, 2013.

[30] M. Bakker -Ecn, A. Brunialti -Sifri, and S. Landolina -European, “Cross-Cutting Technology • RHC-Platform”, Accessed: Oct. 19, 2023. [Online]. Available: www.rhc-platform.org

[31] E. Nadutey, “Wind energy integration with thermal energy storage,” Aalto University, 2019. Accessed: Oct. 19, 2023. [Online]. Available: https://aaltodoc.aalto.fi:443/handle/123456789/40900

[32] Y. Zhang and R. Wang, “Sorption thermal energy storage: Concept, process, applications and perspectives,” *Energy Storage Mater*, vol. 27, pp. 352–369, 2020, doi: https://doi.org/10.1016/j.ensm.2020.02.024.

[33] Y. Ding, *Thermal Energy Storage: Materials, Devices, Systems and Applications*. in Energy and Environment Series. Royal Society of Chemistry, 2021. [Online]. Available: https://books.google.fi/books?id=cYmUzQEACAAJ

[34] H. Nazir *et al.*, “Recent developments in phase change materials for energy storage applications: A review,” *Int J Heat Mass Transf*, vol. 129, pp. 491–523, 2019, doi: https://doi.org/10.1016/j.ijheatmasstransfer.2018.09.126.

[35] K. Faraj, M. Khaled, J. Faraj, F. Hachem, and C. Castelain, “A review on phase change materials for thermal energy storage in buildings: Heating and hybrid applications,” *J Energy Storage*, vol. 33, p. 101913, 2021, doi: https://doi.org/10.1016/j.est.2020.101913.

[36] A. Safari, R. Saidur, F. A. Sulaiman, Y. Xu, and J. Dong, “A review on supercooling of Phase Change Materials in thermal energy storage systems,” *Renewable and Sustainable Energy Reviews*, vol. 70, pp. 905–919, 2017, doi: https://doi.org/10.1016/j.rser.2016.11.272.

[37] I. Shamseddine, F. Pennec, P. Biwole, and F. Fardoun, “Supercooling of phase change materials: A review,” *Renewable and Sustainable Energy Reviews*, vol. 158, p. 112172, 2022, doi: https://doi.org/10.1016/j.rser.2022.112172.

[38] K. Turunen, V. Mikkola, T. Laukkanen, and A. Seppälä, “Long-term thermal energy storage prototype of cold-crystallizing erythritol-polyelectrolyte,” *Appl Energy*, vol. 332, p. 120530, 2023, doi: https://doi.org/10.1016/j.apenergy.2022.120530.

[39] G. Wang *et al.*, “Review on sodium acetate trihydrate in flexible thermal energy storages: Properties, challenges and applications,” *J Energy Storage*, vol. 40, p. 102780, 2021, doi: https://doi.org/10.1016/j.est.2021.102780.

[40] G. Wang, M. Dannemand, C. Xu, G. Englmair, S. Furbo, and J. Fan, “Thermal characteristics of a long-term heat storage unit with sodium acetate trihydrate,” *Appl Therm Eng*, vol. 187, p. 116563, 2021, doi: https://doi.org/10.1016/j.applthermaleng.2021.116563.

[41] K. ’Turunen, “ Long-term thermal energy storage with cold-crystallizing materials - Method, properties and scale-up,” Aalto University, 2023.

[42] M. R. Yazdani, J. Etula, J. B. Zimmerman, and A. Seppälä, “Ionic cross-linked polyvinyl alcohol tunes vitrification and cold-crystallization of sugar alcohol for long-term thermal energy storage,” *Green Chemistry*, vol. 22, no. 16, pp. 5447–5462, 2020.

[43] S. Puupponen and A. Seppälä, “Cold-crystallization of polyelectrolyte absorbed polyol for long-term thermal energy storage,” *Solar Energy Materials and Solar Cells*, vol. 180, pp. 59–66, 2018, doi: https://doi.org/10.1016/j.solmat.2018.02.013.

[44] P. G. Debenedetti, *Metastable liquids : concepts and principles*. Princeton University Press, 1996.

[45] F. S. Javadi, H. S. C. Metselaar, and P. Ganesan, “Performance improvement of solar thermal systems integrated with phase change materials (PCM), a review,” *Solar Energy*, vol. 206, pp. 330–352, 2020, doi: https://doi.org/10.1016/j.solener.2020.05.106.

[46] S. Hirano, “Thermal Energy Storage and Transport,” in *Handbook of Climate Change Mitigation*, W.-Y. Chen, J. Seiner, T. Suzuki, and M. Lackner, Eds., New York, NY: Springer US, 2012, pp. 669–700. doi: 10.1007/978-1-4419-7991-9_20.

[47] “Energy Conservation through Energy Storage Programme Energy Conservation through Energy Storage Program,” 2009.

[48] H. Li, W. Wang, J. Yan, and E. Dahlquist, “Economic assessment of the mobilized thermal energy storage (M-TES) system for distributed heat supply,” *Appl Energy*, vol. 104, pp. 178–186, 2013, doi: https://doi.org/10.1016/j.apenergy.2012.11.010.

[49] A. Hauer, S. Gschwander, Y. Kato, V. Martin, P. Schossig, and F. Setterwall, “Transportation of energy by utilization of thermal energy storage technology,” *ECES-IEA Annex*, vol. 18, 2010.

[50] “Trans-Heat Container.” Accessed: Dec. 12, 2023. [Online]. Available: https://www.nedo.go.jp/content/100899763.pdf

[51] W. Wang and J. Yan, “Mobilized Thermal Energy Storage (M-TES) Technology for Industry Heat Recovery,” *Handbook of Clean Energy Systems*, pp. 1–11, Jul. 2015, doi: 10.1002/9781118991978.HCES127.

[52] “Innovations in Mobile Thermal Energy Storage - Using Waste Heat to Power Communities | PICS.” Accessed: Oct. 19, 2023. [Online]. Available: https://pics.uvic.ca/projects/innovations-mobile-thermal-energy-storage-using-waste-heat-power-communities

[53] M. Shehadeh, E. Kwok, J. Owen, and M. Bahrami, “Integrating mobile thermal energy storage (M-tes) in the city of surrey’s district energy network: A techno-economic analysis,” *Applied Sciences (Switzerland)*, vol. 11, no. 3, pp. 1–12, Feb. 2021, doi: 10.3390/APP11031279.

[54] “Mobile heat storage – Enetech.” Accessed: Oct. 19, 2023. [Online]. Available: https://enetech.com.pl/en/mobile-heat-storage/

[55] “Mobile Heat Storage - Neo Bio Energy.” Accessed: Oct. 19, 2023. [Online]. Available: https://neobioenergy.pl/en/mobile-heat-storage/

[56] S. Guo, J. Zhao, W. Wang, J. Yan, G. Jin, and X. Wang, “Techno-economic assessment of mobilized thermal energy storage for distributed users: A case study in China,” *Appl Energy*, vol. 194, pp. 481–486, 2017, doi: https://doi.org/10.1016/j.apenergy.2016.08.137.

[57] A. C. Tataru and A. Stanci, “Study of the possibility of implementation in Finland of the Passivhaus concept in order to reduce energy consumption,” *MATEC Web Conf.*, vol. 305, 2020, [Online]. Available: https://doi.org/10.1051/matecconf/202030500071

[58] V. M. MOA FESTIN, “Pinch analysis of the Norske Skog Skogn TMP mill,” Chalmers University of Technology, Göteborg, 2009.

[59] C.-E. Grip, J. Isaksson, S. Harvey, and L. Nilsson, “Application of pinch analysis in an integrated steel plant in northern Sweden,” *ISIJ international*, vol. 53, no. 7, pp. 1202–1210, 2013.

[60] A. Rudie and M. Sabourin, “Wood influence on thermomechanical pulp quality: Fibre separation and fibre breakage,” *Journal of pulp and paper science*, vol. 28, no. 11, pp. 359–363, 2002.

[61] B. Talebjedi, T. Laukkanen, H. Holmberg, E. Vakkilainen, and S. Syri, “Advanced energy-saving optimization strategy in thermo-mechanical pulping by machine learning approach,” *Nord Pulp Paper Res J*, vol. 37, no. 3, pp. 434–452, 2022.

[62] J. Isaksson, A. Åsblad, and T. Berntsson, “Comparison Between a Detailed Pinch Analysis and the ‘Heat Load Model for Pulp and Paper’–Case Study for a Swedish Thermo-Mechanical Pulp and Paper Mill,” *CHEMICAL ENGINEERING*, vol. 29, 2012.

[63] “Finland: industrial prices for electricity 2021 | Statista.” Accessed: Oct. 31, 2023. [Online]. Available: https://www.statista.com/statistics/595853/electricity-industry-price-finland/

[64] “Overall Heat Transfer Coefficient | TLV.” Accessed: Nov. 01, 2023. [Online]. Available: https://www2.tlv.com/steam-info/steam-theory/steam-basics/overall-heat-transfer-coefficient

[65] B. Feng, J. Liu, Y. Zeng, and L.-W. Fan, “Atomistic insights into the heat conductance across the interfaces between erythritol and different metals: A non-equilibrium molecular dynamics study,” *Case Studies in Thermal Engineering*, vol. 41, p. 102599, 2023, doi: https://doi.org/10.1016/j.csite.2022.102599.

[66] D. A. Fadare, D. O. Nkpubre, A. O. Oni, A. Falana, M. A. Waheed, and O. A. Bamiro, “Energy and exergy analyses of malt drink production in Nigeria,” *Energy*, vol. 35, no. 12, pp. 5336–5346, 2010, doi: https://doi.org/10.1016/j.energy.2010.07.026.

[67] “Global Beer Consumption by Country in 2019.” Accessed: Oct. 24, 2023. [Online]. Available: https://www.kirinholdings.com/en/newsroom/release/2020/1229_01.pdf

[68] L. Ebrada, M. D. deLuna, F. Manegdeg, and N. Grisdanurak, “Brewery Heat Exchanger Networks Design and Optimization Based on Pinch Analysis at a Single ΔTmin,” *Philippine Engineering Journal*, vol. 36, no. 1, 2015.

[69] Margrét Ormslev Ásgeirsdóttir, “Increasing energy efficiency in industry applying pinch analysis,” University of Iceland & University of Akureyri, 2010.

[70] N. ’Leppäharju, “Kalliolämmön hyödyntämiseen vaikuttavat geofysikaaliset ja geologiset tekijät (Geophysical and geological factors affect the utilization of rock heat),” University of Oulu, 2008.

[71] “Convection Heat Coefficient - 2012 - SOLIDWORKS Help.” Accessed: Dec. 02, 2023. [Online]. Available: https://help.solidworks.com/2012/english/solidworks/cworks/convection_heat_coefficient.htm

[72] “SSAB:n Raahen tehdas - SSAB.” Accessed: Nov. 02, 2023. [Online]. Available: https://www.ssab.com/fi-fi/ssab-konserni/tietoja-ssabsta/tuotantopaikkakunnat-suomessa/raahe

[73] “Valio Oulu - Valio.” Accessed: Nov. 02, 2023. [Online]. Available: https://www.valio.fi/yritys/valion-tehtaat-suomessa/oulu/

[74] “European Market Best-Selling Food Grade Erythritol Wholesale Price CAS 149-32-6 - China Natural Erythritol and Erythritol Bulk.” Accessed: Nov. 17, 2023. [Online]. Available: https://ubchembio.en.made-in-china.com/product/hZyfWGgTrdkX/China-European-Market-Best-Selling-Food-Grade-Erythritol-Wholesale-Price-CAS-149-32-6.html

[75] “Wholesales Price Sodium Polyacrylate Super Absorbent Polymer - China Sodium Polyacrylate and Super Absorbent Polymer.” Accessed: Nov. 17, 2023. [Online]. Available: https://socochem.en.made-in-china.com/product/pdltUSuxvGYM/China-Wholesales-Price-Sodium-Polyacrylate-Super-Absorbent-Polymer.html

[76] “EU Natural Gas - Price - Chart - Historical Data - News.” Accessed: Nov. 17, 2023. [Online]. Available: https://tradingeconomics.com/commodity/eu-natural-gas

[77] “Customized Stainless Steel Copper Finned Tube Heat Exchanger Fin Tube Factory - Buy Heat Exchanger Finned Tube,Fin Tube Evaporator,Extruded Copper Fin Tube Product on Alibaba.com.” Accessed: Nov. 17, 2023. [Online]. Available: https://www.alibaba.com/product-detail/Customized-Stainless-Steel-Copper-Finned-Tube_1600447587201.html?spm=a2700.details.0.0.2dbe73dcvLfY9E

[78] “Stainless Steel Sheet Metal,304 316 Stainless Steel Plate / 304 Stainless Steel Sheet 201 430 316 - Buy 304 Stainless Steel Plate,Stainless Steel Sheet 201,304 Stainless Steel Sheet Product on Alibaba.com.” Accessed: Nov. 21, 2023. [Online]. Available: https://www.alibaba.com/product-detail/stainless-steel-sheet-metal-304-316_1600550001875.html?spm=a2700.galleryofferlist.normal_offer.d_title.5d8c5850Kt8cPb

[79] “Grundfos TP 40-180/2 A-F-A BUBE, 96401986, Inline pump.” Accessed: Nov. 19, 2023. [Online]. Available: https://www.centrifugal-pump-online.com/acatalog/Grundfos-TP-40-180-2-A-F-A-BUBE-1477.html

[80] “Stainless Steel Storage Tank 10000 Liter For Oil - Buy Stainless Steel Storage Tank,Cosmetic Storage Tank 10000 Liter,Can Be Customization Storage Tank Product on Alibaba.com.” Accessed: Nov. 17, 2023. [Online]. Available: https://www.alibaba.com/product-detail/Stainless-Steel-Storage-Tank-10000-Liter_1600383731205.html?spm=a2700.galleryofferlist.normal_offer.d_image.4f9927f4vzyzaj

[81] “In Finland heat pumps sales increased 50% in 2022 - European Heat Pump Association.” Accessed: Dec. 19, 2023. [Online]. Available: https://www.ehpa.org/news-and-resources/news/in-finland-heat-pumps-sales-increased-50-in-2021/

[82] “Ilmalämpöpumppu Midea Xtreme 9 sisä- ja ulkoyksikkö - K-Rauta.” Accessed: Nov. 21, 2023. [Online]. Available: https://www.k-rauta.fi/tuote/ilmalampopumppu-midea-xtreme-9-sisa-ja-ulkoyksikko/6438056305369

[83] “How Long Should Your Heat Pump Last? - Glasco Heating & Air Conditioning.” Accessed: Nov. 19, 2023. [Online]. Available: https://glascohvac.com/heating/heat-pumps/long-heat-pump-last/

[84] “Maalämpöpumppu Bosch LW 6 - K-Rauta.” Accessed: Nov. 15, 2023. [Online]. Available: https://www.k-rauta.fi/tuote/maalampopumppu-bosch-lw-6/4051516783365

[85] “Dispelling the Myths of Ground Source Heat Pumps | Greener Ideal.” Accessed: Nov. 19, 2023. [Online]. Available: https://greenerideal.com/guides/dispelling-myths-ground-source-heat-pumps/

[86] “ENTSO-E Transparency Platform.” Accessed: Oct. 28, 2023. [Online]. Available: https://transparency.entsoe.eu/dashboard/show

[87] B. Talebjedi, T. Laukkanen, H. Holmberg, and S. Syri, “Advanced design and operation of Energy Hub for forest industry using reliability assessment,” *Appl Therm Eng*, vol. 230, p. 120751, 2023, doi: https://doi.org/10.1016/j.applthermaleng.2023.120751.

Appendix 1 – Electricity Price, House's Heating demand and temperature in Oulu

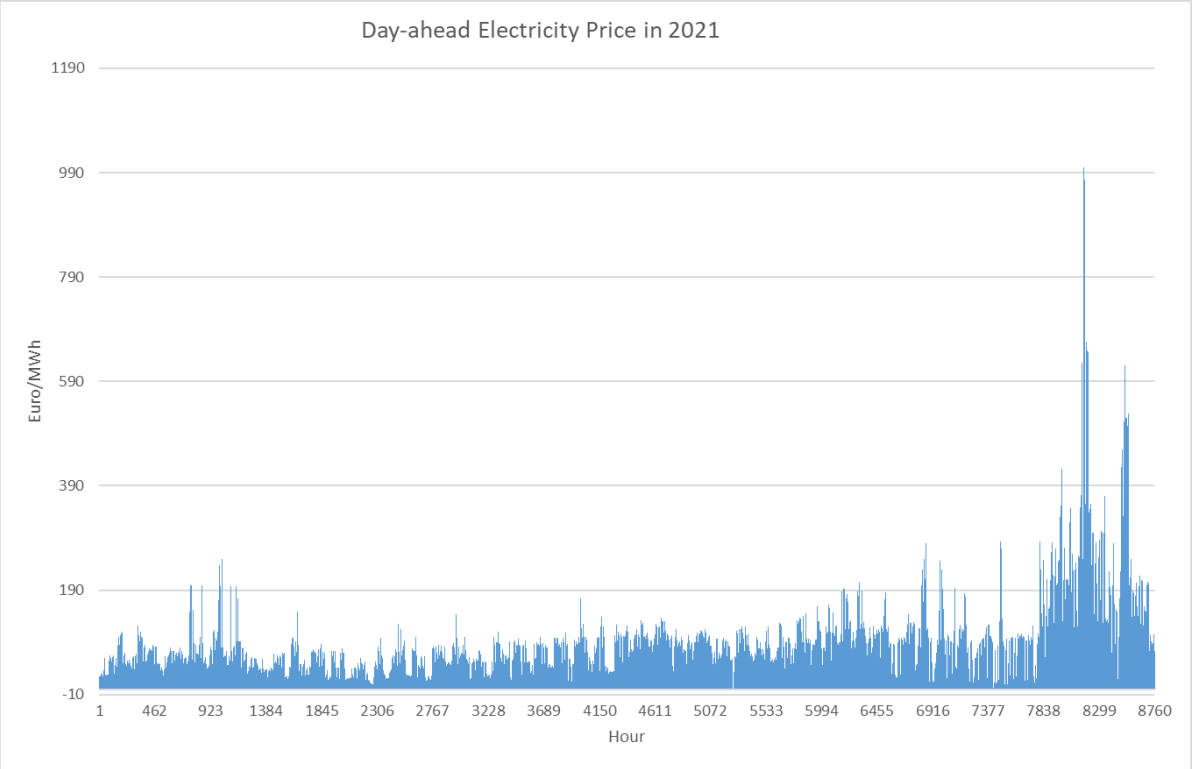

Figure A1.1. Day-ahead Electricity Price in Finland in 2021

Figure A1.1, illustrates the variation in day-ahead electricity price in Finland provided by ENTSO-e [86]. However, the household electricity price differs from the above values as it consists of transmission cost as well as tax.

$$household\ electricity\ price = Dayahead\ \ price + transmission\ \ fee + taxation$$

Transmission fee is 7.27 €/MWh however during winter it increases to 11.27 €/MWh and household electricity tax is 7.03 €/MWh in Finland [87].

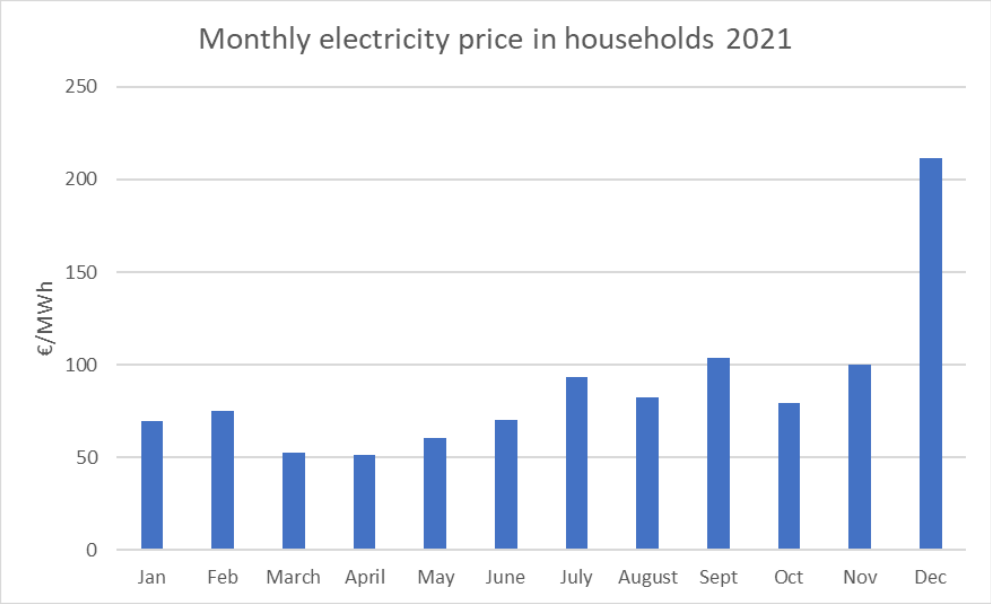

Figure A1.2. Monthly Household's electricity price in Finland in 2021

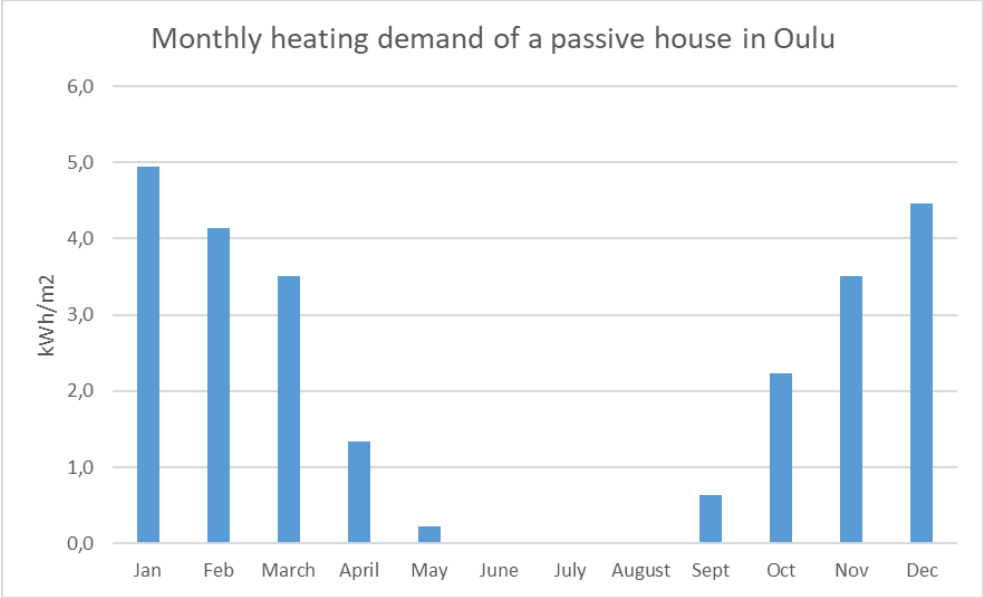

Figure A1.3. Monthly heating demand of a passive house located near Oulu, Finland

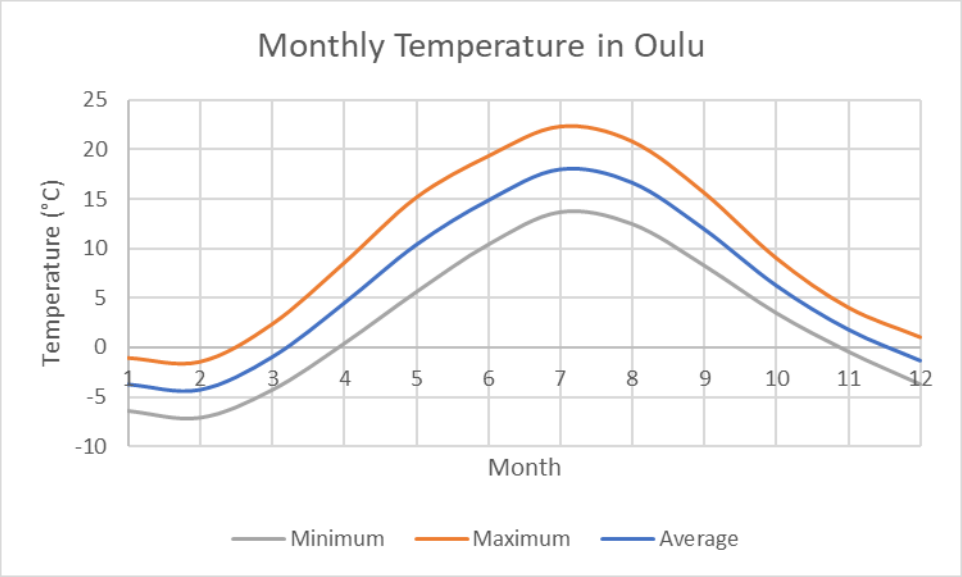

Figure A1.4. Monthly outside temperature in Oulu including maximum, minimum and average temperature

Appendix 2 – Economic Properties of Storage Models

Table A2.1. CAPEX assosiated to the one-time transportation of Storage model 1 consisting one, five, ten storage units

CAPEX Costs	**Number of TES Units**			**Unit**
	1	**5**	**10**	
Storage Tank Cost	11.9	16.4	18.4	k€
ErNa material Cost	37	37	37	k€
Cost of Heat Exchanger	86	97	137	€
Cost of placing Storage Underground	850	850	850	€
SUM	49.8	54.3	56.4	k€

Table A2.2. OPEX assosiated to the one-time transportation of storage model 1 consisting one, five, ten storage units

OPEX Costs	**Number of TES Units**			**Unit**
	1	**5**	**10**	
Reheating cost with electricity	200	176	116	€/a
Transportation Cost	242	247	249	€/a
SUM	443	423	365	€/a

Table A2.3. Annual cash flow, LCOE and NPV associated to one-time transportation of storage model 1 consisting one, five, ten storage units

Parameter	**Number of TES Units**			**Unit**
	1	**5**	**10**	
Annual Cash Flow	-132	-112	-54	€
LCOE	0.59	0.65	0.67	€/kWh
NPV	-51.3	-55.6	-57	k€

Table A2.4. CAPEX of the multiple charging round of one single ErNa storage model

CAPEX Costs	**Number of Charging Rounds**				**Unit**
	1	**2**	**3**	**4**	
Storage Tank Cost	11.9	6	4.2	3.3	k€

ErNa material Cost	37	18.5	12.3	9.2	k€
Cost of Heat Exchanger	86	86	86	86	€
Cost of placing Storage Underground	850	425	283	212	€
SUM	49.8	25	16.9	12.8	k€

Table A2.5. OPEX of the multiple charging round of one ErNa storage model 1

OPEX Costs	**Number of Charging Rounds**				**Unit**
	1	**2**	**3**	**4**	
Reheating cost with electricity	200	213	266	222	€
Transportation Cost	242	363	323	305	€
SUM	442	576	589	527	€

Table A2.6. Annual cash flow, LCOE and NPV associated to multiple charging round of storage model 1

Parameter	**Number of Charging Rounds**				**Unit**
	1	**2**	**3**	**4**	
Annual Cash flow	-131	-265	-278	-216	€
LCOE	0.59	0.3	0.2	0.15	€/kWh
NPV	-51.3	-28	-20.1	-15.3	k€

Table A2.7. CAPEX associated to storage model 2 charged once a year at the industry

CAPEX	**Storage Unit**	**Value**	**Unit**
Storage Tank Cost	ErNa Unit 1	5.1	k€
	ErNa Unit 2	4.6	k€
	ErNa Unit 3	4	k€
	Pure Erythritol	2.4	k€
PCM Cost	ErNa Unit 1	14.3	k€
	ErNa Unit 2	11.9	k€
	ErNa Unit 3	15.5	k€
	Pure Erythritol	5.9	k€
Cost of Heat Exchanger	ErNa Unit 1	95	€
	ErNa Unit 2	186	€
	ErNa Unit 3	67	€
	Pure Erythritol	70	€
Cost of placing Storage Underground	ErNa Units 1-3	740	€

CAPEX	Storage Unit	Value	Unit
Cost of Pump	-	1500	€
Cost of piping and valves	-	1000	€
SUM		67.4	k€